Spring 2011

Structure-activity relationships for interactions of hydroxylated polychlorinated biphenyls with human hydroxysteroid sulfotransferase hSULT2A1

Edugie Jennifer Ekuase
University of Iowa

STRUCTURE-ACTIVITY RELATIONSHIPS FOR INTERACTIONS OF HYDROXYLATED POLYCHLORINATED BIPHENYLS WITH HUMAN HYDROXYSTEROID SULFOTRANSFERASE hSULT2A1

by

Edugie Jennifer Ekuase

An Abstract

Of a thesis submitted in partial fulfillment
of the requirements for the Doctor of
Philosophy degree in Pharmacy
(Medicinal and Natural Products Chemistry)
in the Graduate College of
The University of Iowa

May 2011

Thesis Supervisor: Professor Michael W. Duffel

ABSTRACT

Industrial chemicals known as polychlorinated biphenyls (PCBs) were widely used for decades until their production was banned worldwide due to their persistence and toxicities to humans and other animals. Upon oxidative metabolism by cytochrome P450, hydroxylated metabolites of PCBs (OHPCBs) are formed. OHPCBs have been shown to competitively displace thyroxine from transthyretin, block normal hormonal activity, and inhibit phenol or family 1 sulfotransferases (SULTs) which catalyze sulfation of thyroid hormones and estrogens. Recently, three OHPCBs were shown to also interact with hydroxysteroid or family 2 sulfotransferases that play a role in the homeostasis of steroid hormones such as dehydroepiandrosterone (DHEA).

The objectives of the studies presented in this dissertation were to further examine the effects of selected OHPCBs on the activity of human hydroxysteroid sulfotransferase (hSULT2A1), to develop a three-dimensional quantitative structure activity relationship (3D-QSAR) model for OHPCBs as inhibitors of DHEA-sulfation catalyzed by this enzyme, and to investigate the mechanism of inhibition and binding of OHPCBs to hSULT2A1.

All 15 OHPCBs examined inhibited the sulfation of 1 μM [^{3}H] DHEA, catalyzed by hSULT2A1 with IC_{50} values ranging from 0.6 to 96 μM. The OHPCBs with a 3, 5-dichloro-4-hydroxy substitution were the most potent inhibitors of DHEA sulfation, and they were also shown to be substrates for hSULT2A1. Eight OHPCBs were substrates for hSULT2A1, and seven were solely inhibitors (i.e. they inhibited the sulfation of DHEA, yet they were not themselves sulfuryl-acceptors in hSULT2A1-catalyzed reactions). A 3D-QSAR model was developed utilizing comparative molecular field analysis (CoMFA). The model fit the data well and also had good predictability.

The kinetics of inhibition showed that these OHPCBs were noncompetitive inhibitors of hSULT2A1. Binding studies utilizing the displacement of a fluorescent

probe, 8-anilino-1-naphthalene sulfonic acid, revealed that several of the OHPCBs interact either at more than one binding site or with more than one enzyme conformation. Further exploration of this binding by molecular modeling showed that OHPCBs bind similarly to different conformations of the enzyme. This work has helped in our understanding of the roles of sulfotransferases in the metabolism and toxicities of OHPCBs, and it opens new avenues for future work.

Abstract Approved: _____
Thesis Supervisor

_____
Title and Department

_____
Date

STRUCTURE-ACTIVITY RELATIONSHIPS FOR INTERACTIONS OF HYDROXYLATED POLYCHLORINATED BIPHENYLS WITH HUMAN HYDROXYSTEROID SULFOTRANSFERASE hSULT2A1

by

Edugie Jennifer Ekuase

A thesis submitted in partial fulfillment
of the requirements for the Doctor of
Philosophy degree in Pharmacy
(Medicinal and Natural Products Chemistry)
in the Graduate College of
The University of Iowa

May 2011

Thesis Supervisor: Professor Michael W. Duffel

Graduate College
The University of Iowa
Iowa City, Iowa

CERTIFICATE OF APPROVAL

_____

PH.D. THESIS

_____

This is to certify that the Ph.D. thesis of

Edugie Jennifer Ekuase

has been approved by the Examining Committee
for the thesis requirement for the Doctor of Philosophy
degree in Pharmacy (Medicinal and Natural Products Chemistry)
at the May 2011 graduation.

Thesis Committee: _____
Michael W. Duffel, Thesis Supervisor

_____
Kevin G. Rice

_____
Robert J. Kerns

_____
Jonathan A. Doorn

_____
Larry W. Robertson

To God Almighty who put all the wonderful people in my path to help me realize my dream.

ACKNOWLEDGMENTS

I would like to express my immense gratitude to my advisor, Dr. Duffel. Thank you for your patience, mentorship and support over the years. I could not have achieved this milestone without your help. You were more than a mentor to me; you were like a friend. I came to you with all my problems, be it research related or personal, and you always gave me valuable advice on what to do. I say thank you, thank you and thank you again.

I would like to show my appreciation to my committee members (Dr. Robert Kerns, Dr. Larry Robertson, Dr. Kevin Rice, and Dr. Jonathan Doorn) for the courses they taught. The knowledge I gained from those courses helped me in understanding my project. Most importantly, thank you for your helpful suggestions during the course of writing this dissertation. Also, special thanks to my college professors, Dr. James Mark and Dr. Clinton Dickson, for believing in me and urging me to obtain this PhD degree.

I would like to thank my parents, Felix O. Ekuase, and Beatrice I. Ekuase, for their love, wisdom, and support. Also, thank you for the way you raised my brothers and I. You taught us to always put God first and to believe in ourselves in all that we do, and when we succeed, to have humility. You gave us a sound education and above all showed us how to adapt to every situation in life. Today, I am a woman who adapts quickly to change, confident in her abilities but never arrogant. Also, special thanks to my siblings, Aghasedo Ekuase and Naruna Ekuase for your support and for your wonderful words of encouragement through the years.

Finally, I want to appreciate my son, Olujuwon, for adding so much value to my life. You are an unexpected blessing and a gift from God. Since your arrival, you have made me sigh, cry, and laugh, all at the same time. You always need me, and it feels good to be needed and loved by you. Thank you for making your debut when you did, there could not have been a more appropriate time.

ABSTRACT

Industrial chemicals known as polychlorinated biphenyls (PCBs) were widely used for decades until their production was banned worldwide due to their persistence and toxicities to human and other animals. Upon oxidative metabolism by cytochrome P450, hydroxylated metabolites of PCBs (OHPCBs) are formed. OHPCBs have been shown to competitively displace thyroxine from transthyretin, block normal hormonal activity, and inhibit phenol or family 1 sulfotransferases (SULTs) which catalyze sulfation of thyroid hormones and estrogens. Recently, three OHPCBs were shown to also interact with hydroxysteroid or family 2 sulfotransferases that play a role in the homeostasis of steroid hormones, such as dehydroepiandrosterone (DHEA).

The objectives of the studies presented in this dissertation were to further examine the effects of selected OHPCBs on the activity of human hydroxysteroid sulfotransferase (hSULT2A1), to develop a three-dimensional quantitative structure activity relationship (3D-QSAR) model for OHPCBs as inhibitors of DHEA-sulfation catalyzed by this enzyme, and to investigate the mechanism of inhibition and binding of OHPCBs to hSULT2A1.

All 15 OHPCBs examined inhibited the sulfation of 1 μM [^{3}H] DHEA, catalyzed by hSULT2A1 with IC_{50} values ranging from 0.6 to 96 μM. The OHPCBs with a 3, 5-dichloro-4-hydroxy substitution were the most potent inhibitors of DHEA sulfation, and they were also shown to be substrates for hSULT2A1. Eight OHPCBs were substrates for hSULT2A1, and seven were solely inhibitors (i.e. they inhibited the sulfation of DHEA, yet they were not themselves sulfuryl-acceptors in hSULT2A1-catalyzed reactions). A 3D-QSAR model was developed utilizing comparative molecular field analysis (CoMFA). The model fit the data well and also had good predictability.

The kinetics of inhibition showed that these OHPCBs were noncompetitive inhibitors of hSULT2A1. Binding studies utilizing the displacement of a fluorescent

probe, 8-anilino-1-naphthalene sulfonic acid, revealed that several of the OHPCBs interact either at more than one binding site or with more than one enzyme conformation. Further exploration of this binding by molecular modeling showed that OHPCBs bind similarly to different conformations of the enzyme. This work has helped in our understanding of the roles of sulfotransferases in the metabolism and toxicities of OHPCBs, and it opens new avenues for future work.

TABLE OF CONTENTS

LIST OF TABLES

LIST OF FIGURES

LIST OF ABBREVIATIONS

ADT	Androsterone
AhR	Aryl hydrocarbon receptor
AICc	corrected Akaike information criterion
ANS	8-Anilino-naphthalene sulfonic Acid
11β-HSD1	11β -hydroxysteroid dehydrogenase
BSA	Bovine serum albumin
CoMFA	Comparative Molecular Field Analysis
CScore	Consensus score
CYP	Cytochrome P450
DE52	Diethylaminoethyl cellulose
DHEA	Dehydroepiandrosterone
DHEAS	Dehydroepiandrosterone sulfate
^{3}H-DHEA	Triated dehydroepiandrosterone
DTT	Dithiothreitol
GST	Glutathione-S-transferase
HPLC	High performance liquid chromatography
hSULT2A1	Human hydroxysteroid sulfotransferase
IC_{50}	Half maximal inhibition concentration
IPTG	Isopropyl-1-thio-D-galactopyranoside
K_d	Dissociation constant
K_i	Inhibition constant
K_{cat}	Catalytic constant (turnover number of an enzyme)
K_m	Half maximum velocity
K_{cat}/K_m	Catalytic efficiency
LB	Luria broth

LCA	Lithocholic acid
LOO	Leave-one-out
3-OH-BaP	3-Hydroxybenzo[a]pyrene
MSS	molecular spreadsheet
NADPH	Nicotinamide adenine dinucleotide phosphate
N-OH-2AAF	N-hydroxyl-2-acetylaminofluorene
PAP	Adenosine 3', 5'- diphosphate
PAPS	3'-phosphoadenosine-5'-phosphosulfate
PCB	Polychlorinated biphenyl
PMF-Score	potentials of mean force-score
PREG	Pregnenolone
PREG-S	Pregnenolone sulfate
PRESS	Predictive Residual Sum of Squares
QSAR	Quantitative structural-activity relationships
q^2	Predictive power of QSAR model
r^2	Conventional correlation coefficient
SDS-PAGE	Sodium dodecyl sulfate-polyacrylamide gel electrophoresis
SULT	Sulfotransferase
SULT1E1	Estrogen sulfotransferase
TCDD	2,3,7,8-tetrachlorodibenzo-*p*-dioxin
T_3	Triiodothyronine
T_4	Thyroxine
TRIS-HCL	Tris (hydroxymethyl)aminomethane hydrochloride
TTR	Transthyretin
UGT	Uridine diphosphate-glucuronosyltransferase
v	Velocity
V_{max}	Maximum enzyme velocity

CHAPTER I

INTRODUCTION

Polychlorinated biphenyls

Polychlorinated biphenyls (PCBs) comprise 209 congeners that consist of 1-10 chlorine atoms on a biphenyl ring system (Figure 1) (*1-3*). They were easily synthesized and were sold as mixtures (*2, 4*). In the United States, PCBs were produced in large quantities and marketed under the trade name, Aroclor. The Aroclors were numbered according to the amount of chlorine they possessed. For instance, the last two digits of Aroclor 1254 showed that it was composed of 54% chlorine (*4-5*). In other industrialized countries such as Japan and France, PCBs were sold under the trade names Kanechlor and Phenochlor, respectively (*4-5*).

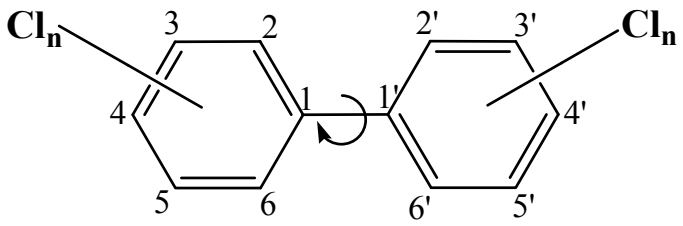

Figure 1. The general structure of polychlorinated biphenyl with possible positions of chlorine atoms denoted by numbers on the carbon atoms. The curved arrow shows possible rotations about the C-C single bond.

PCBs were widely used for many industrial purposes. For example, they were used in paints, fluorescent ballasts, dielectric fluids in capacitors and transformers, caulking materials, plasticizers, surface coating, inks, adhesives, carbonless duplicating paper, wire insulators, fire retardants, elastic sealant and heat insulation (*1, 4, 6*). Owing

to their low reactivity, these versatile compounds were thought to be harmless in the environment and as such were not always properly disposed of (*7*). This improper waste management led to a worldwide pollution because these compounds are very lipophilic and not readily biodegradable in nature (*8-9*). PCB residues have been found in rivers and lakes, the atmosphere, fish, human adipose tissue, blood, and breast milk (*4, 10*). Furthermore, the half-life of PCBs in the human body is 7 to 10 years (*11*).

PCBs were identified in wildlife in 1966 (*12*). This discovery was a cause for concern in the scientific community, and scientists wondered what these compounds could be doing to human health. In 1968, there was accidental exposure to PCBs due to consumption of rice bran oil contaminated with PCB in western Japan (Yusho) (*1-2, 13*). In 1979, there was yet another incident of accidental consumption of PCB in oil in Taiwan (Yu Cheng) (*1, 13-14*). Individuals who consumed the oil became ill and presented with different complaints, such as low birth weights, hyperpigmentation (*1-2, 14*) and comedone (*14-15*). Owing to the occurrence of PCBs in the environment, and the emerging discovery of their biological effects, there was a voluntary restriction on the production of PCBs (*4*) followed by a ban in production in the United States in 1979 (*1*). Although production has now been banned worldwide, PCBs are still in use and a persistent problem.

Exposure to PCBs

The major ways through which humans have been exposed to PCBs are occupational and environmental (*4*). There have been various occupational cases of PCB exposure. Symptoms ranging from elevated serum lipid levels, increased levels of serum enzymes, possible hepatic damage, respiratory problems, chloracne, and related dermal lesions have been observed in individuals who worked in plants where they were exposed to PCBs (*5*). According to one study, when blood plasma PCBs levels of exposed workers in Japan were tested, and compared to plasma PCB levels of the Yusho patients,

the workers had considerably higher PCB levels (*16*). Furthermore, PCB levels in blood and breast milk of mothers who were capacitor workers in Japan were more elevated than those who were not exposed to PCBs (*15*). In Finland, construction workers were shown to be exposed to PCBs that are present in elastic polysulphide sealants during renovation of prefabricated houses (*17*). Their PCBs serum levels were between 0.6 and 17μg/L, and the PCBs in the sealants were primarily from Aroclor 1260 or Aroclor 1254 (*17*).

Exposure to PCBs through the environment has been seen due to the prevalence of these compounds in air, water and soil. Some authors collected air and water samples during their transit from Germany to South Africa, and found out that there were considerable amount of PCBs in the samples they collected (*18*). PCB concentrations reached levels of 3.7 to 220 pg m^{-3} and 0.071 to 1.7 pg L^{-1} in air and seawater, respectively (*18*). Jamshidi and coworkers found that the concentration of PCBs present in some homes in the United Kingdom exceeded that present in the environment (*19*). These authors then suggested that ventilation of indoor air contributes more to outdoor air PCB levels than volatilization of PCBs from the soil (*19*). This suggestion is based on the fact that when soil samples were tested for PCB levels there was enantioselective degradation while those in outdoor air were racemic and comparable to those seen in commercial mixtures (*20*). In addition, in the 1950s and 1960s, PCB-containing wood finishings (*6*) as well as PCB contaminated caulks were used in commercial buildings and in schools (*21-22*). Presently, these are important sources of exposure to PCBs through inhalation as there is evidence of increased blood concentration of lower chlorinated PCBs in humans (*23*). Furthermore, fish are a major source of human exposure to PCBs due to bioaccumulation of these pollutants in fish. For example, in one population where there is high consumption of catfish, PCB serum concentrations were significantly high (*24*). As noted above, accidental exposure to PCBs has been seen in Japan (Yusho) and Taiwan (Yu Cheng). The toxic responses observed in these incidents

were initially linked to PCBs found in the rice bran oil. However, recent evidence suggests that halogenated compounds such as polychlorinated dibenzofurans which are by-products formed from PCB-containing industrial fluids might have been the culprit for some of the toxicities observed (*1-2, 5*).

Effects of PCB exposure

Research has shown that exposure to PCBs correlates with intellectual impairments, lower psychomotor scores and neurotoxicity in children (*25-27*). PCBs have been classified as probable human carcinogens (*28*). However, they are shown to cause mutations and promote cancer in laboratory animals (*1, 29*). PCBs may promote cancer by increasing oxidative stress in the liver (*30*). Oxidative DNA damage by PCBs can lead to formation of 8-hydroxydeoxyguanosine (8-OHdG) (*31*), and the presence of 8-OHdG may be indicative of mutagenesis (*32*). PCBs have also been shown to increase lipid peroxidation in the liver (*33*). Furthermore, they alter behavior, and decrease circulating thyroid hormones in laboratory animals (*34-35*). When rats were given a dose of 3,4,3'4'-tetrachlorobiphenyl (TCB) intraperitoneally, there was considerable decrease in thyroxine (T_4) levels in the plasma due to changes in the metabolism of thyroid hormone (*36*). The decrease in thyroxine could be as a result of hydroxylated metabolites of PCBs blocking transport proteins such as transthyretin (TTR), or it could be due to induced glucuronidation of thyroxine by the parent compounds (*37*). PCBs have also been shown to cause endocrine disruption by interfering with the homeostasis of steroids (*11, 38*). Other reports indicate effects of PCBs on insulin secretion (*39*), arachidonic acid release (*40*), the function of the hypothalamo-pituitary-thyroid axis (*41*) and tissue-specific estrogen-mediated events (*42*). There can also be promotion of hormone-dependent cancers such as breast, ovarian, and testicular cancer (*43*). Furthermore, the ryanodine receptor (in particular, ryanodine receptor type 1 - RyR1), which functions as calcium-induced calcium-release channel, has been shown to have its activity altered by PCB

congeners and their metabolites (*44*).

Coplanar PCBs

More coplanar PCBs, which are also known as ortho-poor PCBs (Figure 2), bind avidly to the aryl hydrocarbon receptor (AhR) (*45*). The non-ortho coplanar PCBs and mono-ortho coplanar PCBs behave like 2, 3, 7, 8-tetrachlorodibenzo-*p*-dioxin (TCDD) in the way they interact with AhR (*4, 8, 45-46*). The non-ortho coplanar PCBs with two para or more meta substitutions are essential for optimum TCDD-like activities (*5*).

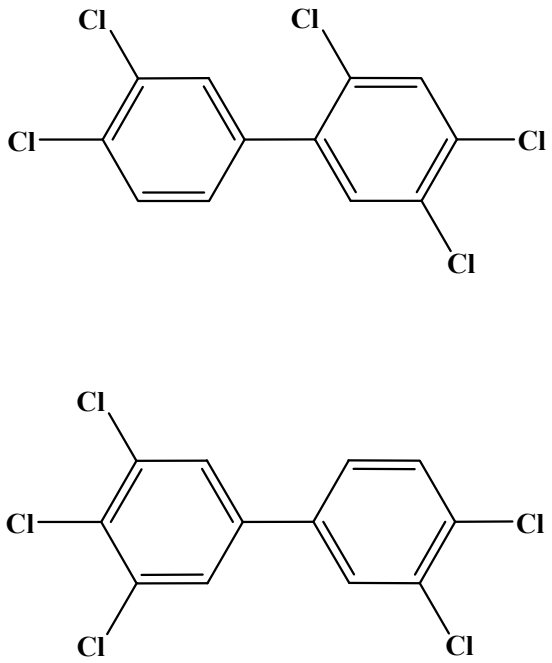

Figure 2. Structure of more coplanar PCBs with one or no ortho chlorines

Furthermore, these compounds behave like 3-methylcholanthrene (3-MC) and TCDD in the way they induce hepatic drug metabolizing enzymes (*47-48*). When 3, 3', 4, 4', 5-pentachlorobiphenyl (PCB 126) was administered to adult male Sprague-Dawley rats, there was increase in the activity of CYP1A1 (*49*). The mono-ortho coplanar PCBs have been reported as mixed-type inducers of drug metabolizing enzymes and have been shown to displace TCDD from the aryl hydrocarbon receptor (AhR) competitively (*50*). Problems seen in reproduction in some animals and humans have be linked to these PCBs (*5*). These observations were based on a toxic equivalency factor (TEF). TEF relates the toxicity of a compound's dioxin-like effect to that of dioxin. However, due to lack of evidence in data collected from *in vivo* work, the use of TEFs for the non-ortho or mono ortho PCBs will not be continued (*46*).

Non-coplanar PCBs

Noncoplanar PCBs having more than one ortho-chlorine atom (Figure 3) are mostly found in humans, Aroclors, and natural bodies of water (*9, 51*)**.** The caudate nucleus (a region of the brain) of patients who had Parkinson's disease while they were alive were collected at autopsy and examined for the levels of PCBs present, and the amount of ortho-substituted PCBs found were very high compared to other PCBs (*52*). In addition, this group of PCBs has been shown to disturb the intracellular second messenger systems needed for growth of neurons and to decrease the dopamine content in the brain (*53*). Furthermore, these noncoplanar PCBs have been reported to stop the absorption of neurotransmitters into brain synaptosomes of rat (*54*).

The diortho-substituted PCB, 2, 2',4, 4',5, 5'-hexachlorobiphenyl (PCB 153), has been shown to promote tumorogenesis and induce enzymes responsible for metabolism of xenobiotics and endogenous compounds (*55*). For example, PCB 153 has been reported to increase the activity of uridine diphosphate glucuronyl transferases (UDPGTs) thereby elevating the elimination of thyroxine (T_4) leading to its reduction in

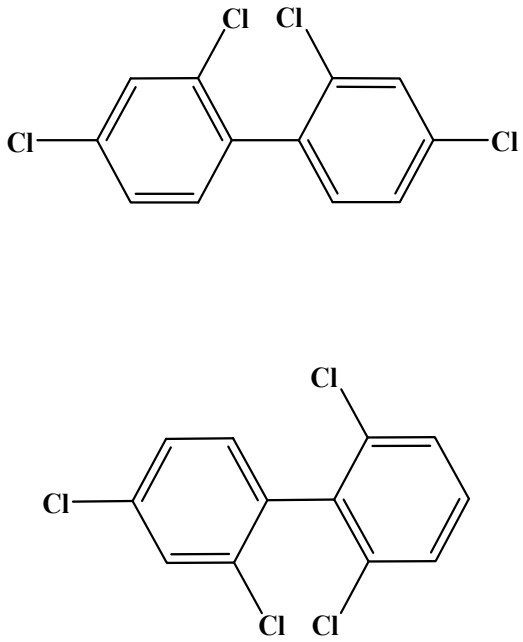

Figure 3. Structure of noncoplanar PCBs with two or more ortho chlorines

serum (*56*). In addition, noncoplanar PCBs have been shown to disrupt the hypothalamic-pituitary-thyroid axis due to reduced levels of serum T_4 concentrations in laboratory animals (*49*). They have been shown to stop the functioning of membranes of proteins by changing their structures (*57*). In addition, the effect of ortho-substituted PCBs on calcium homeostasis has been documented. Reduced levels of calcium are seen with PCBs due to their ability to enter the lipid layer of membrane of rat liver mitochondria and induce damage (*58*).

Volatile PCBs

Airborne PCBs are the lower chlorinated congeners that are released from buildings and from landfills and waters contaminated with PCBs (*59-60*). Volatilization of PCBs results in increased levels of volatile PCBs in air and these have been measured

in cities (*61*) especially during the periods of higher temperatures (*62*). PCBs can be vaporized from landfills, environmental reservoirs as well as from caulks in buildings (*22, 63-64*). Palmer *et al*., 2008, sampled outdoor air for the levels of PCBs in two communities (with the reputation of having a lot of PCB-waste sites) near the Hudson River, and found that PCB concentrations were more elevated in two of the communities they tested than the comparison community located farther away from the Hudson River (*62*). Additionally, large amounts of volatile PCBs have been reported to be released from Lake Michigan into the atmosphere (*65*). According to Persoon *et al*., 2009, 151 airborne PCBs were quantified in two urban areas in the Great Lake region-Cleveland and Chicago (*66*). The authors also found that the average concentrations of PCBs in air in these two cities were not the same and the PCB congeners in the air samples could be likened to those in commercial mixtures (*67*). It should be noted that the lower chlorinated PCB congeners with two or three chlorine atoms (i.e. PCB 12, 15 and 38) were more prevalent at some sites in these cities (*67*). Work by Hu *et al*., 2010, also showed higher levels of di- and tri chlorinated PCBs in Chicago air (*61*).

PCBs are not only found in outdoor air but also in indoor air. Most people spend more than sixteen hours of any given day indoors, and as such may be more exposed to PCBs in indoor air than outdoor air (*68-69*). The presence of PCBs in indoor air can be due to the use of PCB-containing materials such as furniture and furnishings, electrical appliances and fluorescent lights, plastic materials, sealing products, plasticizers and caulks (*69*). In Germany for instance, indoor air contamination by PCBs has been linked to elastic sealant material used in school buildings, and there is a shift towards the lower chlorinated PCBs owing to their volatility (*23*). Furthermore, higher levels of PCB 28 and 52 were observed in air in a school polluted by lower PCBs, and blood samples obtained from teachers in this school contained very high amounts of PCB 28 (*23*). It should be noted that indoor air PCB concentrations are higher than outdoor air concentrations according to some studies. The air in eight non-smoking homes in Rome was tested for

PCB concentrations, and was compared to PCB levels present in air outside the homes (*69*). The result showed that outdoor PCB levels were much lower than indoor PCB levels (*69*). Also, when PCB levels in indoor air were tested in 14 different locations and compared to outdoor air in Birmingham and in the west Midlands area of the United Kingdom, indoor PCB concentrations were greater than outdoor PCB levels (*70*). The results obtained from this study are in agreement with those of Jamishi and coworkers who also found that the concentration of PCBs in indoor air exceeded that of outdoor air in this area (*19*). In general there have been reported cases of elevated PCB levels in homes, schools, offices and laboratories. These airborne PCBs can easily be metabolized when inhaled and may lead to formation of reactive intermediates which may cause cancer (*71*). It is therefore important to investigate further the impact of these compounds to human health.

PCB metabolism

Initial metabolism of PCBs is often catalyzed by cytochrome P450 (CYP) enzymes in reactions whereby the PCBs are oxidized to their hydroxylated forms (OHPCBs) (*4*). Formation of the OHPCB can be by direct insertion of the oxygen atom into the carbon-hydrogen bond or by rearrangement of an epoxide (*72*). PCB metabolites that have been identified in humans include the hydroxylated forms (*73-75*) and in vitro studies showed them to be potent inhibitors of mitochondrial oxidative phosphorylation (*76*). PCB sulfates (*77-78*) or PCB glucuronides (*79*) may be formed as a result of further metabolism of OHPCB by sulfotransferases or UDP-glucuronosyltransferase (UGTs) (Figure 4). Formation of the PCB sulfates may or may not lead to metabolic disposition of these compounds, as some PCB sulfates retain significant lipophilic properties based on calculated octanol/water partition coefficients (*80*). Another group of PCB metabolites are the methylsulfones which are formed as a result of metabolism by glutathione-S-transferase (GST) (*80*). PCB methylsulfones have been shown to be present in tissues

such as the liver, lung and fat, and they induce drug metabolizing enzymes among other effects such as tumor promotion (*81*). Hydroxylated polychlorinated biphenyls (OHPCBs) may not always be metabolized by conjugating enzymes such as SULT, UGT and GST. Further metabolism of OHPCBs by cytochrome P450 monooxygenases may lead to formation of catechols or other dihydroxy metabolites (Figure 4). Mono, di and tri-chlorinated PCBs are known to form catechols in experimental animals, and there are some evidence of the formation of catechols with tetra, penta, and hexachlorinated PCBs as well (*80*). For example, PCB 65 (*82*), PCB 52 (*83*), PCB 101 (*84*), have been shown to form dihydroxylated PCB metabolites in rats, and PCB 153 catechol has been seen in rabbit (*85*). Oxidation of the catechol by cytochrome P450 may result in the formation of PCB-quinone metabolites (Figure 4), and these quinones may bind proteins and DNA to form adducts.

One study showed that the quinones form protein adducts by binding proteins through cysteine residues in treated cells and cause inhibition of topoisomerase (*86*), an enzyme needed for the unwinding and detangling of DNA (*87*). Lower chlorinated PCB quinones such as PCB 3 quinone was shown to be reactive toward nitrogen and sulfur nucleophiles of cells (*88*). In addition, PCB 3 metabolites have been shown to bind purines to form DNA adducts (*89*). Furthermore, there is evidence to show that PCB quinones from lower chlorinated PCBs lead to formation of reactive oxygen species and oxidative stress (*90*).

Hydroxylated PCB metabolites

It has been suggested that PCB metabolism is mainly a detoxication process and the toxic responses observed are due to the parent compounds (*5*). However, according to Lans and coworkers, some hydroxy-PCBs had higher affinity for transthyretin than thyroxine (T_4) (*37*). For example, 4'-hydroxy-2', 3, 3', 4', 5-pentachlorobiphenyl, a PCB metabolite found in blood was shown to competitively displace T_4 from transthyretin

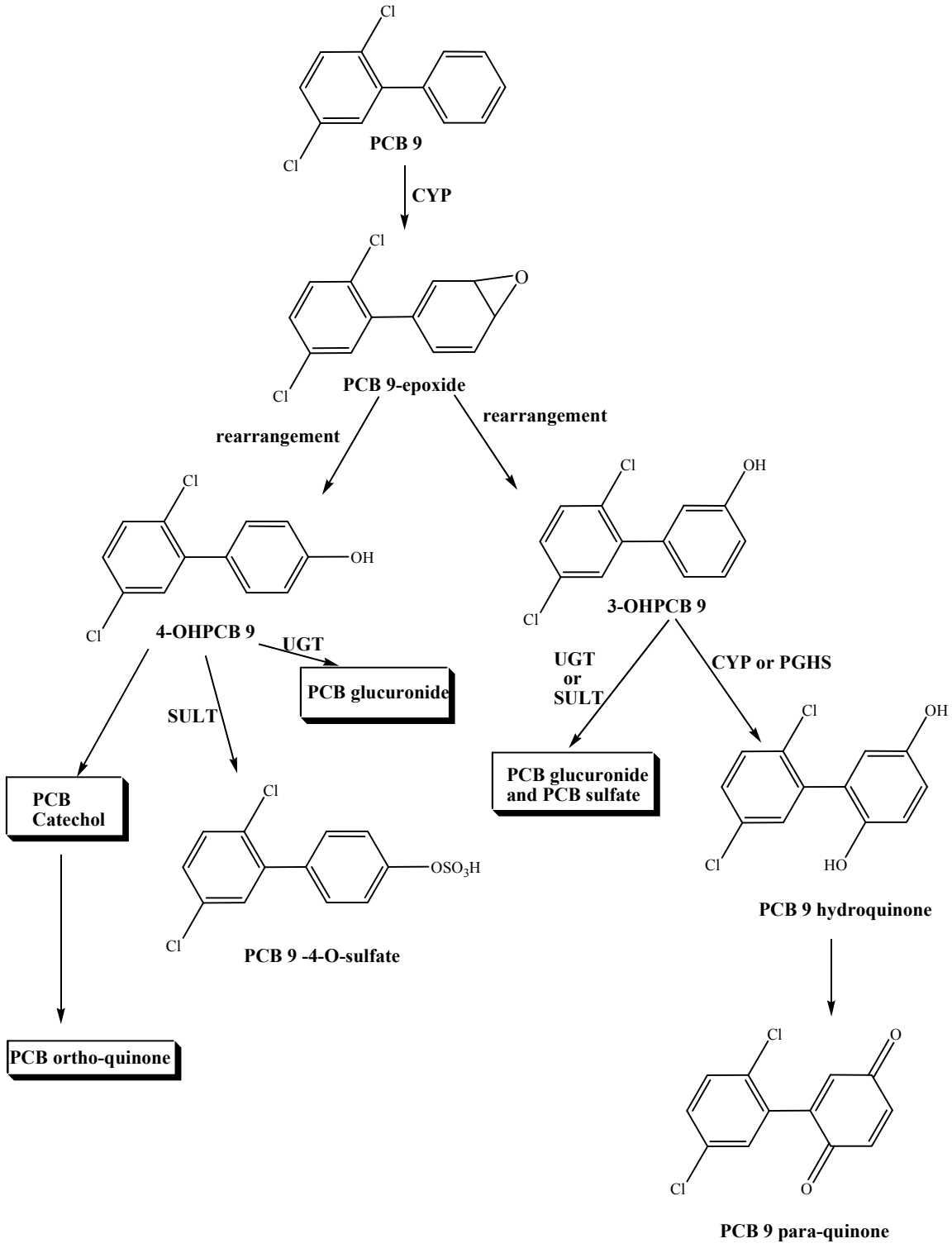

Figure 4. Metabolism of PCB 9 to hydroxy, dihydroxy, quinone and conjugated metabolites

(TTR) with an IC_{50} value in the nanomolar range (*37*). By binding to TTR, OHPCBs can be delivered to the fetus because TTR can cross the placenta and blood-brain barrier, even though it is not the primary transport protein for thyroid hormone in humans (*91*). Furthermore, the displacement of T_4 by OHPCBs leads to decreased serum thyroid hormone levels and this can result in problems in the reproductive and neurological systems (*92-93*). PCB metabolites are implicated in other forms of endocrine disruption (*8, 94*). Estrogenic activity have been seen in the mouse uterus upon binding of 4,4′-dihydroxy-3,3′,5,5′-tetrachlorobiphenyl to the estrogen receptor (*95*). Antiestrogenic activities have also been seen with 4-hydroxy-2, 2', 3', 5', 6- and 2, 2', 3', 4', 6'-pentachlorobiphenyl by disrupting the actions of 17*β*-estradiol in the mouse uterus (*96*). Furthermore, OHPCBs have been shown to inhibit phenol (or family 1) SULTs that catalyze sulfation of thyroid hormones and estrogens (*94, 97*). Inhibition of the estrogen sulfotransferase (SULT1E1) results in an increase of estradiol, and this gives an indirect estrogenic effect. Estradiol is the major form of estrogen circulating in humans and it also plays a role as a tumor promoter through interaction with estrogen receptors (*98*). In addition, metabolites of estradiol (i.e. quinones and semiquinones) cause DNA mutation and may be involved in breast cancer (*99*).

The effects of OHPCBs on family 2 or hydroxysteroid (alcohol) SULTs have not been examined thoroughly. These family 2 SULTs have been shown to play a role in the homeostasis of steroid hormones such as dehydroepiandrosterone (DHEA) and androsterone (*100*), and three OHPCBs have previously been observed to interact with a human family 2 SULT (*77*).

Sulfation reactions

Metabolic sulfation was first observed by Baumann in 1876 when phenyl sulfate was isolated from the urine of a patient treated with phenol (*101*). Sulfation is a reaction catalyzed by enzymes known as sulfotransferases, and these sulfation reactions occur in

bacteria, plants and mammals. The mammalian cytosolic sulfotransferases, SULTs, are responsible for the transfer of a sulfuryl group from the coenzyme, 3'-phosphoadenosine-5'-phosphosulphate (PAPS), to an acceptor molecule (*102-103*) (Figure 5). The donor molecule, PAPS, is very important, as sulfation activity can be dependent on the amount of PAPS present in a given tissue (*104-105*). On the other hand, PAPS availability is dependent on the amount of inorganic sulfate present (*104, 106*) as well as the enzyme, PAPS synthetase in humans and animals (*107*). In lower organisms and plants however, PAPS biosynthesis is dependent on ATP-sulfurylase and APS-kinase (*108-109*). The human bifunctional polypeptide, PAPS synthetase, combines these two enzyme activities in a single protein (*107*). The acceptor molecule in a sulfotransferase-catalyzed reaction either possesses a hydroxyl group or an amino group (*110-111*), and the products formed are PAP and sulfate esters or sulfamates (Figure 5) (*112*). Sulfation reactions are not only important in xenobiotic metabolism, but they can also be involved when endogenous compounds such as steroids need to be transported to the site(s) in the body where they are needed (*113*). For example, DHEA is transported after it has undergone sulfation, to its sulfate ester, DHEA-S. The DHEA-S is circulated through the body and then it is desulfated by another enzyme, sulfatase upon getting to the site where it is needed (*114*). DHEA is a precursor of both androgen and estrogen production and thereby can function as one regulator of steroid biosynthesis (*115*).

Sulfation may render a compound to be less toxic (detoxication), or lead to an enhancement of activity of a compound to get desired effects (prodrug activation) or to an increase in toxicity of a compound to a reactive product in a biological system (bioactivation) (Figure 6).

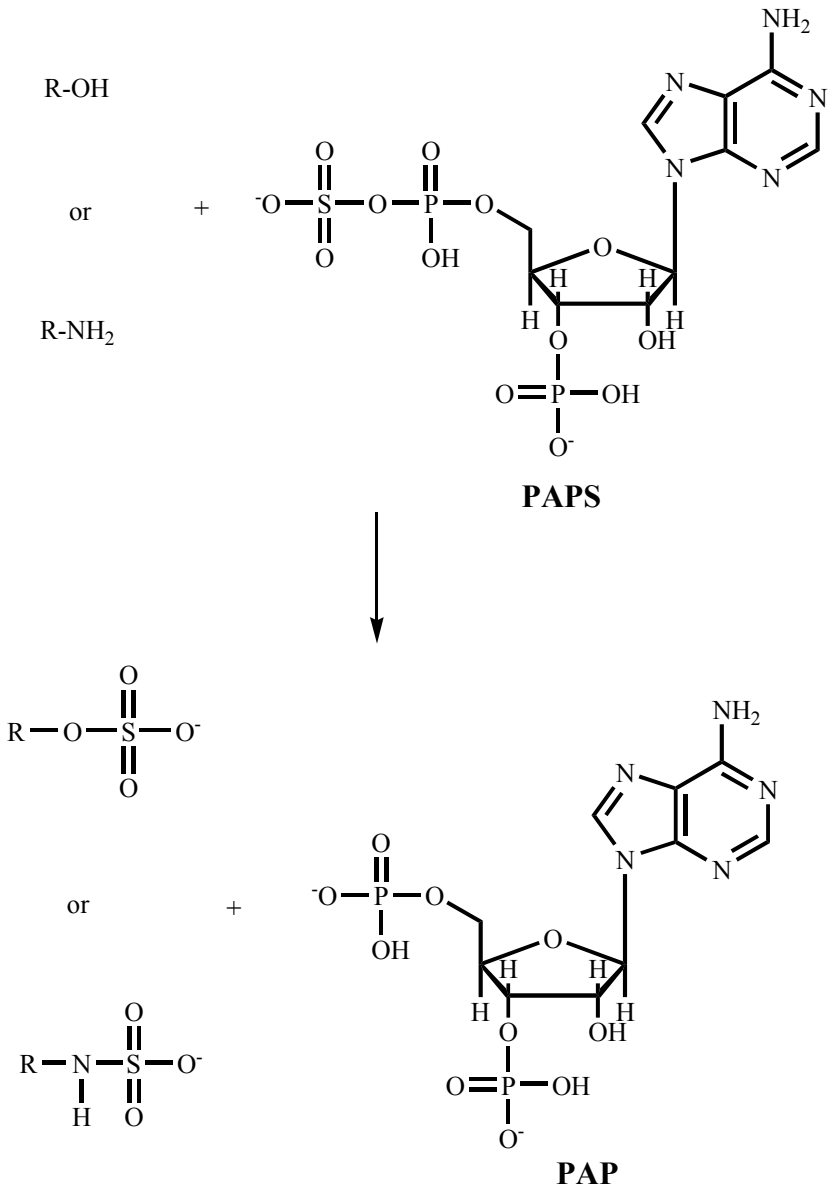

Note: The surfuryl acceptor is represented by R-OH (for phenols, alcohols etc.) or R-NH_2 for amines and PAPS is the donor molecule. The products formed are sulfate esters/sulfamates, and PAP

Figure 5. The general chemical reaction catalyzed by sulfotransferase.

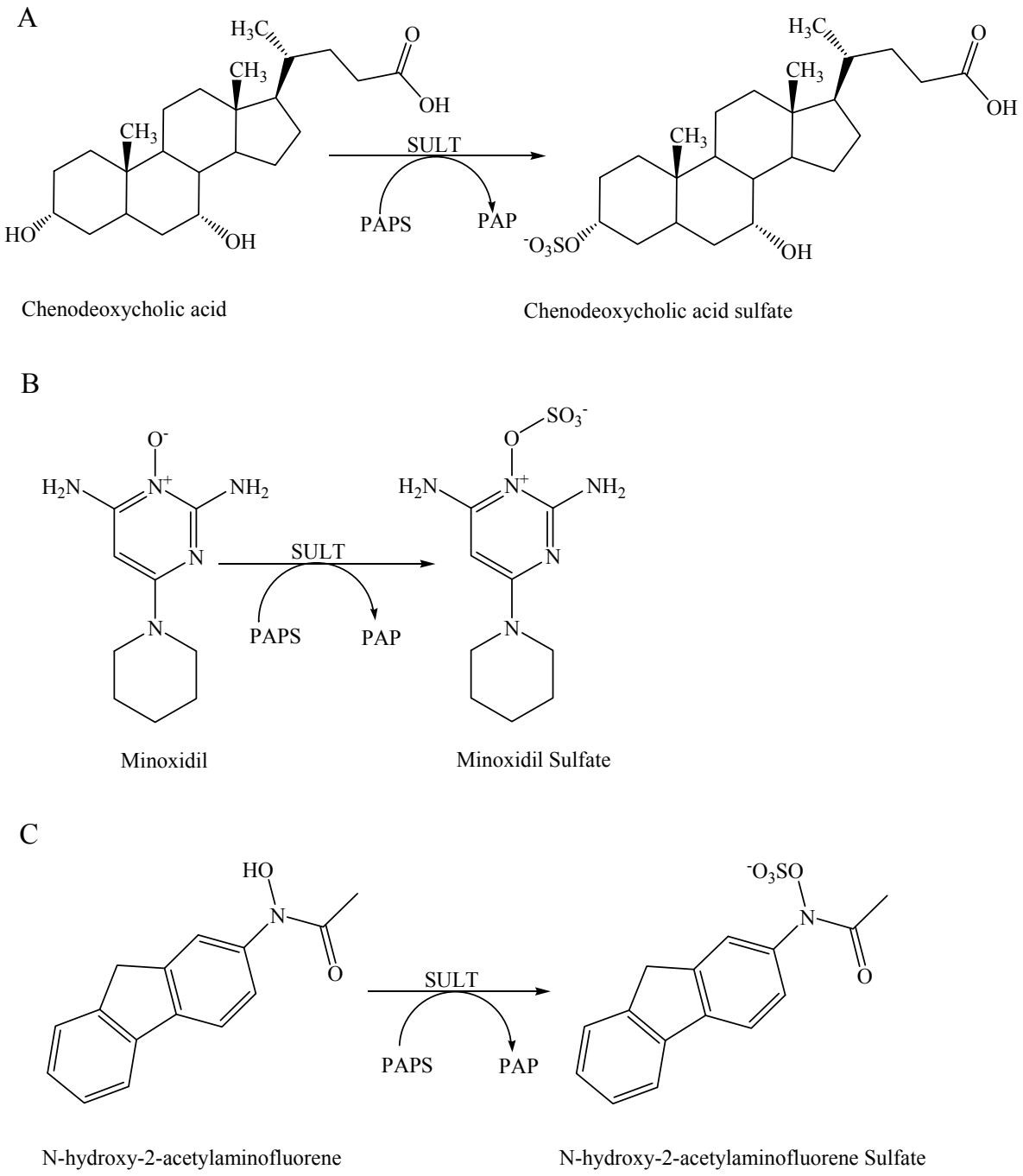

Figure 6. Example of the various forms of sulfation reactions catalyzed by cytosolic sulfotransferases (SULTs) A) Detoxication of the bile acid chenodeoxycolic acid. B) Activation of minoxidil in order to obtain desired pharmacological effect. C) Bioactivation of N-hydroxy-2-acetylaminofluorene to a reactive product that can bind to nucleophilic sites in DNA.

Detoxication

Sulfation reactions often render toxic compounds inactive and facilitate their elimination. Depending upon their chemical structure, the toxic compounds may be first converted into metabolites that can then be sulfated and become more highly soluble in water, thereby increasing their excretion in urine and bile. In other cases, sulfation may occur without additional preliminary metabolism. Detoxication of bile acids is carried out by sulfation. Secondary bile acids are made from primary bile acids, and while primary bile acids are synthesized in the liver, secondary bile acids are made in the intestine by bacteria and they can be toxic to some mammals (*116*). However, in humans, sulfation reaction is important in stopping reabsorption of a secondary bile acid known as lithocholic acid from small intestine thereby protecting tissues from the toxic effects observed in animals (*116-117*). Detoxication by sulfation is also important in the regulation of hormones and homeostasis of neurotransmitters. Thyroid hormone is made inactive by sulfation in order for iodine to be reused for thyroid hormone synthesis (*118*). To make thyroid hormone inactive, the phenolic groups on T_4 and triiodothyronine, T_3, have to be sulfated to facilitate hepatic deiodination (*118*). Catecholamines are circulated in humans in their sulfoconjugated forms, whereas, in rats, glucuronidation of catecholamines is predominant (*119*). More than 70 % of the total epinephrine, norepinephrine and dopamine circulate in the sulfoconjugated forms (*119-120*). Catecholamine sulfates have longer half lives than catecholamines and as such, they can serve as markers in blood pressure regulation (*120*).

Many therapeutic drugs such as salbutamol, fenoterol, albuterol and isoproterenol are eliminated from the body following metabolism that includes sulfation (*121-124*). Furthermore, sulfation in neonates often predominates, as other conjugating enzymes (such as UDP-glucuronosyl transferases) are not highly expressed. The elimination of many drugs or harmful substances from the human fetus and regulation of the activities of several hormones are therefore carried out through reactions catalyzed by

sulfotransferases. While elimination of therapeutic doses of acetaminophen is primarily by glucuronidation in adults, it is predominantly by sulfation in neonates and children (*125*). Also, sulfation of T_3 to its sulfate form, T_3-sulfate (whose concentration increases with fetal age) makes it possible for T_3 to be circulated in the fetus (*126*).

Bioactivation

Many xenobiotics are first metabolized by cytochrome P450 monooxygenase to their hydroxylated forms, followed by the action of conjugating enzymes such as sulfotransferases prior to their elimination. Some sulfate esters are however, not stable and reactive intermediates can be formed that can bind to DNA resulting in mutation or cancer (*106*). The reason this happens is because the sulfate group is an electron-withdrawing group that can easily be cleaved off to leave an electrophilic cation (Figure 7). The electrophilic cation can then react with nucleophilic sites on DNA to form adducts. Sulfotransferases have therefore been implicated in the activation of several classes of compounds (e.g. alkyl-substituted polycyclic aromatic hydrocarbons, aromatic hydroxylamines, benzylic and allylic alcohols, and aryl hydroxamic acids) to their genotoxic forms. For example, the α-hydroxylated metabolite of tamoxifen and *N*-hydroxy-2-acetylaminofluorene (*N*-OH-2AAF), when activated by sulfation, become more toxic and form DNA and/or protein adducts (*127-128*) as illustrated in Figure 8. Furthermore, cyproterone acetate (a synthetic steroidal hormone widely used for acne and prostate cancer) has also been shown to be hepatocarcinogenic in rats as well as in humans upon undergoing sulfation reaction (*129*). Various forms of cancer (*130-131*) and other disease states such as entry of HIV have also been linked to sulfation reactions (*132*). HIV entry has been associated with sulfation of tyrosyl residues present on the chemokine receptor CCR5 which allows HIV gb120 to bind and facilitates viral delivery (*132*).

Although bioactivation of some compounds by sulfotransferase leads to the

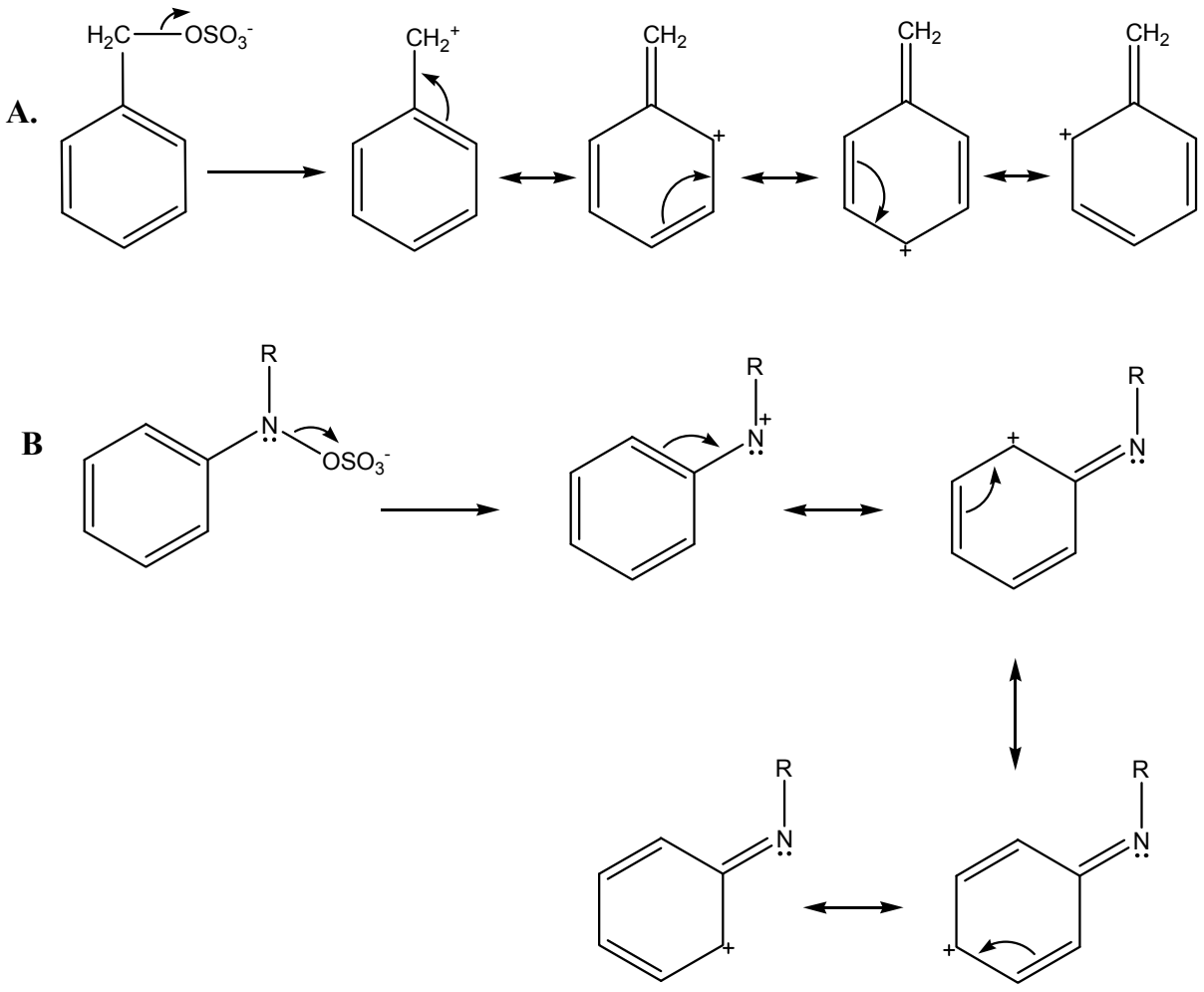

Figure 7. Resonance stabilization of cations formed heterolytically from sulfuric acid esters of benzylic alcohols (A) and aromatic hydroxylamines (B). Adapted from (*133*) with slight modification.

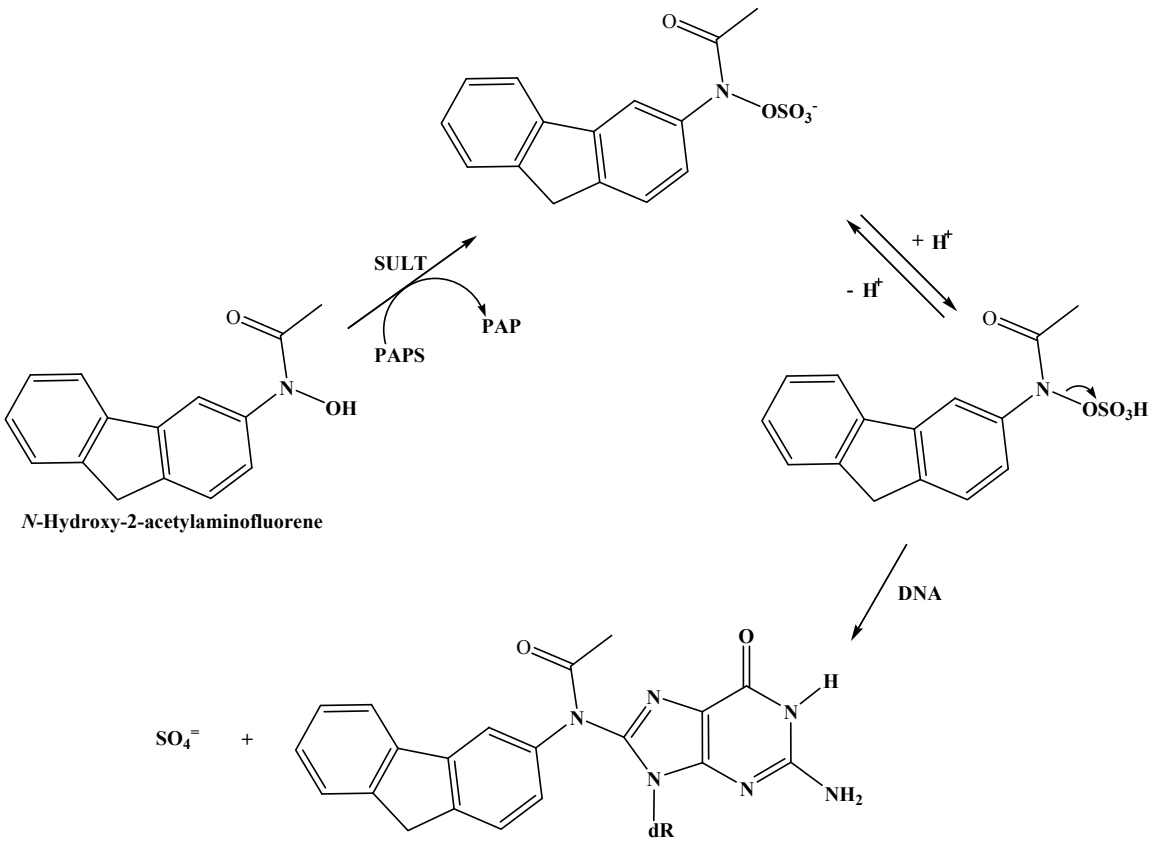

Figure 8. Activation of N-hydroxy-2-acetylaminofluorene by sulfotransferase. Adapted from (*134*) with modification

formation of toxic reactive metabolites, sulfation reactions are, however, essential for the activation of some drugs to obtain their pharmacological activity. For example, minoxidil (Figure 6) has to be activated through a sulfation reaction in order to obtain the desired hypotensive effects, vascular effects (vasodilation) and hair growth-stimulating effects of the drug (*135-137*). Minoxidil ester, unlike most sulfate esters possesses an inner salt (*138*), and this makes it more hydrophobic than its parent compound and less readily excreted in urine or bile (*139*). In addition, specific sulfate esters of triamterene, morphine, and cicletanine have been shown to have enhanced biological activity relative to their parent compounds (*140-142*).

Classification of sulfotransferases

Sulfotransferases can be broadly classified into membrane-bound sulfotransferases and cytosolic sulfotransferases (SULTs) (*105-106*). Membrane-bound sulfotransferase are found in the Golgi apparatus of most cells and can catalyze sulfation of macromolecules such as carbohydrates, glycosaminoglycans, and proteins, but not the sulfation of small exogenous molecules such as drugs or other xenobiotics (*106*).

The cytosolic or soluble SULTs (*143*), the focus of this dissertation, are, however, expressed in the liver, kidney, adrenals, platelets, brain, skin, lung, and gut (*105*), and they are involved in the sulfation of both endogenous compounds (e.g. catecholamine, steroids, bile acids, thyroid hormones) and exogenous compounds (e.g. drugs, carcinogens and other xenobiotics) (*110, 112, 144*). There are at least 14 cytosolic SULTs in humans and they are divided into four families, the phenol SULTs (SULT1), the hydroxysteroid SULTs (SULT2), SULT4, and SULT6 (*145*). SULT1A1, SULT1A2, SULT1A3, SULT1A4, SULT1B1, SULT1C1, SULT1C2, SULT1C3, and SULT1E1 are all members of the SULT1 family; SULT 2A1, SULT2B1a and SULT2B1b belong to the SULT2 family; SULT4A and SULT6 only have one member each, SULT4A1 and SULT6B1 respectively (*145*). SULT4A1, which has been identified in the brain (*146*), and SULT6B1, expressed in the testis (*147*), have not been fully characterized for their substrate specificities. The family1 SULTs have often been characterized as mainly catalyzing sulfation of phenols, thyroid hormones, catecholamines, and estradiol; family 2 SULTs have usually been described as sulfotransferases mainly responsible for the sulfation of hydroxysteroids and hydrophobic alcohols. However, there is considerable cross-reactivity of substrate classes for these two families, where more subtle features than simple functional groups define specificity of the SULTs (*145*).

Nomenclature of cytosolic sulfotransferase

The nomenclature of sulfotransferases is still evolving. With more sulfotransferases found, it became more confusing to name the different isoforms of the enzymes. Therefore the nomenclature of these enzymes became very inconsistent. Isoforms were initially named according to the substrates they sulfated (e.g. phenol sulfotransferases, bile acid sulfotransferases and hydroxysteroid sulfotransferases). For example, SULT2A1 catalyzes sulfation of DHEA and has often been referred to as DHEA-sulfotransferase, and SULT1E1 catalyzes the sulfation of estrogen and was referred to as estrogen sulfotransferase. However, these enzymes possess the ability to catalyze the sulfation of a wide variety of molecules with overlapping substrate specificity, and this compounded the problem of naming these enzymes. Nagata and Yamazoe developed a system whereby the prefix ST preceded the cytotolic families (*148*). In this system the gene families were divided into subfamilies based on sequence similarity and substrate specificity (*148*). However, naming these enzymes based on the Yamazoe and Nagata system was not widely accepted, primarily due to conflicts with the nomenclature system adopted for human genome.

More recently however, a systematic nomenclature was developed that is now more widely used in the scientific community (*149*). Sixty five complementary DNAs and eighteen genes of sulfotransferases previously obtained have this nomenclature system applied to them (*149*). The SULTs were named based on their amino acid sequence. Those SULTs with at least 45% amino acid sequence identity are assigned to the same gene family, those with at least 60% sequence identity are in the same subfamily, and those with at least 97% identity are designated as the same isoform (*149*). In this system, the species name serves as a prefix to the protein designated as SULT followed by the family represented as an Arabic numeral with a subfamily in capital letter. The isoform in the subfamily is also shown, and it is based on the order of that

protein's sequence. For example (HUMAN) SULT2A1 or hSULT2A1 is a human cytosolic sulfotransferase of family 2, subfamily A and isoform 1.

Structures of sulfotransferases

In terms of structures, all sulfotransferases have an α/β domain that is made up of five-stranded parallel β-sheet that is involved in the binding site of the coenzyme (i.e. PAPS) as well as the active site (*103, 150*). Cytosolic SULTs are usually homodimers in their active catalytic forms, with mouse estrogen SULT (*151*) and rat aryl SULT (*152*) being the exceptions. The first x-ray crystal structure of a SULT ever solved was that of mouse estrogen sulfotransferase (mEST): mEST was cocrystallized with PAP followed by soaking the crystals with estradiol (*153*). Important three dimensional features were obtained from this x-ray crystal structure for both the coenzyme and substrate binding sites (*153*). Subsequently, x-ray crystal structures were solved for the human family 1 sulfotransferases, and the human estrogen sulfotransferases, hSULT1E1, in complex with PAPS was the first structure solved that contained the active sulfuryl donor (*154*). Important information about sulfotransferases mechanism of S_N2-like inline displacement reaction that involves a highly conserved histidine residue was obtained (*154*). The authors also concluded that the involvement of two residues, Lys47 and Ser137, may contribute to the hydrolysis of PAPS when substrates are not present (*154*). The human dopamine/catecholamine sulfotransferase, hSULT1A3, in complex with SO_4^{2-} and PAP (*155*) showed that two other residues, Glu146 and Asp 86 are also important in the function of hSULT1A3. There is an electrostatic bond formation seen between Glu146 and dopamine, this may be important in the activity and selectively of hSULT1A3 while Asp86 may explain the activity of hSULT1A3 on dopamine and tyrosine by interacting with manganese having an oxidation state of +2 (*155*). The first crystal structure solved that contained a foreign compound (p-nitrophenol) and PAP was that of hSULT1A1 (*156*). The x-ray crystal structure showed that two molecules of p-nitrophenol can bind

at the catalytic site of the enzyme, and it gave insights into how this enzyme can modify its structure to allow various compounds with different shapes and sizes to bind in order to catalyze their sulfation (*156*). It also provided an hypothesis for how substrate inhibition results with some substrates (*156*). A crystal structure of hSULT1E1 in the presence of PAP and a OHPCB, 4,4'-dihydroxyl-3,3',5',5' tetrachlorinated biphenyl, showed that the OHPCB binds in a non-coplanar manner similar to the way 17-beta-estradiol binds at the active site of the enzyme (*157*). Thus this gives structural evidence for how certain OHPCBs have been proposed to serve as endocrine disruptors, through inhibition of this sulfotransferase *(85, 142).*

For the family 2 enzymes, three crystal structures of hSULT2A1 have been solved: SULT2A1 in complex with PAP (*150*), SULT2A1 in complex with DHEA (*158*) and SULT2A1 in complex with androsterone (*100*). Rehse *et al*., 2002, showed that DHEA can bind in two different modes with the first binding mode reflecting the catalytic site and the second binding reflecting the substrate inhibition site (*158*). In the androsterone-bound structure, the authors showed that androsterone (ADT) binds more tightly to SULT2A1 than DHEA, and ADT serves as cognate substrate for the enzyme (*100*). The crystal structure for cholesterol sulfotransferase, hSULT2B1b in complex with pregnenolone and PAP has also been solved (*159*). It provided an explanation of the preference of the different substrates seen with the two isoforms of the family 2 sulfotransferases.

The information that can be deduced from the structures as seen in Figure 9 is that the overall 3-dimensional structures of cytosolic sulfotransferases are similar; however there are some notable differences as well. The important residues at the PAPS binding site are conserved in all the cytosolic sulfotransferases (*150*). At the PAPS site, serine and lysine are important residues for the binding of PAPS and activation of the sulfuryl group (*160*). In addition, a histidine residue that is conserved in all SULTs is involved in the sulfuryl transfer (*160*). There are differences in the sulfuryl acceptor binding sites and

A) hSULT1E1:PAPS

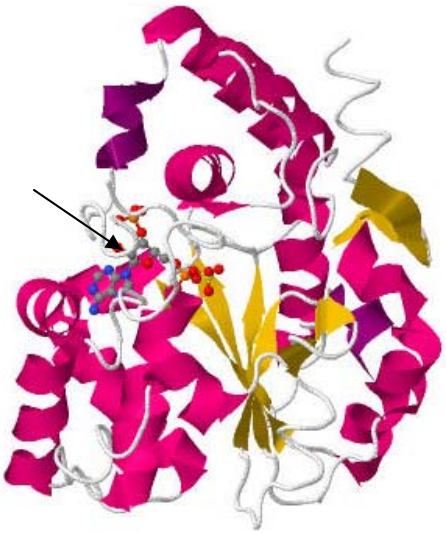

B) hSULT2A1:PAP

C) hSULT2B1b:Pregnenolone:PAP

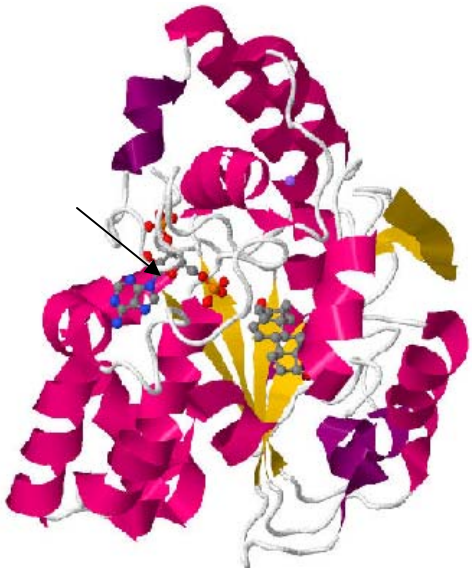

D) hSULT1A1:PNP:PAP

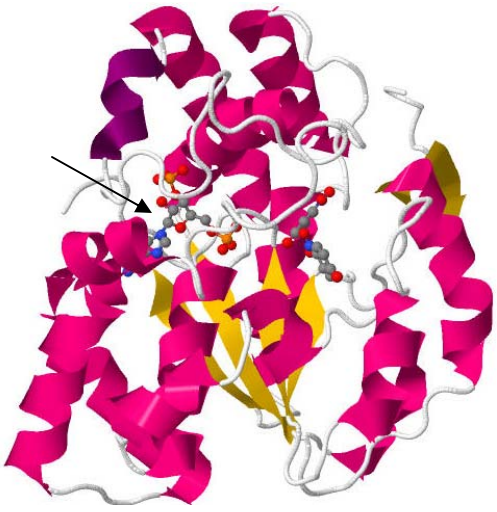

Figure 9. Crystal structures of A) human estrogen sulfotransferase, hSULT1E1 B) human hydroxysteroid sulfotransferase, hSULT2A1 C) human cholesterol sulfotransferase, hSULT2B1b D) human phenol sulfotransferase, hSULT1A1. The PAP/PAPS binding site is similar, however, there are differences at the substrate binding site that allow for substrate specificity among the different isoforms represented. Arrow in each structure indicates the PAP/PAPS binding site. Adapted from refs (*150, 154, 156, 159*).

they are important in determining substrate specificities of individual SULTs. For example, in hSULT2A1 and hSULT1E1, there are some differences in the way Pro14-Ser20, Glu79-Ile82 and Tyr234-Gln244 loops are oriented (*150*). This observation does not come as a surprise as different sulfotransferases have a lot of substrates that they act on (*160-161*).

Human hydroxysteroid sulfotransferase hSULT2A1

Human hydroxysteroid sulfotransferase hSULT2A1, also known as DHEA-ST, is the major family 2 SULT in humans, and it plays an important role in the sulfation of steroids, bile acids and xenobiotics (*162*). It is a homodimer composed of two identical subunits (*163*) with each subunit having a mass of approximately 34kDa (*158*). hSULT2A1 is expressed in the reticular layer of the adrenal, liver and small intestine (*164*). In addition, Javitt *et al*., 2001 discovered with the use of real time polymerase chain reaction (RT-PCR), that SULT2A1 is not only expressed in the adrenal, small intestine and liver but also in the ovary, prostate, stomach and colon (*165*). Immunochemical analysis also showed that SULT2A1 is expressed in the kidney, the liver of the human fetus, and the fetal adrenal (*166*). SULT2A1 is involved in the biosynthesis and secretion of DHEA-sulfate in the adrenal (*167*). In the liver, it catalyzes the sulfation of therapeutic drugs, bile acids and xenobiotics (*168*), and it is the only family 2 SULT isoform identified in the liver (*163*).

Specificity of hSULT2A1

Human hydroxysteroid sulfotransferase (hSULT2A1) plays a vital role in the sulfation of cytotoxic bile acids in the liver, because reduced levels of hSULT2A1 in the liver have been linked to chronic liver disease (*169*). Work by Kitada *et al*., 2003, showed that hSULT2A1 protects liver from the toxicity that can be caused by lithocholic acid (LCA) by converting LCA to its sulfate (*170*). SULT2A1 is also involved in the sulfoconjugation of 3α- and 3β- hydroxysteroids, the phenolic hydroxyl of some

estrogens, the 17-hydroxyl of testosterone (*163*) and therapeutic compounds such as budesonide (*171*) and tibolone (*172*). In addition, pentachlorophenols, once seen as phenol sulfotransferases inhibitors have been shown to be substrates for hSULT2A1 (*173*). hSULT2A1 is therefore an enzyme with broad substrate specificity (*163, 168*).

SULT2A1 and steroid metabolism

Sulfation is important in the metabolism of steroids. Steroid sulfation leads to a loss of biological activity of the steroids. In addition, steroid sulfates are the form in which steroids are stored and transported within the body. Pregnenolone (PREG) and dehydroepiandrosterone (DHEA) are representative steroids that are sulfated in reactions catalyzed by SULT2A1.

Pregnenolone (PREG) is important in the human fetus because it is the precursor for the biosynthesis of DHEA. PREG is first conjugated to its sulfate ester by SULT2A1 (*38*). Metabolism of Pregnenolone sulfate leads to formation of 17α-hydroxypregnenolone sulfate and further metabolism on the latter by desmolase results in formation of DHEA-sulfate (DHEAS) (*174*). DHEAS is also formed directly from the action of hSULT2A1 on DHEA (*143*). DHEA serves as the main precursor for the production of estrogen in the placental during pregnancy (*174*) while DHEAS is involved in the softening of the cervix before parturition (*175*).

Furtheremore, DHEA is a hormone with immunoenhancing, anti-cancer, neurotropic, and anti-aging effects (*176*). DHEA and DHEAS are thought to play protective roles in hypercholesterolemia (*177*), Alzheimer's disease (*178*), cancer (*179*), and cardiovascular diseases (*180-181*).

Inhibition of hSULT2A1 and how it affects steroid metabolism

One theory is that when hSULT2A1 activity is blocked, the cellular DHEA level may increase and there may be an imbalance in synthesis of steroid hormones because

DHEA-sulfate serves as an intermediate in the production of estrogens and androgens. This may then lead to formation of sex hormone-dependent tumors that may result in cancer. There is no clear evidence for this as of yet. However, higher levels of DHEA and reduced levels of DHEA-sulfate in the cerebrospinal fluid have been linked with Alzheimer's disease and Vascular Dementia (*182*). Studies by Tagawa *et al*., 2000, have also shown DHEA-sulfate and pregnenolone-sulfate (PREG-S) to be elevated in patients with hyperthyroidism, while patients with hypothyroidism had reduced levels of DHEA, DHEAS and PREG-S in serum (*183*).

Interaction of compounds with hydroxysteroid sulfotransferase

Many compounds interact with sulfotransferases either as substrates or as inhibitors. Compounds that inhibit sulfotransferase activity could be pure inhibitors, or they could serve as alternate substrates for the enzyme and thus compete for binding at the active site. This inhibition may be as a result of either binding to the PAPS/PAP-site or binding to the substrate-site (*114*).

Xenobiotics or endogenous compounds that serve as substrates for an enzyme can inhibit sulfation of other substrates. For example, hSULT2A1 catalyzes the sulfation of an endogenous steroid, testosterone, and this results in the inhibition of budesonide sulfation (*184*). Some food-derived flavonoids, such as apigenin, myricetin, baicelein, galangrin and 7-hydroxyflavone have been shown to have considerable effects on the sulfation of DHEA catalyzed by hSULT2A1 with K_i values in the sub-micromolar range (*38*). Furthermore, flavonoids such as quercetin, kaempferol, genistein, daidzein were also shown to inhibit DHEA sulfation catalysed by hydroxysteroid sulfotransferase (SULT2A1) that was cloned from rat liver with IC_{50} values in the micromolar range (*185*). Among the inhibitors of SULT2A1, two of the flavonoids, genistein and diadzein, were actually substrates for the enzyme (*185*). Seven natural products, two coumarins and

five xanthones, were evaluated for their inhibitory effect on DHEA sulfation catalyzed by hSULT2A1 and were shown to inhibit hSULT2A1 (*186*). One of the coumarins, Mammea C/OA, however, also served as substrate for hSULT2A1 with a K_m of 3.7μM and a V_{max} of 4.5 nmol/mg/min (*186*). Xenoestrogens (i.e. synthetic estrogen mimics) such has bisphenol A and alkylphenols are chemicals mostly used in detergents and plastics, and they have been shown to inhibit hSULT2A1 activity and reduce the expression of enzymes needed for the synthesis of the coenzyme PAPS (*43*).

When a molecule binds to the active site of an enzyme, competitive inhibition and noncompetitive inhibition are two of the major mechanisms that are possible. Competitive inhibition is a result of an inhibitor binding at the active site of an enzyme, thereby competing with a given substrate for the enzyme active site. Competitive inhibition can also result from allosteric binding of an inhibitor (*187*). Noncompetitive inhibition is defined as binding of an inhibitor at a site either different from or near the active site of an enzyme. However, noncompetitive inhibition patterns can also result from several instances where an inhibitor binds at the catalytic site of an enzyme (*187*).

Noncompetitive binding patterns have been seen with enzymes that make use of an exosite for substrate binding, isomechanism enzymes, enzymes with two-step binding inhibitors and bisubstrate enzymes (*187*). Exosites are regions that differ from the active site of some enzymes, but their physiological substrates bind more avidly to these sites than their catalytic sites (*187*). A good example of such enzymes having these exosites regions to bind their very large substrates are the serine proteases (*187*). Inhibitors can bind at the active site and show a noncompetitive inhibition mechanism, and their binding would not disrupt the binding of their preferred substrates (*187*). Isomechanism enzymes follow many different states in order to complete a catalytic cycle (*188*). During these different states, some compounds can bind and inhibit the enzyme noncompetitively because some steps are not fast enough and are rate limiting (*188*). In this process, it should be noted that the substrate and the compound which inhibits the enzyme both bind

at the catalytic site, however binding occurs at varying times and at such the two compounds do not have to compete for the active site of the enzyme (*187*). As the name implies, with the two-step binding inhibitors mechanism, inhibitors bind in two steps. The inhibitor first exhibits fast kinetics in the way it is bound and released from the enzyme resulting in competition with a preferred substrate (*187*). Then the binding of the inhibitor causes the change in enzyme conformation to slow down, and this stabilizes the enzyme-inhibitor complex (*187*).

Some bisubstrate enzymes go through a process that is mandatory. The substrates first bind, and then products are given off next in a very ordered fashion, and the mechanism of inhibition by inhibitors of these enzymes may be of a noncompetitive type even though the inhibitor is binding at the same site as one of the substrates (*187*). For example, metabolism of cortisone is carried out by 11β-hydroxysteroid dehydrogenase (11β-HSD1) using the cofactor NADPH (*189*). However, the binding of compound C to 11β-HSD1 inhibits cortisone metabolism in a noncompetitive inhibition pattern (*189*). The noncompetitive inhibition pattern is due to binding of compound C to the enzyme-product complex (i.e. 11β-HSD1-NADP complex) which causes a conformational change that does not allow cortisone to bind (*187*). Another example is with zolpolrestat which binds to the active site of human aldose reductase (ALR2) in the presence of the cofactor, NADPH, in a noncompetitive inhibitory binding pattern (*190*). The noncompetitive inhibition observed with zolpolrestat, may be as a result of binding to the ALR2-NADP complex (*187*). The importance of substrate binding to enzyme-product complex and forming a dead end or ternary complex (enzyme-product-substrate complex) in hSULT2A1 (*191*) and in rSULT1A1 (*192*) has been shown as well.

CHAPTER II

STATEMENT OF THE PROBLEM

Sulfation reactions are carried out by enzymes known as sulfotransferases. Sulfotransferases are important in hormone regulation, detoxication of endogenous bile acids as well as xenobiotics, and metabolic activation of xenobiotics leading to chemical carcinogenesis and other toxicities *(105,115,117, 120,132).* One role of sulfotransferases in toxicology relates to environmental pollutants that interfere with the transfer of the sulfuryl moiety to endogenous acceptor molecules such as physiologically important steroids. Dehydroepiandrosterone (DHEA) is one such steroid and it is a precursor to androgens and estrogens (*115*).

Polychlorinated biphenyls (PCBs), which persist as worldwide pollutants and are implicated in a variety of adverse health effects, are metabolized by cytochrome P450s to their hydroxylated forms (OHPCBs) *(4)*. The formation of OHPCBs may sometimes lead to their detoxication, however, these metabolites have been shown to be retained in blood, liver, and adipose tissue (*4, 10*). In addition, they were previously shown to inhibit the activities of three isoforms of the human phenol (family 1) sulfotransferases, hSULT1A1 and hSULT1B1 involved in thyroid hormone sulfation, and hSULT1E1 involved in estrogen sulfation (*94, 97*). However, there is a lack of understanding as to how these compounds interact with the family 2 enzyme, human hydroxysteroid sulfotransferase (hSULT2A1). Work done previously in our laboratory, showed that three OHPCBs do interact with hSULT2A1 (*77*). However, there was a need to extend our studies on the effect of OHPCBs on hSULT2A1 activity. The research presented in this dissertation, aims to provide valuable information on the interactions of the metabolites of semi-volatile PCBs (i.e. those with lower numbers of chlorine atoms) with hSULT2A1.

The hypothesis of this study is that hydroxylated polychlorinated biphenyls are substrates and inhibitors of hSULT2A1 and these interactions can be explained on the

basis of structural features of OHPCBs. The long term goal of this project is to be able to predict the effect of OHPCBs on hSULT2A1 based on structural characteristics. In order to test the hypothesis, the first aim was to examine the ability of OHPCBs to inhibit the sulfation of DHEA catalyzed by hSULT2A1 and to determine those cases where the inhibition was due to the OHPCB serving as an alternate substrate for hSULT2A1 (Figure 10). The OHPCBs, whether as pure inhibitors or alternate substrates, may disrupt

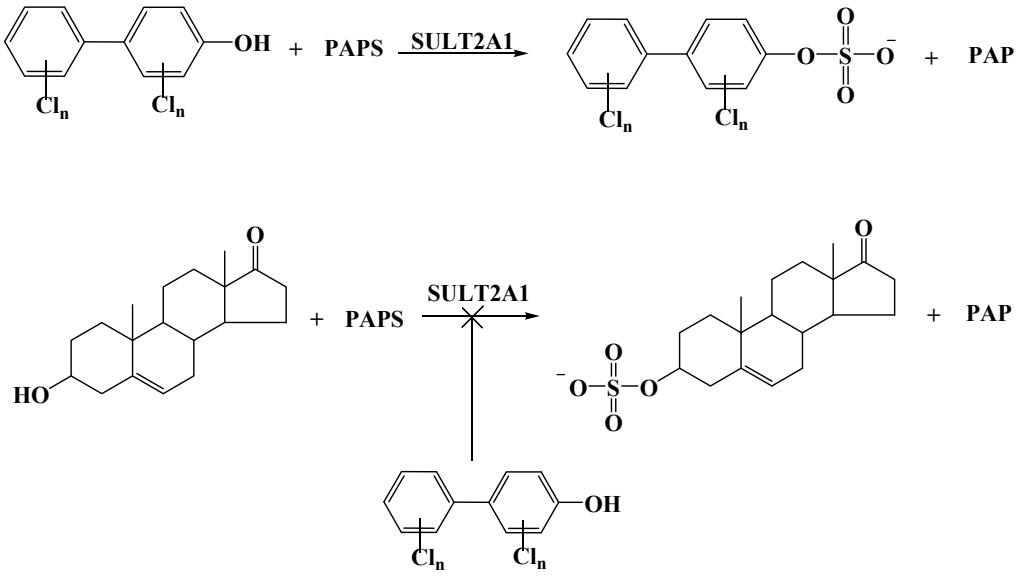

Figure 10. Hydroxylated polychlorinated biphenyls (OHPCBs) as substrates and inhibitors of hSULT2A1

the cellular balance of sulfation and desulfation of DHEA. This is also important as it suggests the ability for these compounds to inhibit the sulfation of other endogenous steroids that are substrates for hSULT2A1 (e.g., pregnenolone and androsterone), thereby causing endocrine disruption. In addition, sulfation of other xenobiotics or drugs may be

altered as these compounds bind to the active site of hSULT2A1. Moreover, sulfation of OHPCBs might also serve as a potential route of elimination of these compounds from the body, although this remains to be determined. The second aim was to study the quantitative structure-activity relationships for OHPCBs as inhibitors of DHEA-sulfation catalyzed by hSULT2A1. This will aid in predicting the actions of other similar OHPCBs on hSULT2A1, since there is a large number of OHPCBs, and it would not be feasible to experimentally test them all. The third aim was to determine the mechanism of inhibition of hSULT2A1 by OHPCBs and to study the binding affinities of OHPCBs with purified hSULT2A1. The rationale for determining the mechanism of inhibition, and dissociation constants is to use the information in connection with results on molecular modeling to learn more about the specific interaction of OHPCBs with the active site of hSULT2A1. An additional component of this aim was to utilize known crystal structures of hSULT2A1 and molecular modeling of substrate and inhibitor interactions with hSULT2A1 to further understand how OHPCBs bind to the enzyme.

CHAPTER III

RESULTS AND DISCUSSION

Inhibitory effects of OHPCBs on the sulfation of DHEA catalyzed by hSULT2A1

A total of 15 hydroxylated polychlorinated biphenyls were examined for their ability to inhibit sulfation of DHEA catalyzed by hSULT2A1 (Figure 11). The analysis was done using a radiochemical assay with purified recombinant hSULT2A1. The sigmoidal curves (Figure 12) were derived by plotting the reaction rate as a percentage of the control rate for DHEA sulfation versus the log of the concentration of OHPCB. A complete dose-dependent inhibition was observed with all of the OHPCBs. A range of concentrations was used depending on the solubility limit for a given OHPCB. The IC_{50} values obtained from the sigmoidal curves are listed in Table 1. There was a greater than 100-fold range in inhibitory ability for the OHPCBs seen in Table 1. 4-OHPCB 34 and 4-OHPCB 68 were the most potent inhibitors of DHEA sulfation with IC_{50} values of 0.6 and 0.8 μM respectively. These compounds clearly had the highest inhibition potency for the enzyme of all the other compounds tested. They both possess one chlorine atom ortho to the ring junction and have a 3, 5-dichloro substitution on the phenolic ring. The OHPCBs with higher inhibition potency possess either one ortho chlorine atom (4'-OHPCB 33 and 4'-OHPCB 25) or a meta chlorine atom with two chlorine atoms flanking the hydroxy group (4-OHPCB 36). Dichlorinated OHPCBs (4'-OHPCB 6, 4-OHPCB 8, 4'-OHPCB 9, 4-OHPCB 11, 4'-OHPCB 12, and 4-OHPCB 14) have high inhibition potency, with IC_{50} values ranging from 8μM to 16μM. However, those with ortho chlorine substitutions (4'-OHPCB 9, 4'-OHPCB 6 and 4-OHPCB 8) are the best among this group, with 4'OHPCB 9 having an IC_{50} value of 8 μM and 4'-OHPCB 6 and 4-OHPCB 8 both having an IC_{50} value of 10 μM. Ortho substitution seemed to be important for inhibition as 4'-OHPCB 3 is a 3-fold weaker inhibitor than 4-OHPCB 8, and the difference between these two compounds is the ortho chlorine present in the latter.

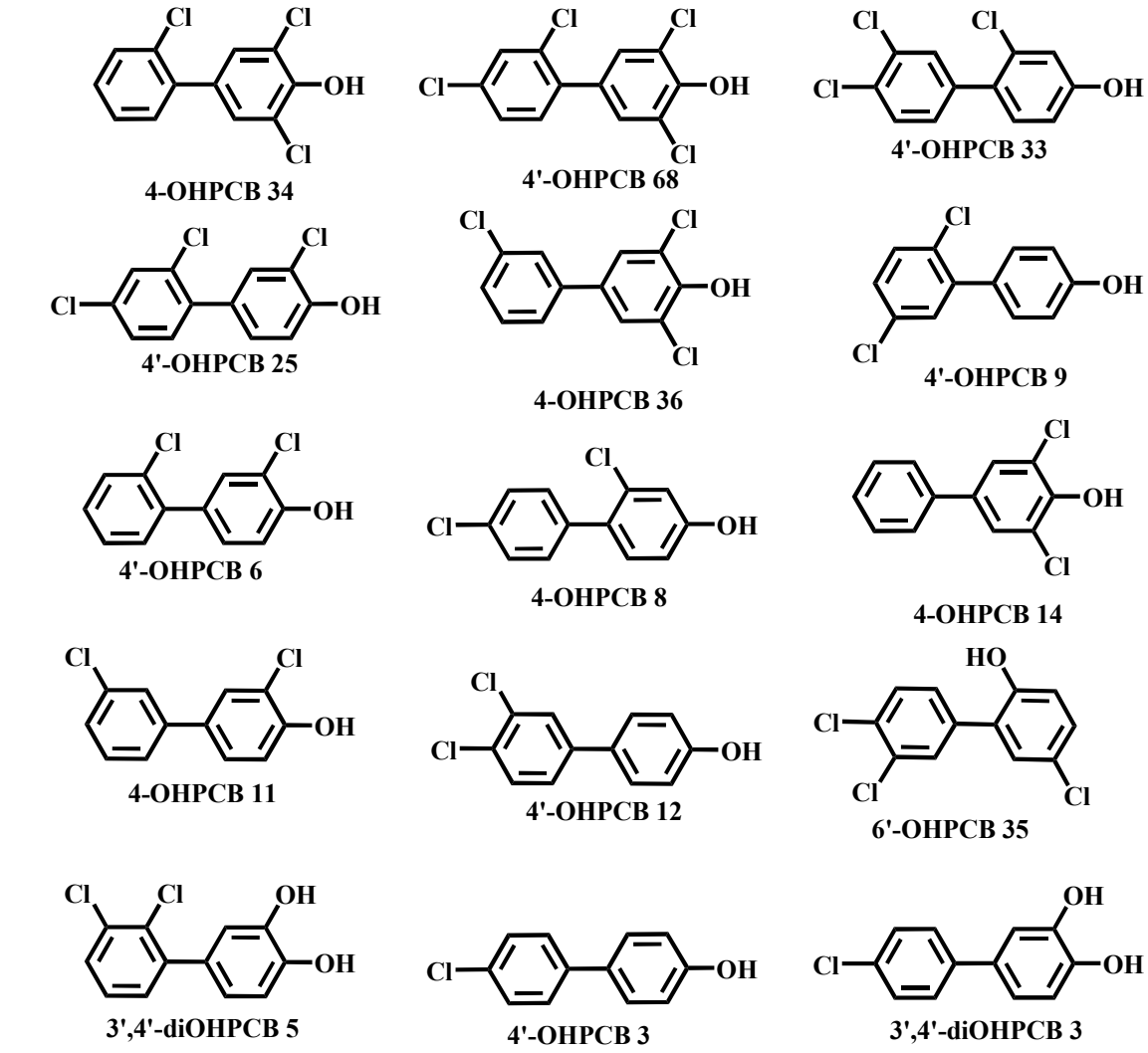

Figure 11. Structures of OHPCBs used in this study. The full name of each compound is given in the methods section.

A.

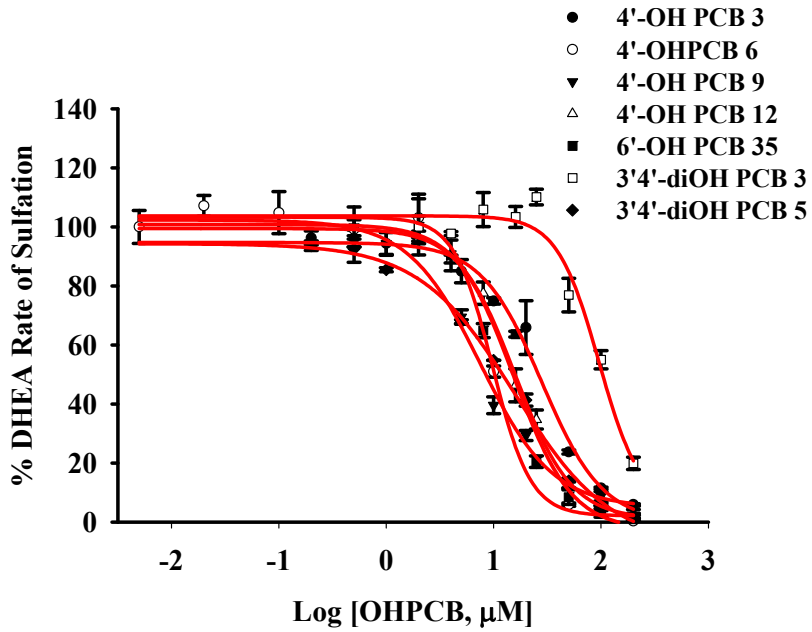

B.

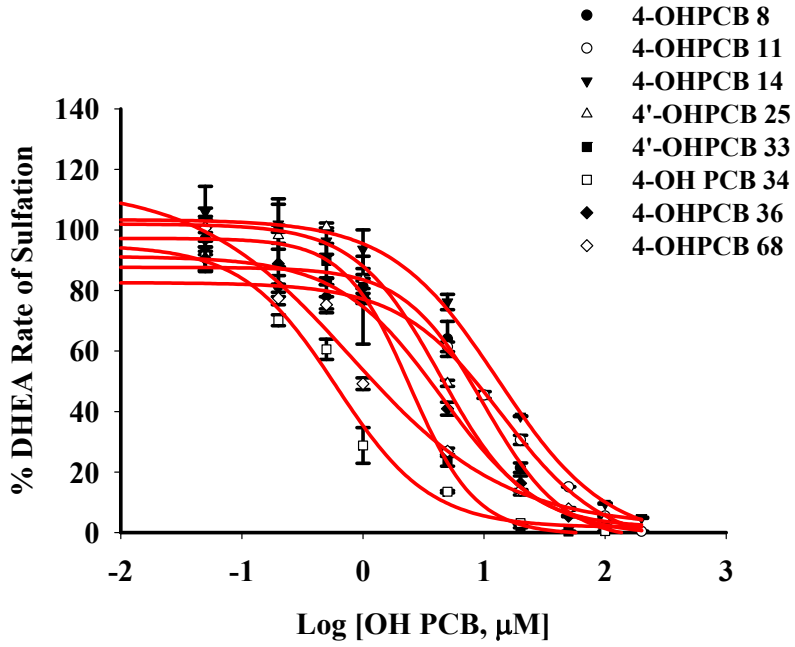

Figure 12. Inhibitory effects of OHPCBs on the sulfation of DHEA catalyzed by hSULT2A1. Radiochemical assays using 1µM ^{3}[H]DHEA were carried out at pH 7.0 with variable concentrations of OHPCBs as described in Methods. (A) Those OHPCBs that were solely inhibitors and (B) Those OHPCBs that inhibited the sulfation of DHEA, but also served as alternate substrates. Data points are the means ± standard error of triplicate determination.

Table 1. Inhibition of human SULT2A1 activity by hydroxylated PCBs (OHPCBs)[a]

Compound	IC_{50} (μM)
4-hydroxy-2',3,5-trichlorobiphenyl (4-OHPCB 34)	0.6 ± 1.2[b]
4'-hydroxy-2,3',4,5'-tetrachlorobiphenyl (4'-OHPCB 68)	0.8 ± 1.3[b]
4'-hydroxy-2'3,4-trichlorobiphenyl (4'-OHPCB 33)	2.5 ± 1.1
4'-hydroxy-2,3',4-trichlorobiphenyl (4'-OHPCB 25)	4.4 ± 1.3
4-hydroxy-3,3'5'-trichlorobiphenyl (4-OHPCB 36)	4.4 ± 1.2
4'-hydroxy-2,5-dichlorobiphenyl (4'-OHPCB 9)	7.5 ± 1.1
4'-hydroxy-2,3'-dichlorobiphenyl (4'-OHPCB 6)	9.8 ± 1.1
4- hydroxy-2,4'-dichlorobiphenyl (4-OHPCB 8)	10 ± 1.2
4-hydroxy-3,5-dichlorobiphenyl (4-OHPCB 14)	13 ± 1.1
4-hydroxy-3,3'-dichlorobiphenyl (4-OHPCB 11)	14 ± 1.2
4'-hydroxy-3,4-dichlorobiphenyl (4'-OHPCB 12)	16 ± 1.1
6'-hydroxy-3,3',4-trichlorobiphenyl (6'-OHPCB 35)	16 ± 1.1
3',4'-dihydroxy-2,3,-dichlorobiphenyl (3',4'-diOHPCB 5)	16 ± 1.1
4'-hydroxy-4-monochlorobiphenyl (4'-OHPCB 3)	28 ± 1.1
3',4'-dihydroxy-4-monochlorobiphenyl (3',4'-diOHPCB 3)	96 ± 1.2

[a] Structures of these compounds are shown in Figure 11. IC_{50} values are the micromolar concentrations of OHPCB resulting in 50 % inhibition of the sulfation of 1μM DHEA catalyzed by hSULT2A1. IC_{50} values are expressed as the means and standard error of triplicate determinations.

[b]Standard errors are higher than the IC_{50} values. This may be due to the fact that they are substrates and upon binding, result in structural changes. It may also be due to the fit of the data.

In addition, an ortho or a meta substitution increased binding affinity for those compounds having a 3, 5-dichloro-4-hydroxy substitution. Those with an ortho chlorine substitution (4-OHPCB 34 and 4'-OHPCB 68) were the most potent inhibitors, and these were followed by 4-OHPCB 36 with meta chlorine substitution and then 4-OHPCB 14 with no ortho or meta chlorine substitution. A meta chlorine substitution may be more effective than a meta hydroxy substitution (compare 4'-OHPCB 12 and 3', 4'-diOHPCB 3) for interaction with the enzyme. Furthermore, a meta chlorine substitution is important in increasing affinity, as seen by comparing 4'-OHPCB 33 and 4-OHPCB 8, and by examining 4-OHPCB 36 and 4-OHPCB 14. 6'-OHPCB 35 and 3'4'-diOHPCB 5 both possess an IC_{50} value of 16 μM. Thus, the ortho-OH substitution in 6'-OHPCB 35 does not seem to increase inhibition potency. These data have given us important new insights on structural requirements of OHPCBs for the inhibition of SULT2A1 activity.

Sulfation of OHPCBs catalyzed by hSULT2A1

Since substrate-binding to the active site of hSULT2A1 could serve to inhibit the sulfation of DHEA, it was necessary to determine which OHPCBs were substrates for the enzyme. Of the 15 OHPCBs that were inhibitors of hSULT2A1-catalyzed sulfation of DHEA, eight were substrates. The effect of increasing OHPCB concentration on the activity of purified recombinant hSULT2A1 was then investigated using a range of concentrations of OHPCBs (depending upon solubility limit of each individual OHPCB) and a saturating concentration of PAPS (200 μM). As seen in Figure 13, as the substrate OHPCB concentration increased, there was an increase in the rate of sulfation until it reached a maximum, and then the velocity began to decrease at higher concentrations of substrate. This decrease in rate of sulfation is known as substrate inhibition. Substrate inhibition is typical with many sulfotransferases, and it is usually a result of the formation of a dead-end complex (i.e. an Enzyme-PAP-Substrate complex) (*191*). The kinetics of sulfation were fitted to a substrate inhibition equation $v = V_{max}/(1+ (K_m/[S])+[S]/K_{is})$

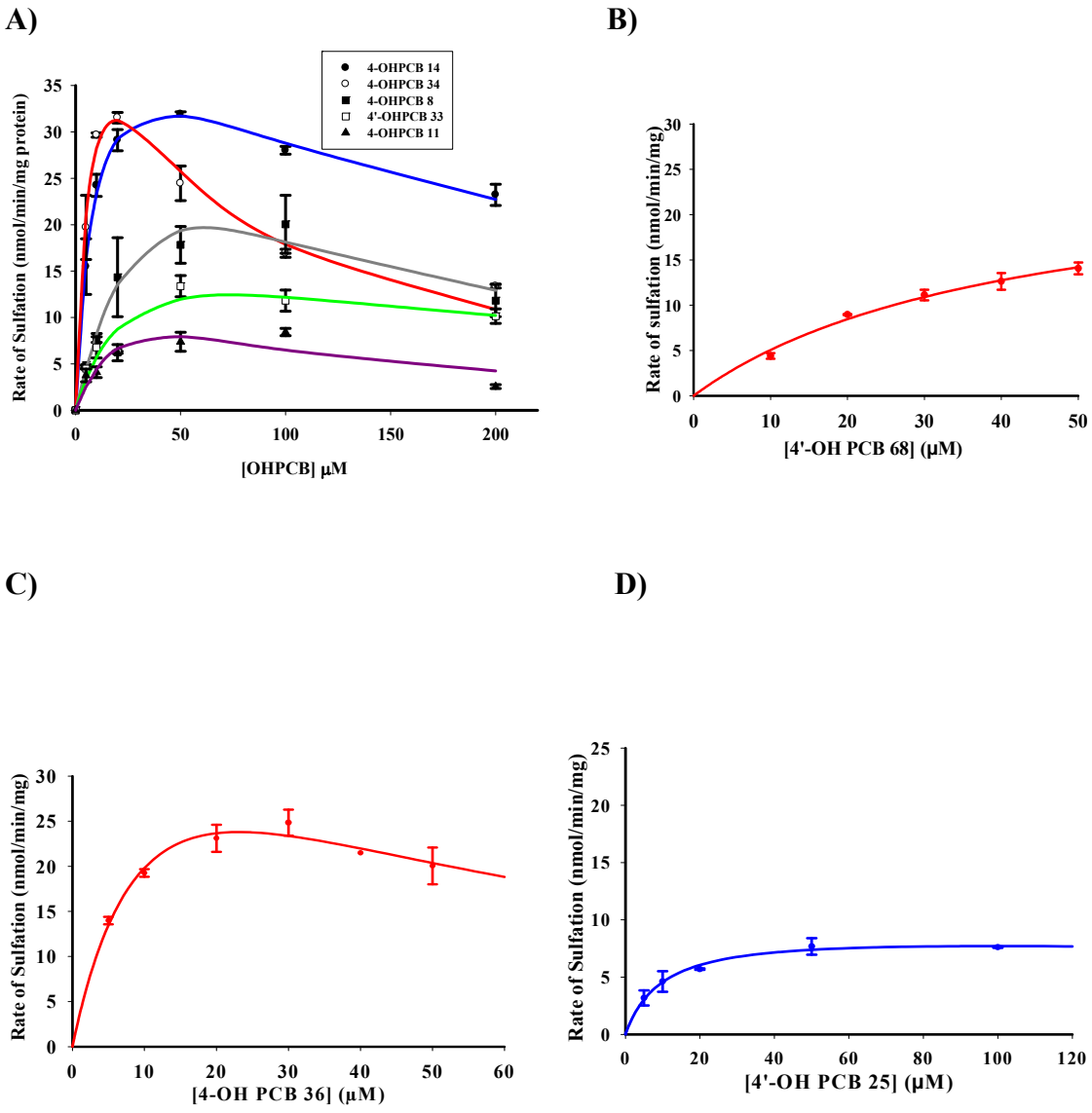

Figure 13. The ability of purified recombinant hSULT2A1 to catalyze sulfation of OHPCBs was investigated with HPLC assay for substrate-dependent formation of PAP. Assays were conducted at pH 7.0 with a saturating concentration of PAPS (200 µM) as described in the chapter on methods. Panel A, corresponds to sulfation of 4-OHPCB 14, 4-OHPCB 34, 4-OHPCB 8, 4'-OHPCB 33, and 4-OHPCB 11. Panels B, C, D correspond to sulfation of 4'-OHPCB 68, 4-OHPCB 36 and 4'-OHPCB 25 respectively. Kinetic data for 4'-OHPCB 68 provided by Y. Liu (*67).*

(Table 2). In Table 2, the V_{max} (i.e. the maximum reaction velocity) values ranged from 8.5 to 57 nmol/min/mg and, among the OHPCBs examined, the V_{max} value was highest for 4- OHPCB 34 and lowest for 4'-OHPCB 25. The K_m (i.e. the concentration of substrate at half maximal velocity) ranged from 8.1 μM to 57 μM with 4-OHPCB 34 having the lowest K_m value. The substrate inhibition constant, K_{is}, ranged from 39 to 220 μM. Substrate inhibition was most prevalent with increasing concentration of 4-OHPCB 34 and 4-OHPCB 36. Three OHPCBs with a 3, 5-dichloro- 4-hydroxy substitution pattern (4-OHPCB 34, 4-OHPCB 36, and 4-OHPCB 14) showed the highest catalytic efficiency (K_{cat}/K_m) with the enzyme and these values reached approximately ten times those of the OHPCBs without the 3, 5-dichloro-4-hydroxy substitution pattern (i.e. 4-OHPCB 8, 4-OHPCB 11, 4'-OHPCB 25, 4'-OHPCB 33).

Table 2. Kinetic parameters for sulfation of OHPCBs catalyzed by hSULT2A1

OHPCB	V_{max} (nmol/min/mg)	K_m (μM)	K_{is} (μM)	k_{cat}/K_m ($min^{-1}mM^{-1}$)
4-OHPCB 14	44.3 ± 3.9	8.5 ± 1.8	220 ± 56	176
4-OHPCB 34	57.1 ± 11.4	8.1 ± 3.2	47.4 ± 16.2	238
4-OHPCB 36	51.8 ± 16.3	13.6 ± 6.7	39.4 ± 23.1	129
4-OHPCB 8	56.1 ± 42.6	56.8 ± 58.2	65.4 ± 73.8	33
4'-OHPCB 33	21.0 ± 7.4	26.2 ± 16.2	217 ± 189	27
4'-OHPCB 25[a]	8.5 ± 0.5	8.6 ± 2.0	-	33
4-OHPCB 11	21.4 ± 18.3	36.6 ± 43.9	51.9 ± 65.7	20

[a] While 4'-OHPCB 25 and 4'-OHPCB 68 (not shown) were substrates for hSULT2A1, reliable kinetic constants for K_{is} (both OHPCBs) and for K_m and V_{max} (4'-OHPCB 68) were not obtained due to low solubilities. Values of K_m and V_{max} for 4'-OHPCB 25 were estimated using the Michaelis-Menten equation. Note: k_{cat}/K_m values are based on a subunit M_r of 33,785.

Development of three dimensional quantitative structure-activity models (3D-QSAR) for the interaction of OHPCBs with hSULT2A1

Lower polychlorinated biphenyls have been found in urban air, and their hydroxylated metabolites have been shown to interact with hSULT2A1. One goal of this research was to develop a method to predict interactions of these OHPCBs with this enzyme. Although the development of linear models (2D-QSAR) for the use of pKa and log *P* values of OHPCBs in predicting inhibition of DHEA sulfation catalyzed by hSULT2A1 was attempted (Figure 14), no useful correlations were seen between the log IC_{50} and either log *P* or pKa. The r^2 values for linear curve-fitting with both plots were approximately 0.7, and this was not considered to be useful for predictive purposes.

To improve assessment of the ability of these chlorinated OHPCBs to interact with hSULT2A1, a 3D-QSAR based on comparative molecular field analysis (CoMFA) was then developed. The model can help in prescreening other lower chlorinated OHPCBs having similar substitution patterns for their effects on hSULT2A1. The 3D-QSAR model was derived for a set of 15 OHPCBs which were built in SYBYL 8.0 (Tripos, St. Louis Mo, USA), and the IC_{50} values used for 3D-QSAR development are shown in Table 1. The IC_{50} values were converted into pIC_{50} (-log IC_{50} (M)) values for the CoMFA analysis. The IC_{50} values covered a range of 2 orders of magnitude and were evenly distributed over this range. For alignment purposes, seven compounds were used as templates based on a common substructure to get the best alignment for our model. The use of 3'4'-diOHPCB 5 as template gave the highest q^2 (0.742) and r^2 (0.981) values at 7 components (Table 3). Other templates also gave high q^2 values at a high optimum number of components. However, using a high number of components means running the risk of over-fitting the data to noise. In order not to over train the model, the template (4'-OHPCB 68) with lower number of components with a somewhat lower q^2 value, was used for the 3D-QSAR model. The superimposition of all the compounds on the

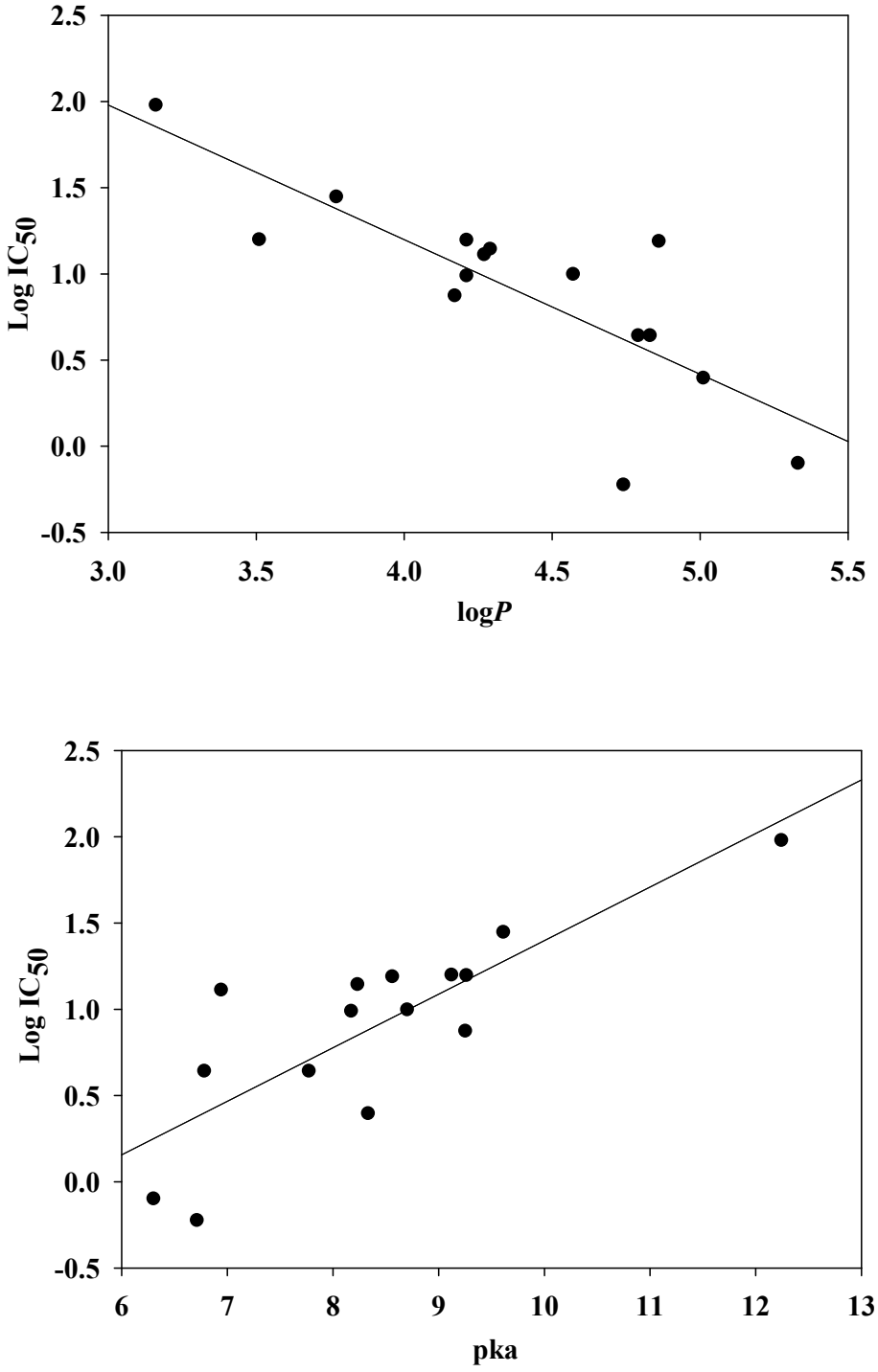

Figure 14. Linear models (2D-QSAR) for the use of log *P* and pKa of OHPCBs in predicting inhibition of DHEA sulfation catalyzed by hSULT2A1. Log *P* and pKa values were calculated at pH 7.0. using the ACD/I-Lab Web service, Advanced Chemistry Development Inc. (Ontario, Canada)

Table 3. Evaluation of each of the seven OHPCBs for use as a template for alignment in CoMFA

Template	Optimum # of components	q^2	r^2	S.E	S.C. (%)	E.C. (%)
4-OHPCB 3	6	-0.156	0.980	0.105	26	74
4'-OHPCB 9	5	0.625	0.975	0.112	19	81
4-OHPCB 12	7	0.260	0.972	0.134	25	75
4'-OHPCB 25	7	0.717	0.980	0.114	36	74
4'-OHPCB 68	5	0.697	0.949	0.159	38	62
3',4'-diOH PCB 3	7	0.715	0.982	0.108	23	77
3',4'-diOH PCB 5	7	0.742	0.981	0.109	21	79

Note: q^2 is the predictive power of the model, r^2 is the fit of the data to the model, S.E is the standard error, S.C. is steric contribution and E.C is the electrostatic contribution.

template molecule 4'- OHPCB 68 is shown in Figure 15. The CoMFA model ultimately derived was statistically significant with a q^2 value of 0.697, an r^2 value of 0.949, and a standard error (S.E.) of 0.159 at 5 components. The steric and electrostatic contributions were 38% and 62%, respectively. The experimental and predicted binding affinities, expressed in pIC_{50} values, are shown in Table 4. The difference between the actual pIC_{50} and predicted pIC_{50} is less than 0.5 (Table 4). 4-OHPCB 34 had the highest inhibitory activity with an experimental value of 6.22 and predicted value of 6.02. There is good correlation between actual pIC_{50} and predicted pIC_{50} without any real outliers as shown in Figure 16. It should be noted that substrates for hSULT2A1 were the most potent inhibitors of the sulfation of DHEA catalyzed by hSULT2A1 (Figure 17)

The q^2 (0.697) derived proves that the model is useful. However, it is ideal to test the external predictive power of the 3D-QSAR model developed. Our training set contained 15 compounds and to get a perfect model, at least 15 compounds are usually

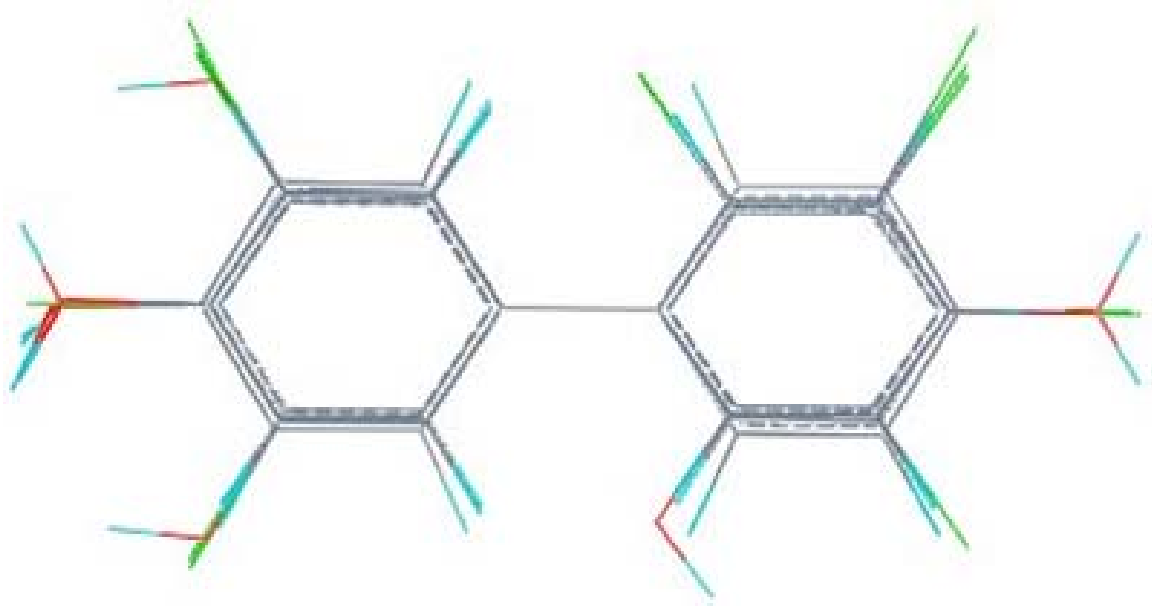

Figure 15. Superimposition of all 15 hydroxylated polychlorinated biphenyls (OHPCBs) with 4'-OHPCB 68 as template molecule using a common substructure-based alignment.

desired. However, a good model can still be derived with slightly fewer compounds. Therefore for external validation purposes 3 compounds (4-OHPCB 14, 4-OHPCB 25 and 4-OHPCB 12) were removed from the training set, and a model was derived using the remaining 12 compounds (i.e. model 2, Figure 18). It should be noted that care was taken not to choose compounds with highest or lowest pIC_{50} in order to maintain 2 orders of magnitude between the lowest and highest value of IC_{50}. The 3 compounds chosen were moderately inhibitory. As observed in Table 5, the prediction of IC_{50} values for 4-OHPCB 12 and 4-OHPCB 25 were in agreement with the experimental IC_{50} values obtained. However, the predicted and actual IC_{50} values for 4-OHPCB 14 were 3.8 fold different. This was, however, only slightly more than the 0.5 log unit criteria that is commonly used to evaluate predicted vs. actual values in CoMFA. The q^2, r^2, and S.E for the model based on the 12 compounds were 0.540, 0.957 and 0.163, respectively, at 4

Table 4. Experimental and predicted IC_{50} values of 15 OHPCBs for the inhibition of DHEA sulfation catalyzed by hSULT2A1

Compound	IC_{50} (μM)	Actual pIC_{50}	CoMFA	Predicted pIC_{50}	Difference
3',4'-diOH PCB 3	95.7	4.019	90	3.947	0.072
3',4'-diOH PCB 5	15.9	4.799	90	4.853	0.054
4'-OHPCB 12	15.8	4.801	84	4.763	0.039
4'-OHPCB 25	4.4	5.357	92	5.273	0.084
4'-OHPCB 3	28.1	4.551	86	4.525	0.026
4'-OHPCB 33	2.5	5.602	92	5.503	0.099
4'-OHPCB 6	9.8	5.009	88	5.117	0.108
4'-OHPCB 68	0.8	6.097	94	6.153	0.056
4'-OHPCB 9	7.5	5.125	86	5.114	0.011
4-OHPCB 11	14.0	4.854	84	4.843	0.011
4-OHPCB 14	13.0	4.886	88	5.082	0.196
4-OHPCB 34	0.6	6.222	88	6.022	0.199
4-OHPCB 36	4.4	5.357	92	5.268	0.088
4-OHPCB 8	10.0	5.000	92	5.303	0.303
6'-OHPCB 35	15.5	4.810	92	4.721	0.088

Note: The difference between the experimental and the predicted pIC_{50} values is seen in the column labeled Difference.

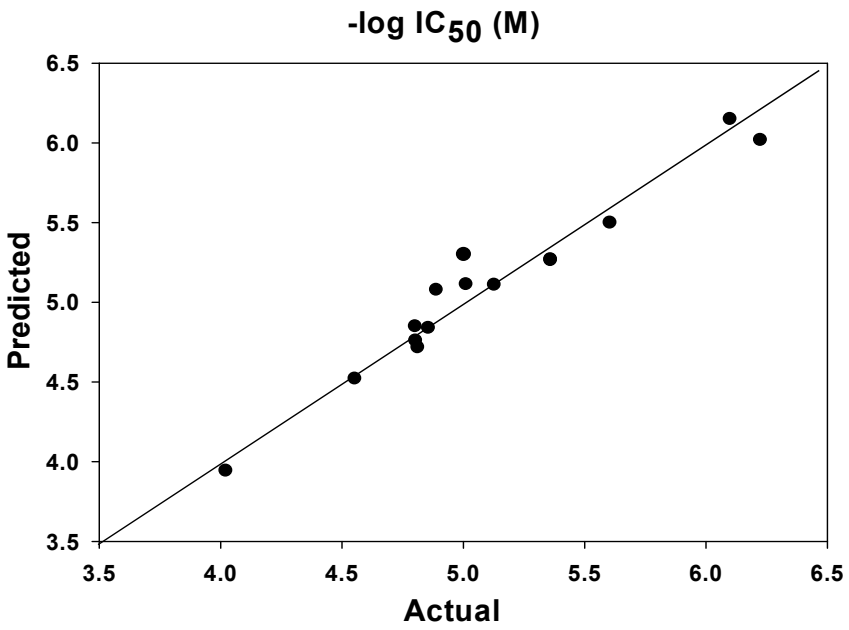

Figure 16. Actual versus predicted - log IC_{50} values for a set of 15 OHPCBs inhibitors of DHEA sulfation catalyzed by hSULT2A1. The predicted and experimental pIC_{50} values are in good agreement. The predictive power (q^2) of the model is 0.697 and the fit of the data to the model (r^2) is 0.949.

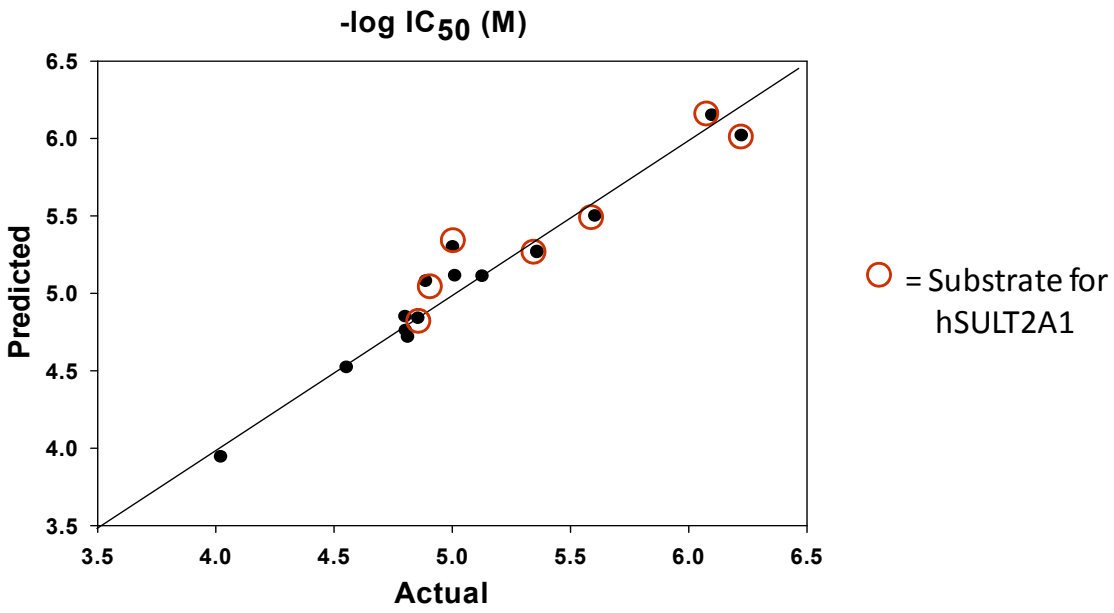

Figure 17. OHPCB substrates of hSULT2A1 are the most potent inhibitors of DHEA sulfation. The predictive power (q^2) of the model is 0.697 and the fit of the data to the model (r^2) is 0.949.

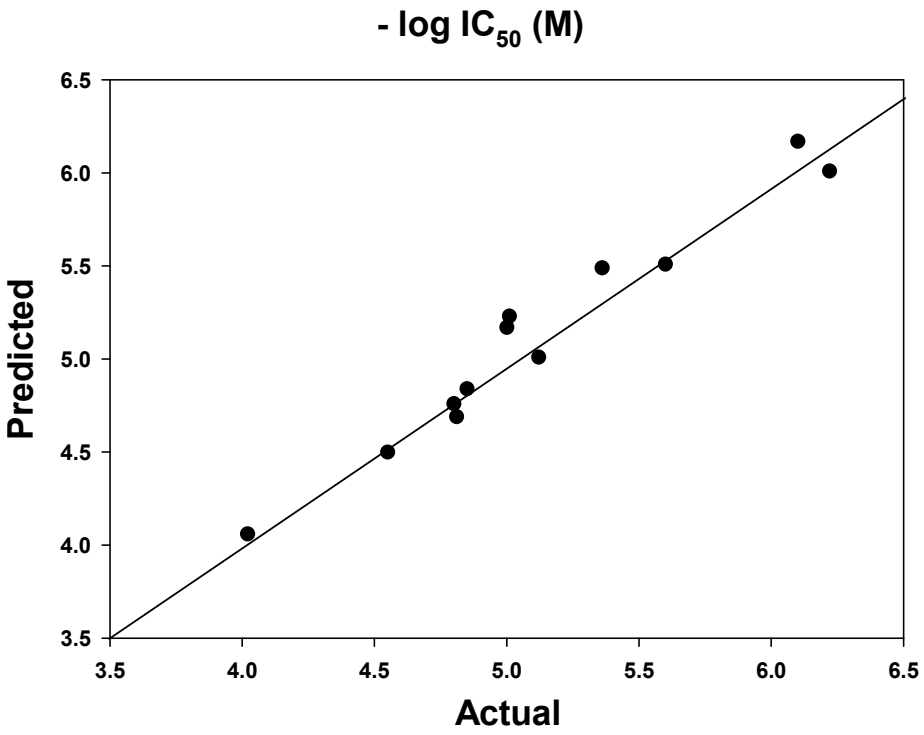

Figure 18. Actual versus predicted - log IC_{50} values for the 12-compound model (model 2). The predicted and experimental pIC_{50} values are in good agreement. The predictive power (q^2) of the model is 0.540 and the fit of the data to the model (r^2) is 0.957.

Table 5. Predicted and actual IC_{50} values of test compounds

Test compounds	Predicted (pIC_{50})	Actual (pIC_{50})	Predicted IC_{50} (μM)	Actual IC_{50} (μM)
4'-OHPCB 12	4.73	4.80	18.6	15.8
4-OHPCB 25	5.39	5.36	4.10	4.40
4-OHPCB 14	5.47	4.89	3.37	13.0

Note: Three compounds were removed from the training set in Model 1, and a second model derived based on the 12 remaining compounds. This second model was used to predict the IC_{50} values for 4'-OHPCB 12, 4-OHPCB 25 and 4-OHPCB 14.

components. The steric contribution was 29% and the electrostatic contribution was 71%.

We also examined an additional OHPCB that has been shown to be present in serum (4-OHPCB 165) but was not part of either CoMFA model. This compound however, was very different from the compounds in the training set, in terms of its chlorine substitution pattern and number of chlorine atoms it possesses. It has two ortho chlorines at the bridge and, due to its highly chlorinated nature, is very lipophilic. However, owing to its very low solubility limit under our assay conditions, it was not possible to determine a valid IC_{50} value. The solubility limit of 4-OHPCB 165 is 1 μM and this was determined using a previously described light scattering method (*193*) with modification to excitation and emission wavelength. The excitation was set at 380 nm with a slit width of 2.5 nm, and emission was set at 400 nm with a slit width of 4 nm.

Mechanism of Inhibition of hSULT2A1 by OHPCBs

In order to investigate the mechanism by which OHPCBs inhibit sulfation of DHEA catalyzed by hSULT2A1, the same radiochemical assay described in the methods section (chapter V) was used with fixed concentrations of DHEA (0.2 μM, 0.4 μM, 0.6 μM and 1 μM) in the presence and absence of variable concentrations of OHPCBs. The DHEA concentrations used were below the concentration where substrate inhibition occurred (*191*). Data obtained were fitted by nonlinear regression to four different kinetic models (competitive, noncompetitive, mixed, and uncompetitive inhibition) (Enzyme Kinetics Module, Sigma Plot 11) using the following equations: competitive (full) equation (Eq. (1a)) competitive (partial) equation (Eq. (1b)), noncompetitive (full) equation (Eq. (2a)), noncompetitive (partial) equation (Eq. (2b)), mixed (full) equation (Eq. (3a)), mixed (partial) equation (Eq. (3b)), uncompetitive (full) equation (Eq. (4a)), and uncompetitive (partial) equation (Eq. (4b)). The model having a high R^2 with the lowest AICc value was chosen to be the most likely model for the mode of inhibition (Table 6). The Akaike Information Criterion (AIC) is useful in comparing statistical

$$v = V_{max}/(1+(K_m/S)*(1+I/K_i)) \quad (1a)$$

$$v = V_{max}/(1+(K_m/S)*(1+I/K_i)/(1+I/(\alpha K_i))) \quad (1b)$$

$$v = V_{max}/((1+I/K_i)*(1+K_m/S)) \quad (2a)$$

$$v = V_{max}/((1+K_m/S)*(1+I/K_i)/(1+I*\beta/K_i)) \quad (2b)$$

$$v = V_{max}/((K_m/S)*(1+I/K_i)+(1+I/\alpha K_i))) \quad (3a)$$

$$v = V_{max}*((1+\beta*I/(\alpha K_i))/(1+I/(\alpha K_i)))/(1+(K_m/S))*(1+I/K_i)/(1+I/(\alpha K_i))) \quad (3b)$$

$$v = V_{max}/(1+I/Ki+K_m/S) \quad (4a)$$

$$v = V_{max}*(1+\beta*(I/K_i))/(1+I/K_i+K_m/S) \quad (4b)$$

models in order to select the right model that has the best-fit to the data (*194*). It provides the information lost when a model is related to a real process (*195*). It is however more useful for larger sample sizes (i.e. n > 40) (*196*). The corrected version of Akaike Information Criterion (AICc) has been utilized in this work because it is more preferred to the AIC for smaller sample sizes (*196*). In addition, under each statistical model there is an extensive search in order to make sure the model is the likely model and this makes the AICc more powerful than the AIC (*197*). The lines corresponding to the various concentrations of OHPCBs intersect to the left of the y-axis in plots of 1/v versus 1/DHEA. Eleven OHPCBs showed a complete noncompetitive inhibition while three OHPCBs (4'-OHPCB 9, 4'-OHPCB 25, and 4'-OHPCB 68) showed a partial noncompetitive inhibition with respect to DHEA. 4-OHPCB 36 was the only OHPCB that exhibited a partial competitive inhibition. The OHPCB substrates were the most potent inhibitors of DHEA sulfation catalyzed by hSULT2A1, and they bind at the active site of hSULT2A1. In noncompetitive inhibition the inhibitor binds to the free enzyme (*E*) and enzyme-substrate complex (*ES*) (*198*). It possesses two dissociation constants: the dissociation constant for binding of the inhibitor to the free enzyme (K_i) and binding of the inhibitor to the enzyme-substrate complex (αK_i) (*198*). The K_i values for the

inhibitors are listed in Table 7. Alpha (α) shows the effect of a substrate on the affinity of the enzyme for an inhibitor and vice versa (*199*). Therefore, it reflects a change in the dissociation constant upon binding of substrate to enzyme (*199*). Fourteen OHPCBs have an α value of 1 and their reciprocal plots intersect on the x-axis (Figures 19 to 25), meaning that these inhibitors have equal affinity for both the free enzyme (*E*) and enzyme-substrate (*ES*) complex. In addition, 4'-OHPCB 9, 4'-OHPCB 25, and 4'-OHPCB 68 also possess beta (β) values of 0.11 ± 0.02, 0.19 ± 0.06, 0.23 ± 0.07,

Table 6. Comparison of the statistic parameters of enzyme kinetic models of inhibitor equation fits

OHPCBs	Noncompetitive (full)		Mixed (full)		Competitive (full)		Uncompetitive (full)	
	R^2	AICc	R^2	AICc	R^2	AICc	R^2	AICc
4'-OHPCB 33	0.97	40.9	0.97	43.7	0.96	48.0	0.94	58.0
4'-OHPCB 68[a]	0.97	6.4	0.97	9.9	0.97	8.4	0.95	23.4
4'-OHPCB 6	0.99	17.7	0.99	19.4	0.99	23.4	0.96	59.2
4-OHPCB 36[b]	0.98	31.4	0.98	27.4	0.98	24.6	0.96	55.1
4-OHPCB 8	0.97	38.8	0.97	41.5	0.97	40.8	0.95	60.9
4-OHPCB 14	0.97	40.6	0.97	43.3	0.97	43.5	0.94	60.0
4'-OHPCB 9 [a]	0.99	-1.1	0.99	0.8	0.99	4.1	0.98	42.5
4-OHPCB 11	0.97	53.2	0.97	54.1	0.96	60.3	0.95	64.4
4'-OHPCB 3	0.96	43.3	0.96	45.5	0.95	47.9	0.94	53.5
4'-OHPCB 12	0.98	20.6	0.98	23.3	0.98	23.0	0.97	44.6
4'-OHPCB 25 [a]	0.97	45.8	0.97	48.0	0.96	52.9	0.95	61.0
3',4'-diOH PCB 3	0.98	33.9	0.98	35.6	0.97	45.0	0.97	43.8
3',4'-diOH PCB 5	0.98	21.8	0.98	23.4	0.98	25.7	0.96	46.7
6'-OHPCB 35	0.98	10.8	0.99	11.4	0.97	25.0	0.97	33.9
4-OHPCB 34	0.97	37.1	0.97	38.7	0.96	47.2	0.96	46.9

[a] fit to partial noncompetitive inhibition equation

[b] fit to partial competitive inhibition equation

Table 7. Dissociation constants for 15 OHPCBs as inhibitors of sulfation of DHEA catalyzed by hSULT2A1

Polychlorinated biphenyls (OHPCBs)	K_i (μM)[a]
4-hydroxy-2',3,5-trichorobiphenyl (4-OHPCB 34)	0.8 ± 0.1
4'-hydroxy-2,3',4,5'-tetrachlorobiphenyl (4'-OHPCB 68)	0.6 ± 0.1
4'-hydroxy-2'3,4-trichlorobiphenyl (4'-OHPCB 33)	3 ± 0.2
4'-hydroxy-2,3',4-trichlorobiphenyl (4'-OHPCB 25)	3 ± 0.6
4-hydroxy-3,3'5'-tricrobiphenyl (4-OHPCB 36)	3.4 ± 0.8
4'-hydroxy-2,5-dichlorobiphenyl (4'-OHPCB 9)	0.7 ± 0.1
4'-hydroxy-2,3'-dichlorobiphenyl (4'-OHPCB 6)	5.4 ± 0.2
4- hydroxy-2,4'-dichlorobiphenyl (4-OHPCB 8)	5.0 ± 0.4
4-hydroxy-3,5-dichlorobiphenyl (4-OHPCB 14)	13.5 ± 1.0
4-hydroxy-3,3'-dichlorobiphenyl (4-OHPCB 11)	12 ± 0.9
4'-hydroxy-3,4-dichlorobiphenyl (4'-OHPCB 12)	4 ± 0.3
6'-hydroxy-3,3',4 trichlorobiphenyl (6'-OHPCB 35)	9 ± 0.5
3',4'-dihydroxy-2,3,-dichlorobiphenyl (3',4'-diOHPCB 5)	14 ± 0.8
4'-hydroxy-4-monochlorobiphenyl (4'-OHPCB 3)	17 ± 1.5
3',4'-dihydroxy-4-monochlorobiphenyl (3',4'-diOHPCB 3)	32 ± 2.3

[a] K_i is calculated using nonlinear regression analysis fit to noncompetitive inhibition

respectively. The β values signify formation of product (i.e., DHEA-sulfate) in the presence of these three OHPCBs. While it is sometimes assumed that only competitive inhibitors interact at the same site on the enzyme as the substrate, this is not always the case. Noncompetitive inhibitors can also bind at the active site of the enzyme (*187*). The key difference is that different forms of the enzyme are involved. Moreover, noncompetitive inhibition has been seen with most inhibitors of sulfotransferases. For example, the mode of inhibition of the sulfation of 3-OH-BaP by triclosan and by OHPCBs has been reported as noncompetitive (*200-201*). Triethylamine was also shown to be a noncompetitive inhibitor of DHEA sulfation (*202*). Furthermore, quercetin has been shown to noncompetitively inhibit sulfation of minoxidil and acetaminophen (*203-204*).

The noncompetitive inhibition observed by the OHPCBs studied might suggest multiple sites of binding of the inhibitors to the enzyme, but it would also be consistent with interaction solely at the DHEA-binding site. There have been studies that show the possibility of two substrates simultaneously occupying the active site in two isoforms of a family 1 sulfotransferase (*156, 205*). The tertiary structures at the catalytic sites among the cytosolic sulfotransferases are similar, and the sulfuryl acceptor binding site for the family 1 enzyme is large enough to accommodate two molecules of substrate at the same time. While Rehse *et al*., 2002, showed two binding modes for DHEA by overlaying two crystal structures of hSULT2A1 in complex with DHEA (*158*), there are no studies to support having two molecules of DHEA simultaneously at the active site of hSULT2A1.

A noncompetitive inhibition pattern would also arise if the OHPCB bound to the DHEA binding site in both the free enzyme and the form of the enzyme with PAPS or PAP already bound. Indeed, DHEA has been shown to have two alternate binding modes to hSULT2A1, in the open conformation (without PAP) and in the closed conformation (with PAP) (*206*). Thus, the noncompetitive binding pattern seen with OHPCBs is likely the result of different enzyme conformation depending on whether or not the nucleotide

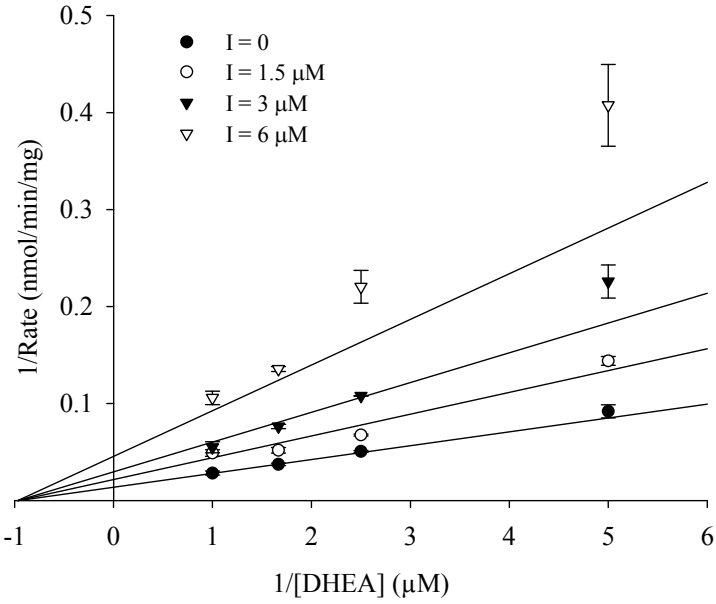

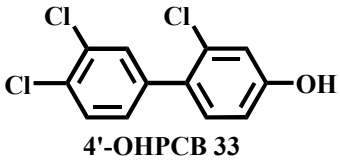

4'-OHPCB 33

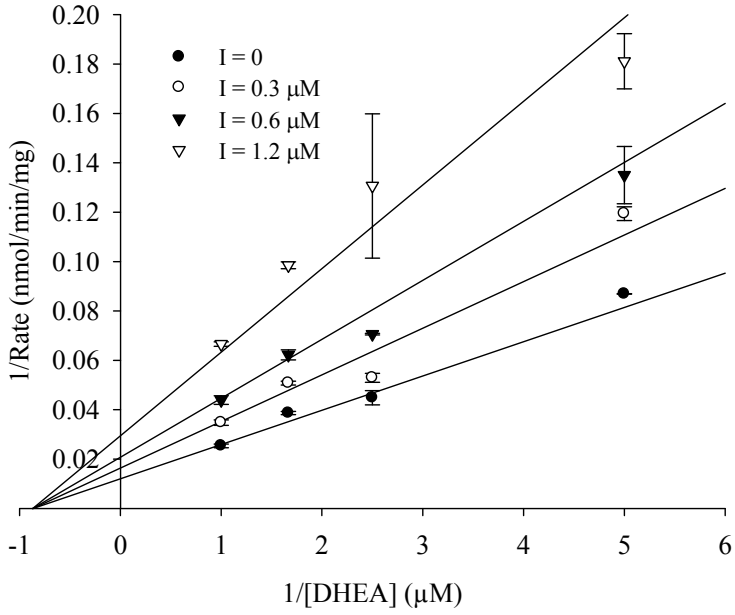

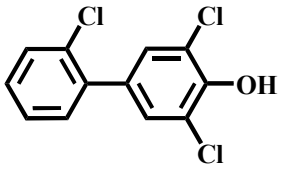

4-OHPCB 34

Figure 19. Kinetic analysis of OHPCBs as inhibitors of DHEA sulfation catalyzed by hSULT2A1. Nonlinear regression fits to noncompetitive inhibition by 4'-OHPCB 33 and 4-OHPCB 34 are shown. The data points are the means ± standard error of triplicate determination. AICc values for 4'-OHPCB 33 and 4-OHPCB 34 are 40.9 and 37.1 respectively, and R^2 is 0.97 for both OHPCBs.

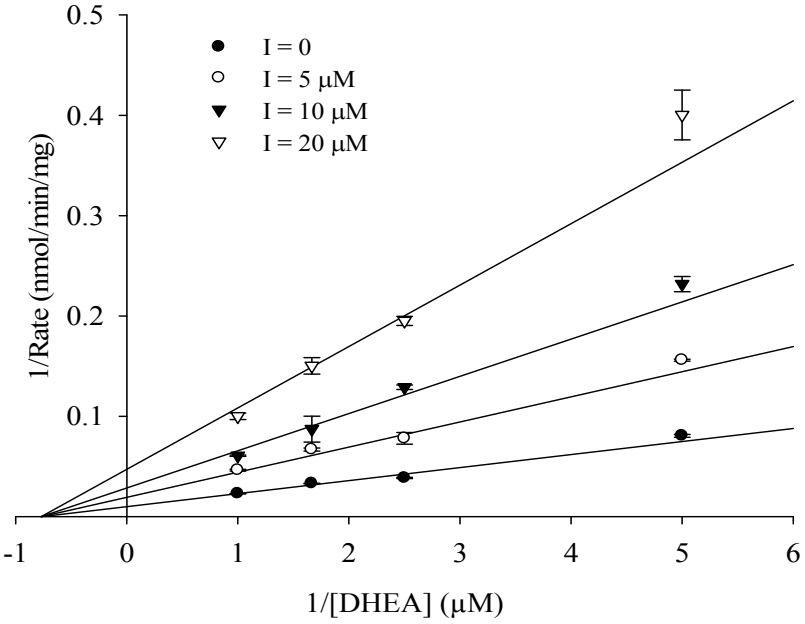

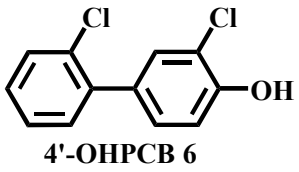

4'-OHPCB 6

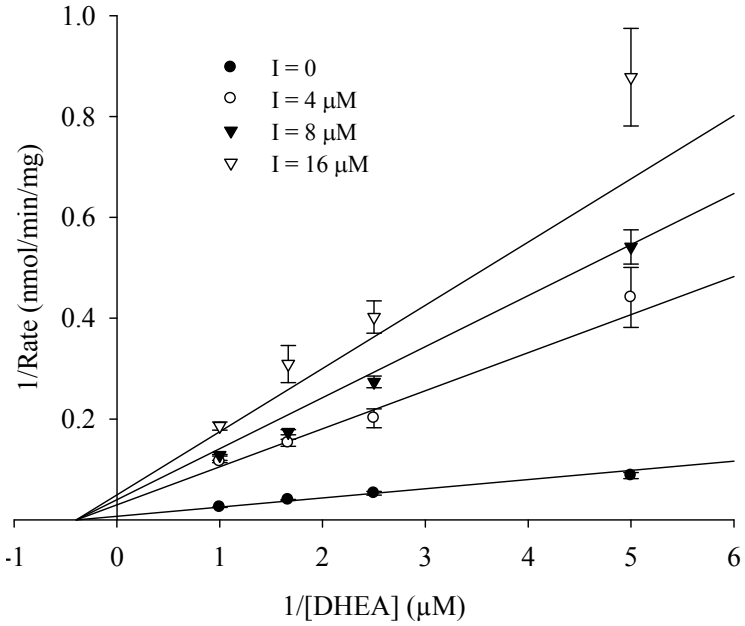

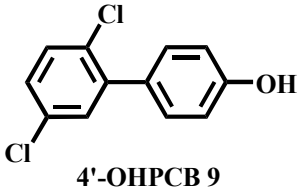

4'-OHPCB 9

Figure 20. Kinetic analysis of OHPCBs as inhibitors of DHEA sulfation catalyzed by hSULT2A1. Nonlinear regression fits to noncompetitive inhibition (full) and noncompetitive (partial) inhibition by 4'-OHPCB 6 and 4'-OHPCB 9 respectively are shown. AICc values for 4'-OHPCB 6 and 4'-OHPCB 9 are 17.7 and -1.1 respectively, and R^2 is 0.99 for both OHPCBs.

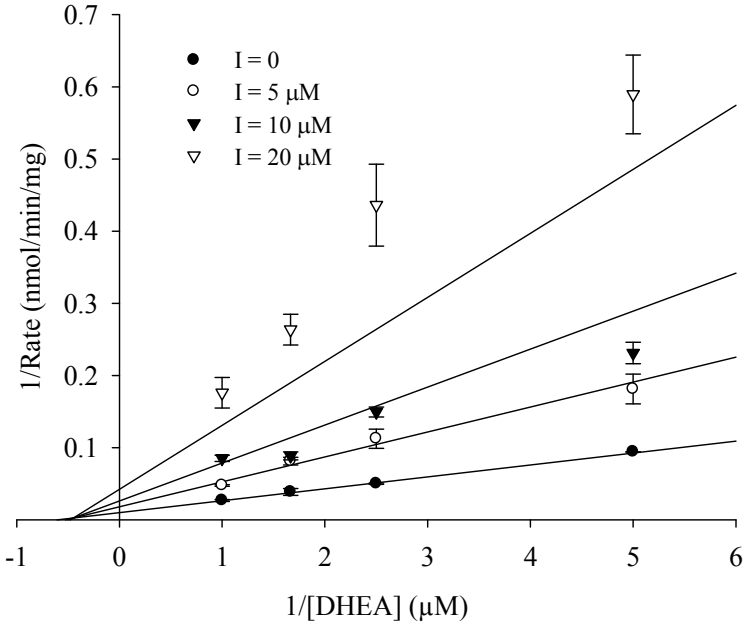

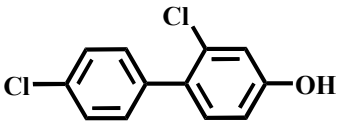

4-OHPCB 8

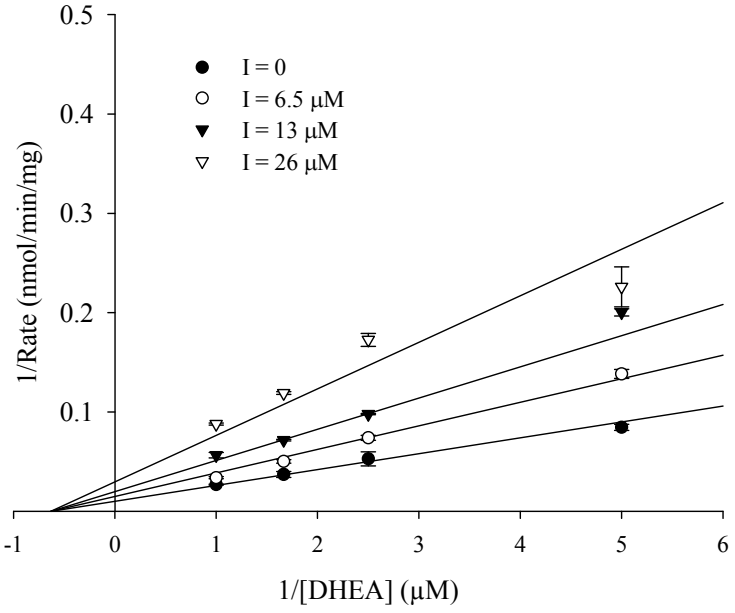

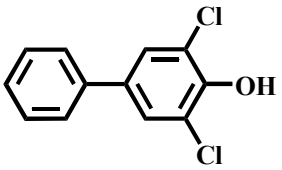

4-OHPCB 14

Figure 21. Kinetic analysis of OHPCBs as inhibitors of DHEA sulfation catalyzed by hSULT2A1. Nonlinear regression fits to noncompetitive inhibition of 4-OHPCB 8 and 4-OHPCB 14 are shown. AICc values for 4-OHPCB 8 and 4-OHPCB 14 are 38.8 and 40.6 respectively, and R^2 is 0.97 for both OHPCBs.

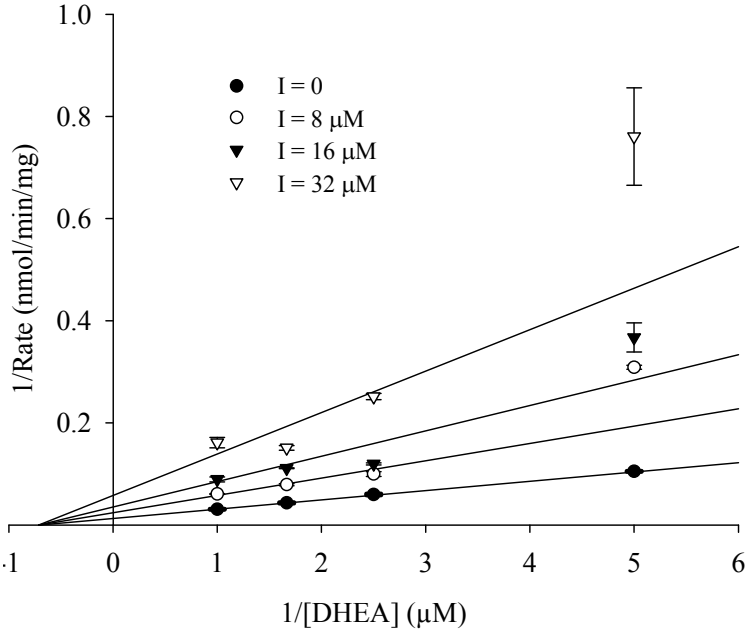

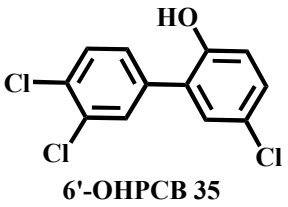

6'-OHPCB 35

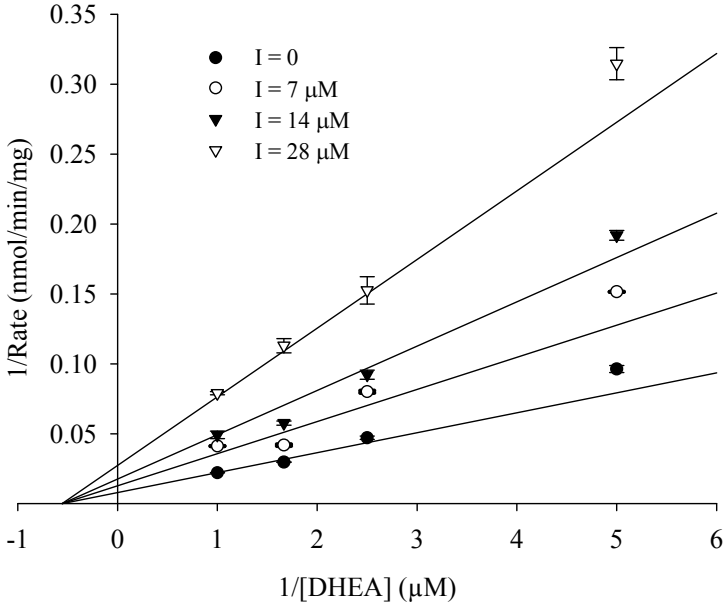

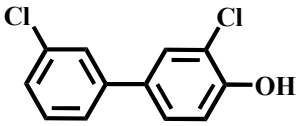

4-OHPCB 11

Figure 22. Kinetic analysis of OHPCBs as inhibitors of DHEA sulfation catalyzed by hSULT2A1. Nonlinear regression fits to noncompetitive inhibition by 6'-OHPCB 35 and 4-OHPCB 11 are shown. AICc values are 10.8 and 53.2, and R^2 are 0.98 and 0.97 for 6'-OHPCB 35 and 4-OHPCB 11 respectively.

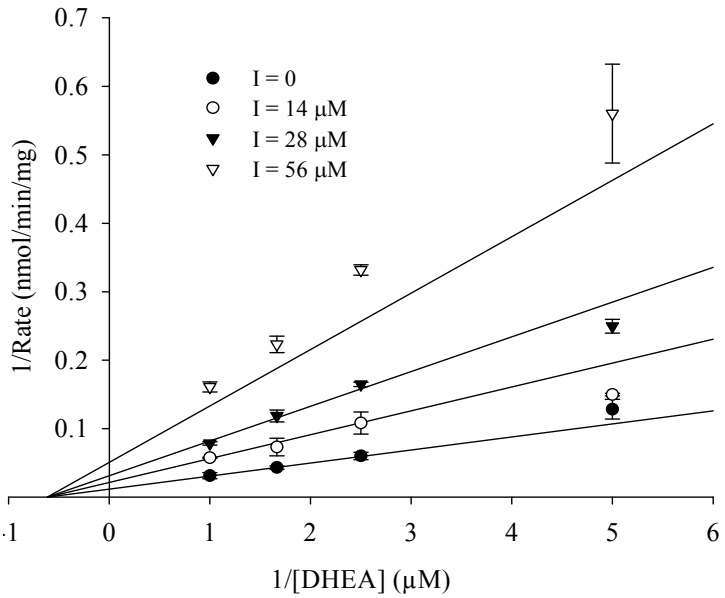

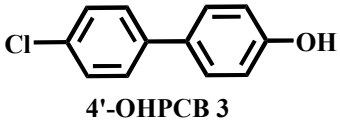

4'-OHPCB 3

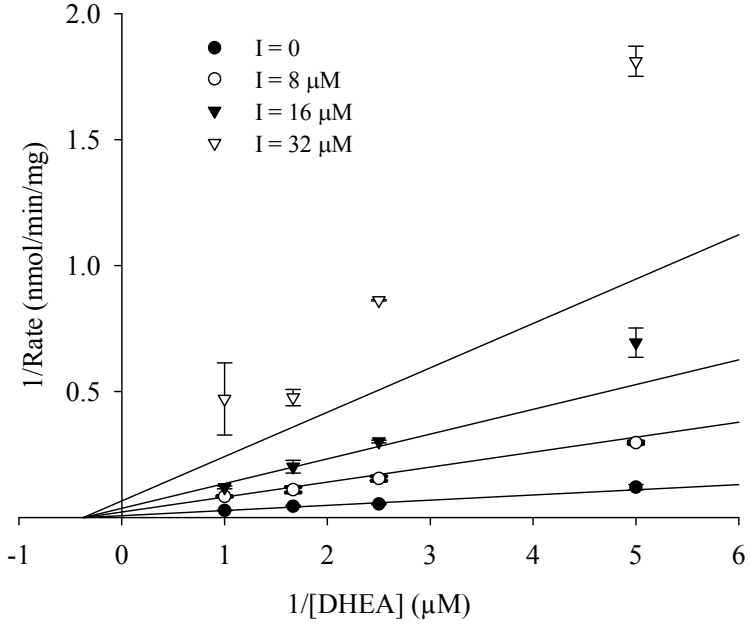

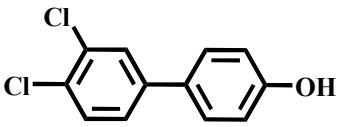

4'-OHPCB 12

Figure 23. Kinetic analysis of OHPCBs as inhibitors of DHEA sulfation catalyzed by hSULT2A1. Nonlinear regression fits to noncompetitive inhibition by 4'-OHPCB 3 and 4'-OHPCB 12 are shown. AICc values are 43.3 and 20.6, and R^2 are 0.96 and 0.98 for 4'-OHPCB 3 and 4'-OHPCB 12, respectively.

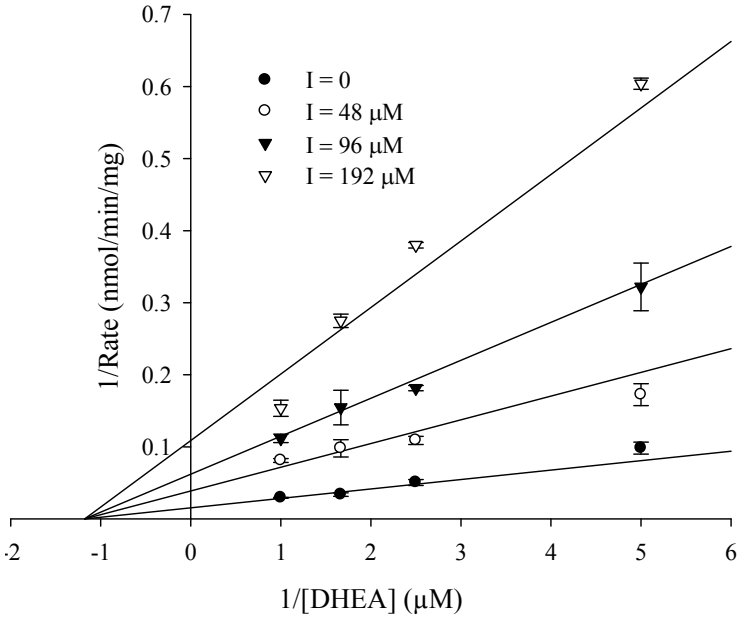

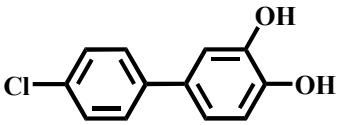

3',4'-diOHPCB 3

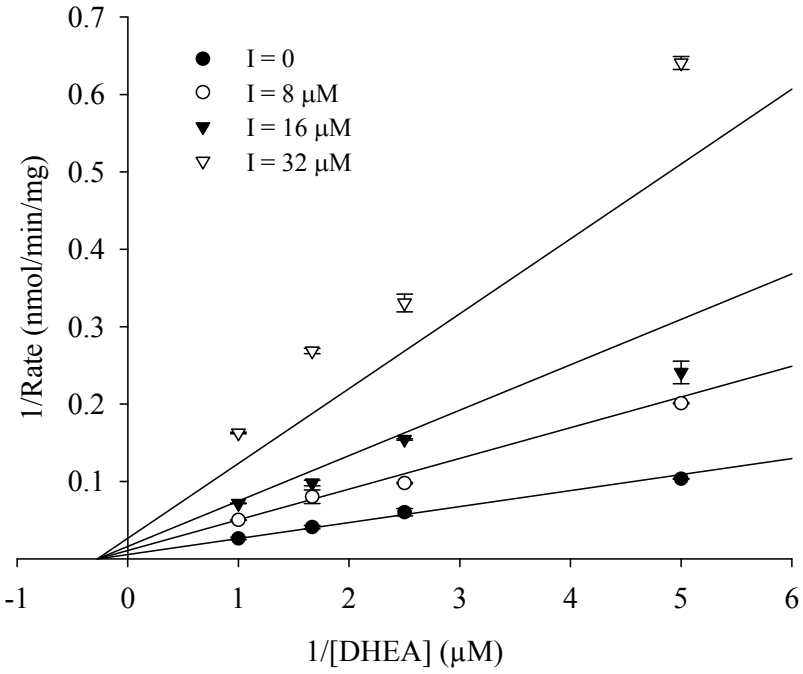

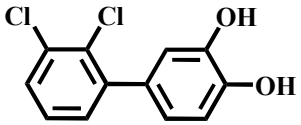

3',4'-diOHPCB 5

Figure 24. Kinetic analysis of OHPCBs as inhibitors of DHEA sulfation catalyzed by hSULT2A1. Nonlinear regression fits to noncompetitive inhibition by 3', 4-diOHPCB 3 and 3', 4'-diOHPCB 5 are shown. AICc values are 33.9 and 21.8 for 3', 4'-diOHPCB 3 and 3', 4'-diOHPCB 5 respectively, and R^2 is 0.98 for both OHPCBs.

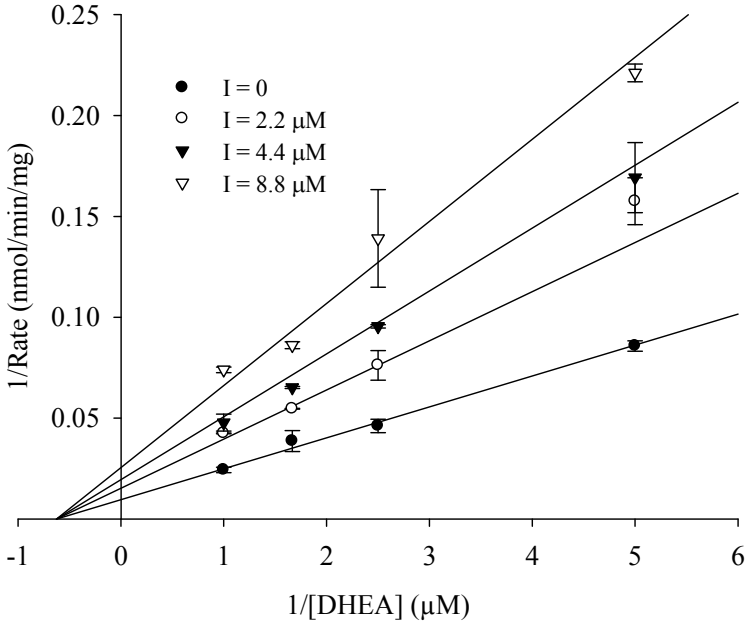

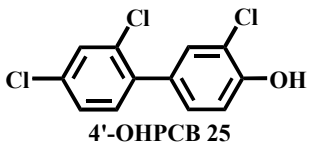

4'-OHPCB 25

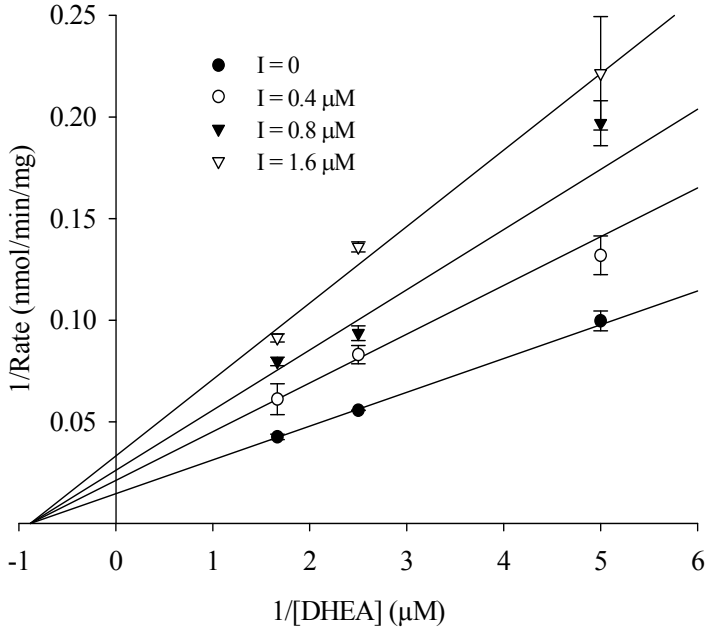

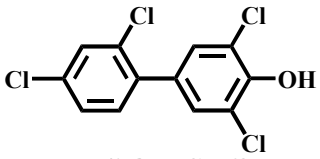

4'-OHPCB 68

Figure 25. Kinetic analysis of OHPCBs as inhibitors of DHEA sulfation catalyzed by hSULT2A1. Nonlinear regression fits to noncompetitive (partial) inhibition by 4'-OHPCB 25 and 4'-OHPCB 68 are shown. AICc values are 45.8 and 6.4 for 4'-OHPCB 25 and 4'-OHPCB 68 respectively and R^2 is 0.97 for both OHPCBs.

(i.e., either PAPS or PAP) is bound to the sulfotransferase. 4-OHPCB 36 showed a partial competitive inhibition with respect to DHEA and it had α value of 4.2, and lines intersect above the x-axis (Figure 26), indicating that this OHPCB binds to the free enzyme. Competitive inhibition is where the substrate (in this case DHEA) binds with a higher affinity to the free enzyme than the enzyme-complex. However, the inhibition of DHEA by 4-OHPCB 36 is not a complete inhibition, therefore the enzyme is converted into a modified, but still functional enzyme-substrate-inhibitor complex (*207*).

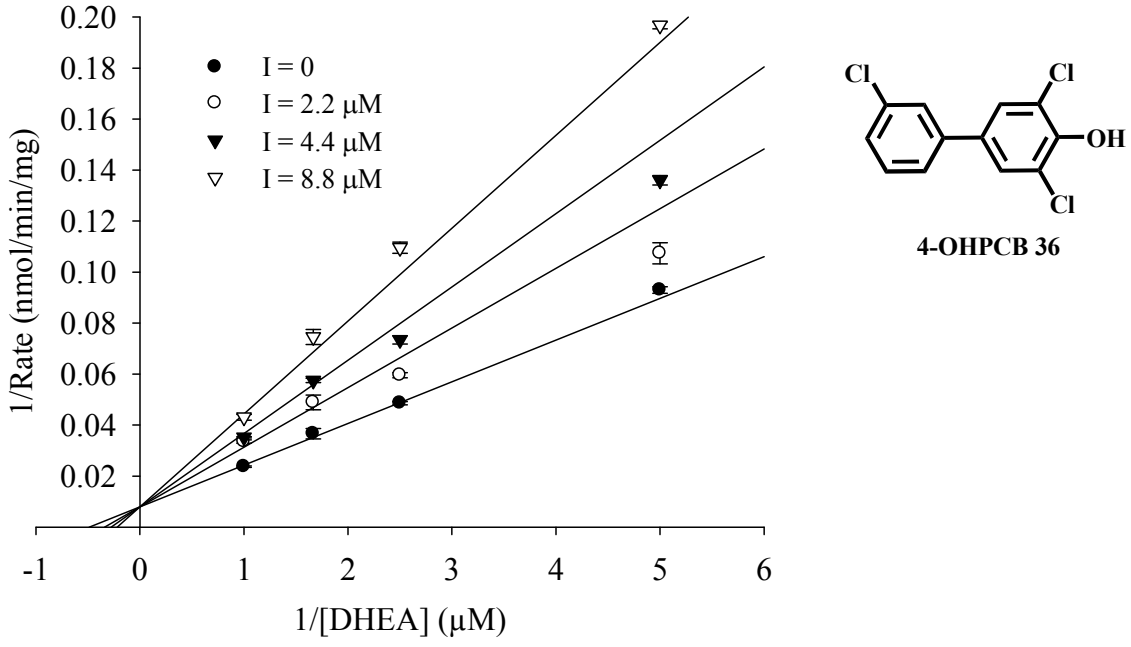

Figure 26. Kinetic analysis of 4-OHPCB 36 as inhibitor of DHEA sulfation catalyzed by hSULT2A1. The nonlinear regression fit to competitive (partial) inhibition is shown. AICc and R^2 are 24.6 and 0.98, respectively.

The Binding of OHPCBs to hSULT2A1

Studies to determine dissociation constants for the binding of OHPCB were carried out using the fluorescent probe molecule, 8-anilino-1-naphthalene sulfonic acid (ANS), shown in Figure 50 in the Methods section. ANS is used for the detection of structural and functional changes of proteins, and it is particularly useful for the analysis of the binding of ligands to proteins (*208*). The binding of ANS to protein is noncovalent, and therefore, it can be displaced by a specific substrate or inhibitor. A decrease in the fluorescence of ANS is observed when it is displaced from a hydrophobic region of a protein into a more polar environment.

Most proteins have been reported to have more than one binding site for ANS (*209*). It is therefore important to use a concentration of this probe molecule that would saturate all potential binding sites on the enzyme. Preliminary experiments to determine the binding of ANS to hSULT2A1 were carried out in order to know the saturating concentration of ANS needed in subsequent OHPCB-titration studies. Titrations with ANS were done in the presence and absence of hSULT2A1 (duplicate determinations) and the fluorescence intensity was plotted as a function of the concentration of ANS (Figure 27). A dissociation constant (K_d) of approximately 12 μM was obtained. The difference of the means (mean with enzyme minus mean without enzyme) of the two assays, also represented in Figure 27, clearly showed that saturation occurred at a concentration of 40 μM. This concentration was over 3-fold higher than the K_d, and this was the concentration used in the subsequent titration studies to determine dissociation constants for OHPCBs.

The binding of OHPCBs to hSULT2A1 was analyzed in the presence of 40 μM ANS as described in chapter V, and the absolute value of the change in fluorescence was plotted versus concentration of OHPCB (Figures 28 to 35). It should be noted that the increase in the absolute value of the change in ANS fluorescence with OHPCB titration actually represents a decrease in the fluorescence intensity of ANS observed.

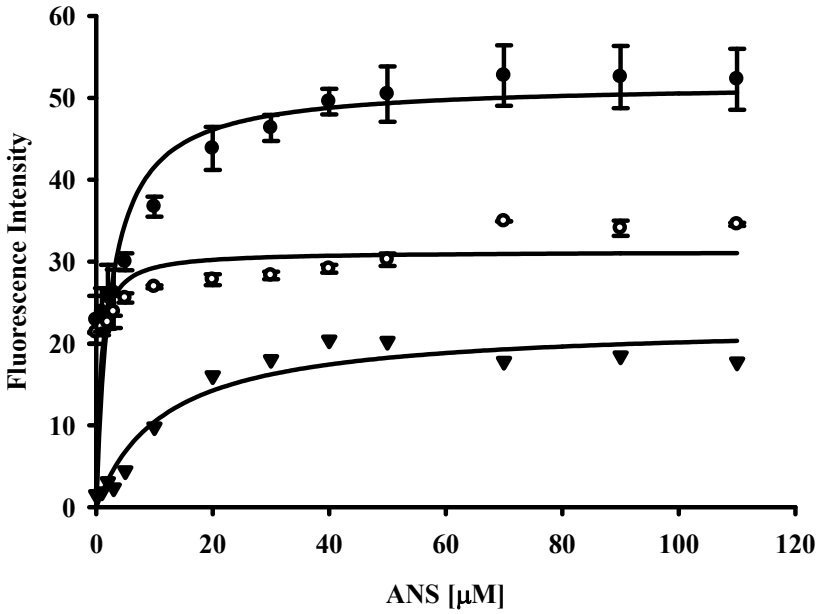

Figure 27. Binding of ANS to hSULT2A1. The excitation wavelength was 380 nm and the emission wavelength was 465 nm. Data points are the mean ± standard error of duplicate determinations (●) assays done in the presence of enzyme. (○) assays carried out in the absence of enzyme. (▼) the difference between the means of the duplicate determinations in the presence and absence 3 μg of enzyme.

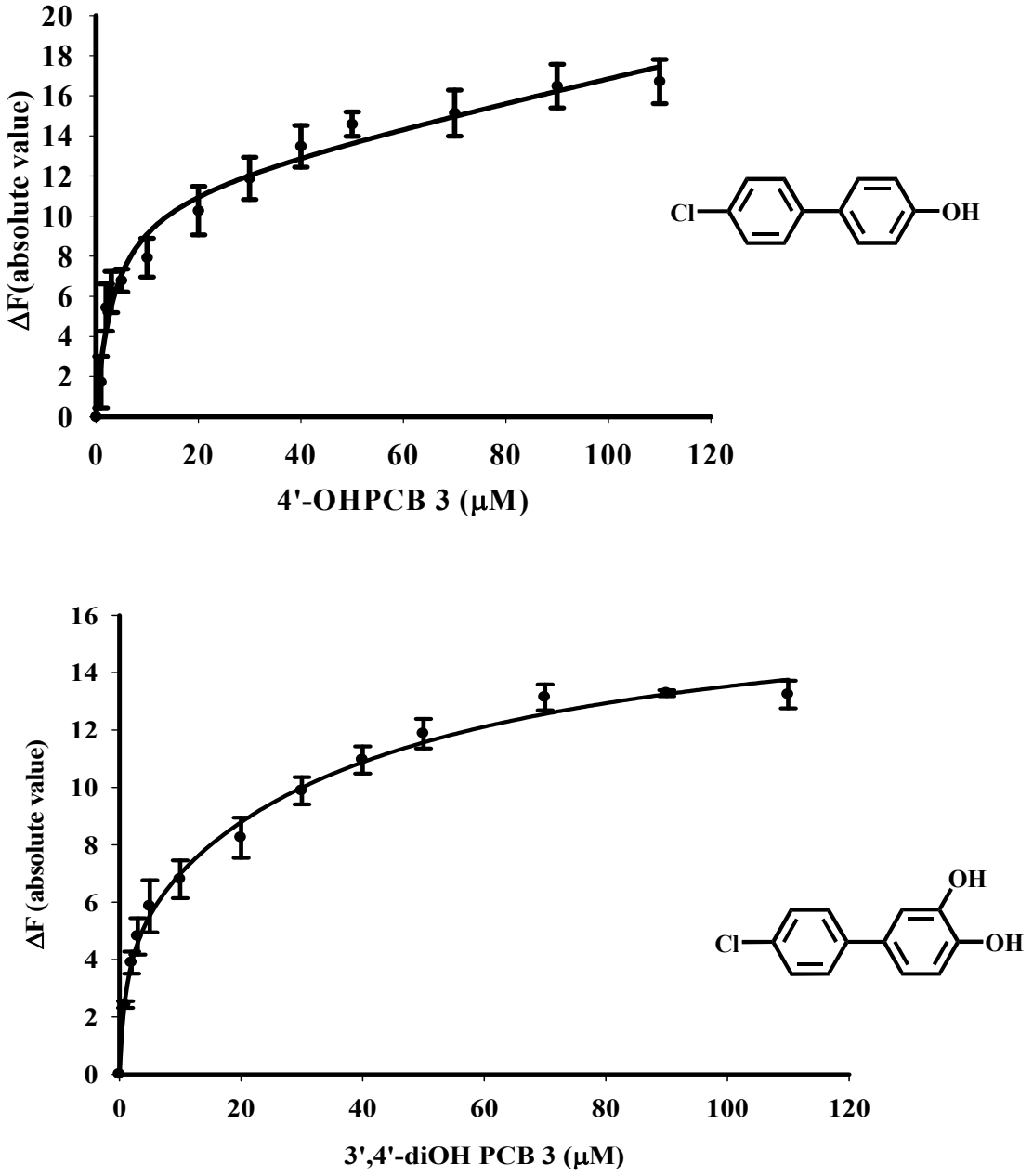

Note: The y-axis represents the absolute value of the decrease in fluorescence of the probe molecule (ANS) at 465 nm (excitation at 380 nm).

Figure 28. Binding 4'-OHPCB 3 and 3', 4'-diOH PCB 3 to hSULT2A1. A plot of the absolute value of the fluorescence change versus OHPCBs concentration is shown. Assays were carried out with a saturating concentration of ANS (40 μM). Data points are the mean ± standard error of triplicate determinations. The curves represent the fit to a single-site binding equation for 4-OHPCB 3 ($r^2 = 0.92$), and a double-site binding equation for 3', 4-diOHPCB 3 ($r^2 = 0.97$).

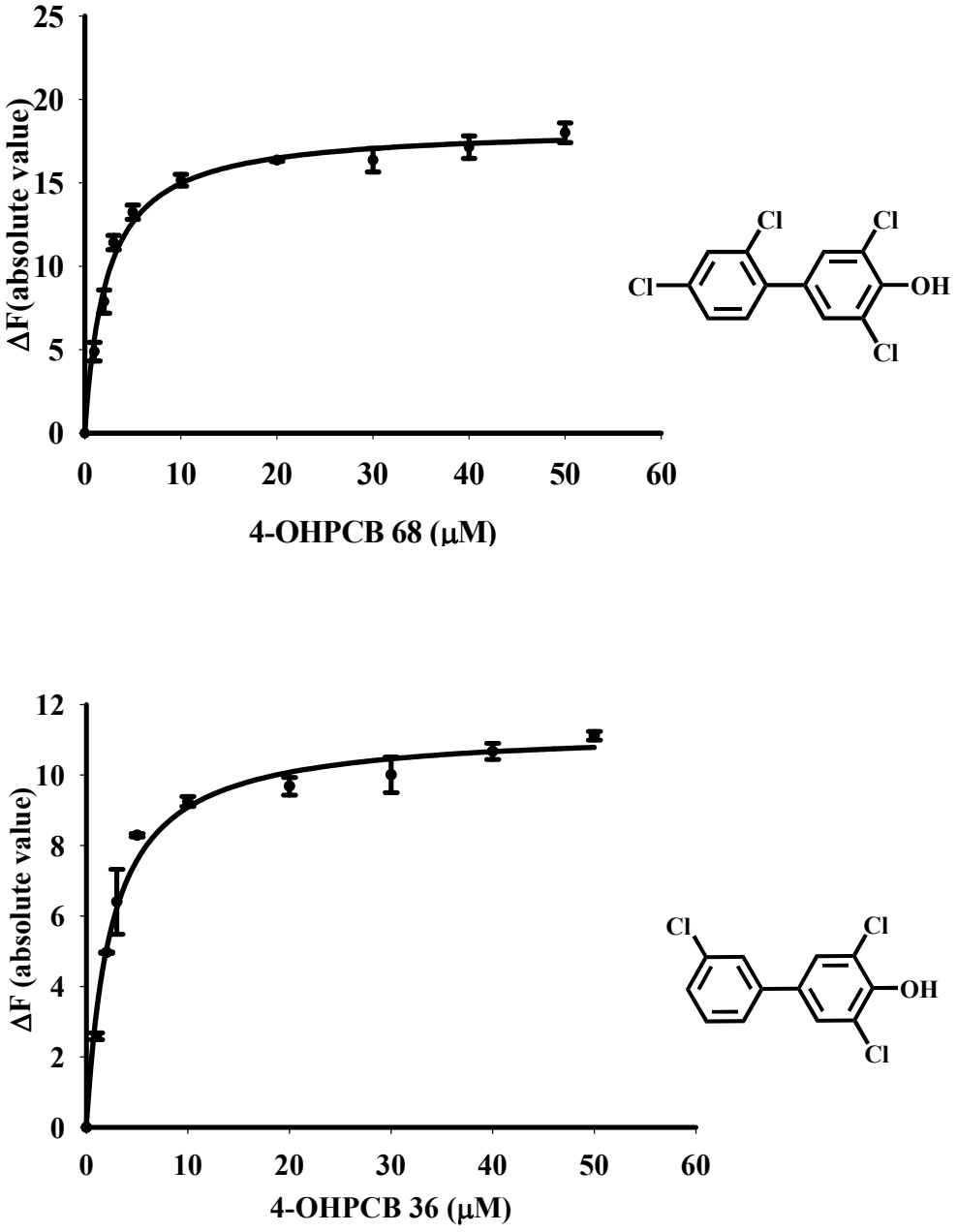

Note: The y-axis represents the absolute value of the decrease in fluorescence of the probe molecule (ANS) at 465 nm (excitation at 380 nm).

Figure 29. Binding of 4-OHPCB 68 and 4-OHPCB 36 to hSULT2A1. A plot of the absolute value of the fluorescence change versus OHPCBs concentration is shown. Assays were carried out with a saturating concentration of ANS (40 μM). Data points are the mean ± standard error of triplicate determinations. The curves represent the fit to a single-site binding equation ($r^2 = 0.98$ for both 4-OHPCB 68 and 4-OHPCB 36).

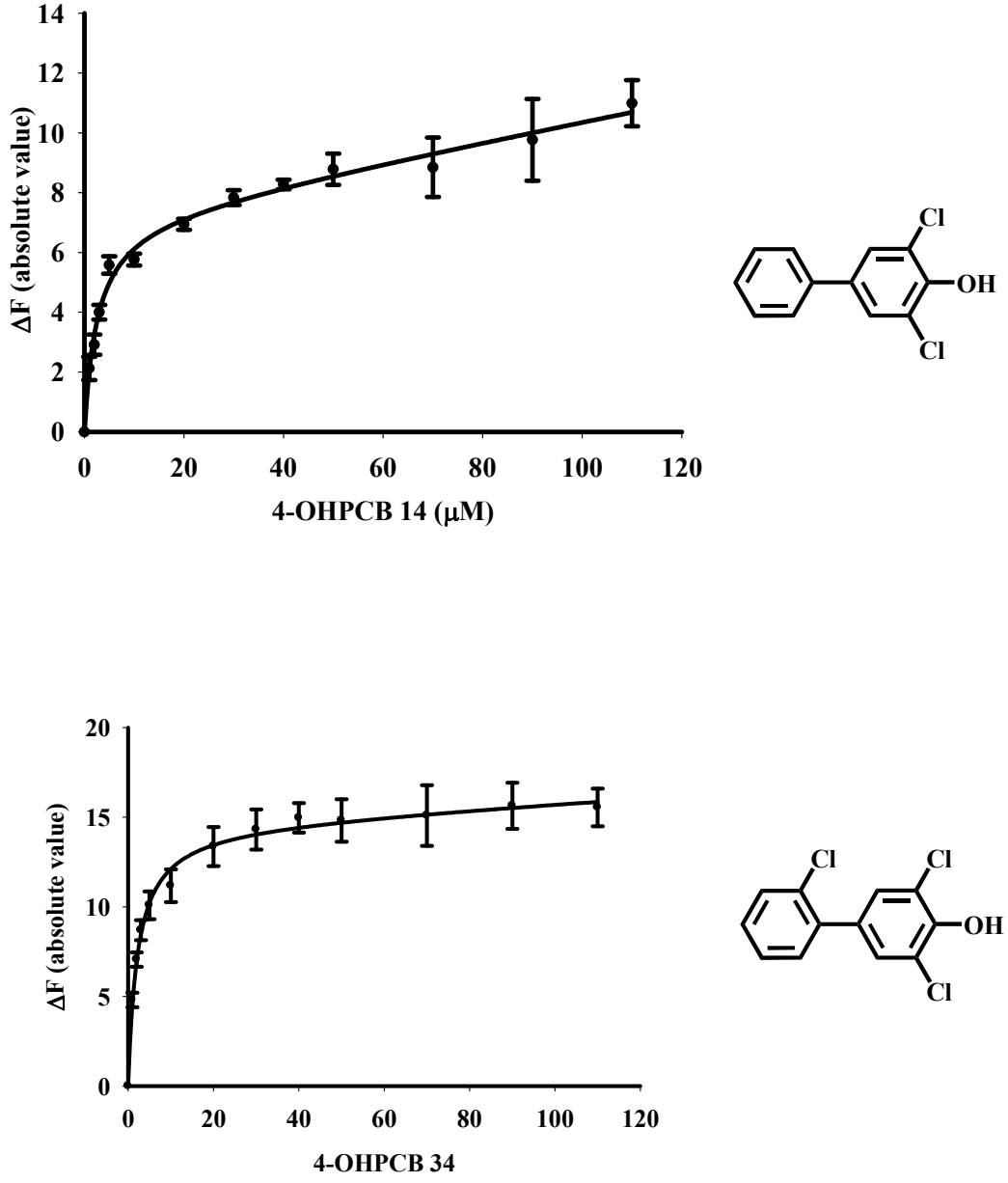

Note: The y-axis represents the absolute value of the decrease in fluorescence of the probe molecule (ANS) at 465 nm (excitation at 380 nm).

Figure 30. Binding of 4-OHPCB 14 and 4-OHPCB 34 to hSULT2A1. A plot of the absolute value of the fluorescence change versus OHPCBs concentration is shown. Assays were carried out with a saturating concentration of ANS (40 μM). Data points are the mean ± standard error of triplicate determinations. The curves represent the fit to a single-site binding equation ($r^2 = 0.93$ for both 4-OHPCB 14 and 4-OHPCB 34).

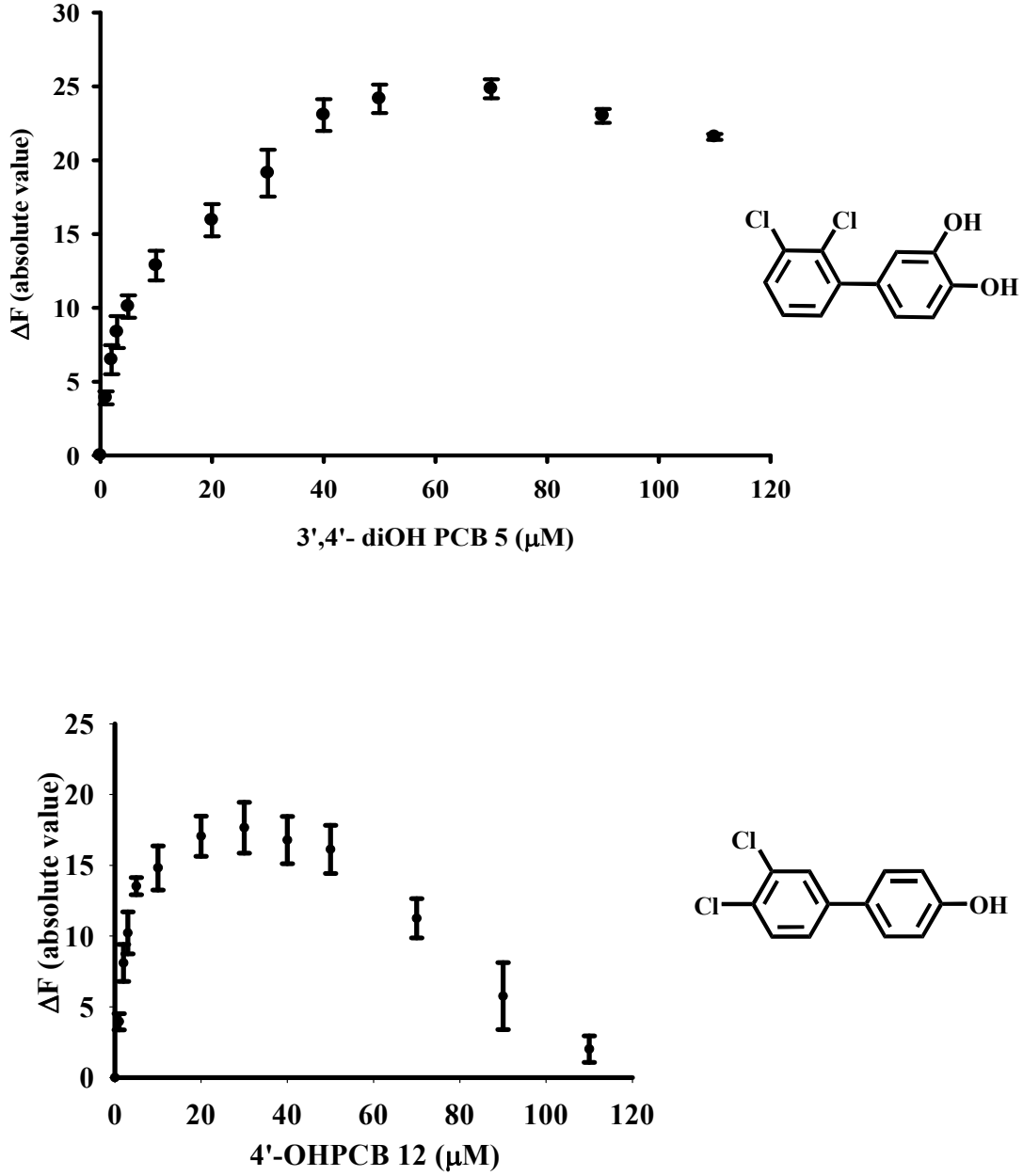

Note: The y-axis represents the absolute value of the decrease in fluorescence of the probe molecule (ANS) at 465 nm (excitation at 380 nm).

Figure 31. Binding 3', 4'-diOH PCB 5 and 4'-OHPCB 12 to hSULT2A1. A plot of the absolute value of the fluorescence change versus OHPCBs concentration is shown. Assays were carried out with a saturating concentration of ANS (40 μM). Data points are the mean ± standard error of triplicate determinations.

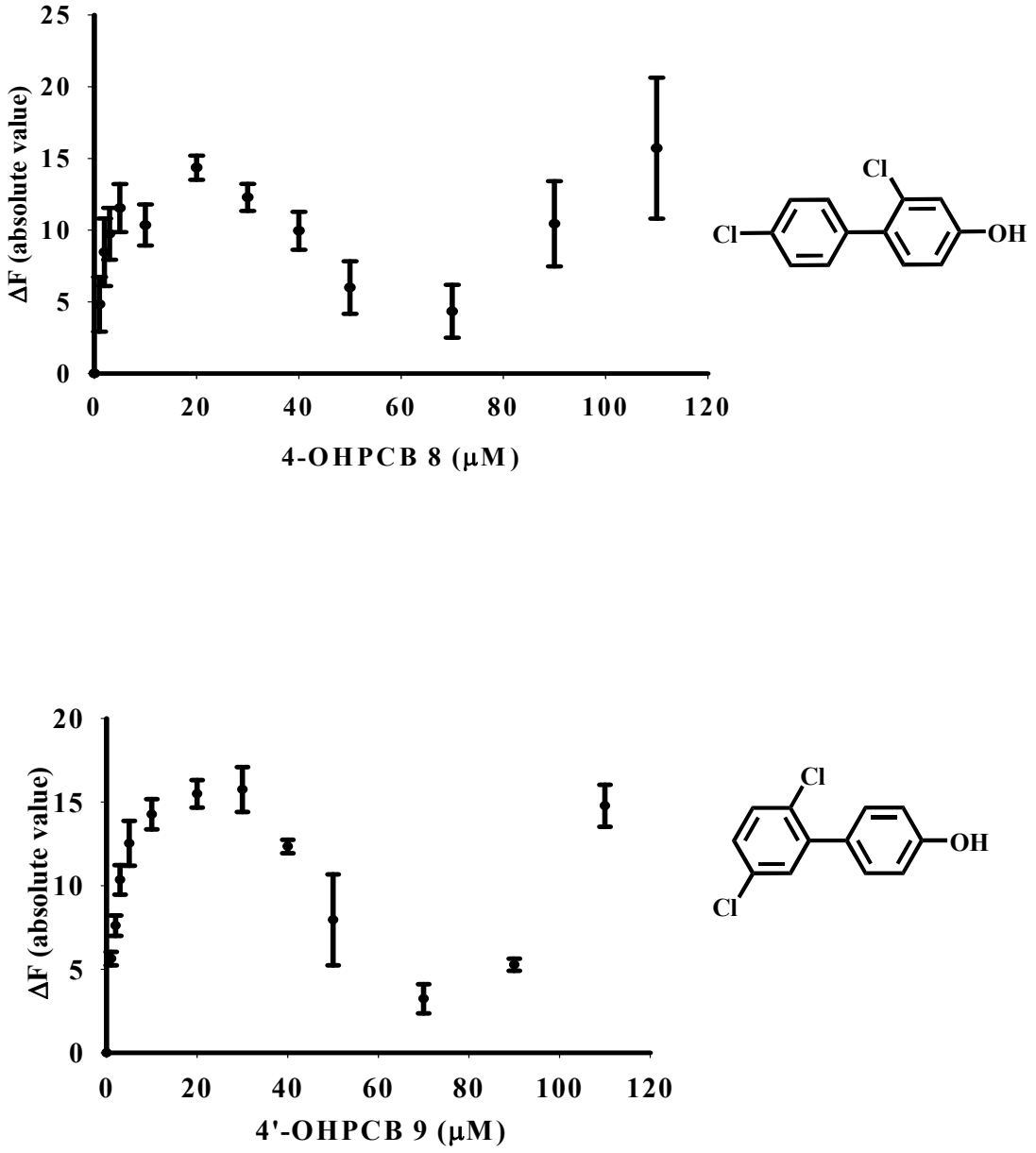

Note: The y-axis represents the absolute value of the decrease in fluorescence of the probe molecule (ANS) at 465 nm (excitation at 380 nm).

Figure 32. Binding 4-OHPCB 8 to 4'-OHPCB 9 to hSULT2A1. A plot of the absolute value of the fluorescence change versus OHPCBs concentration is shown. Assays were carried out with a saturating concentration of ANS (40 μM). Data points are the mean ± standard error of triplicate determinations

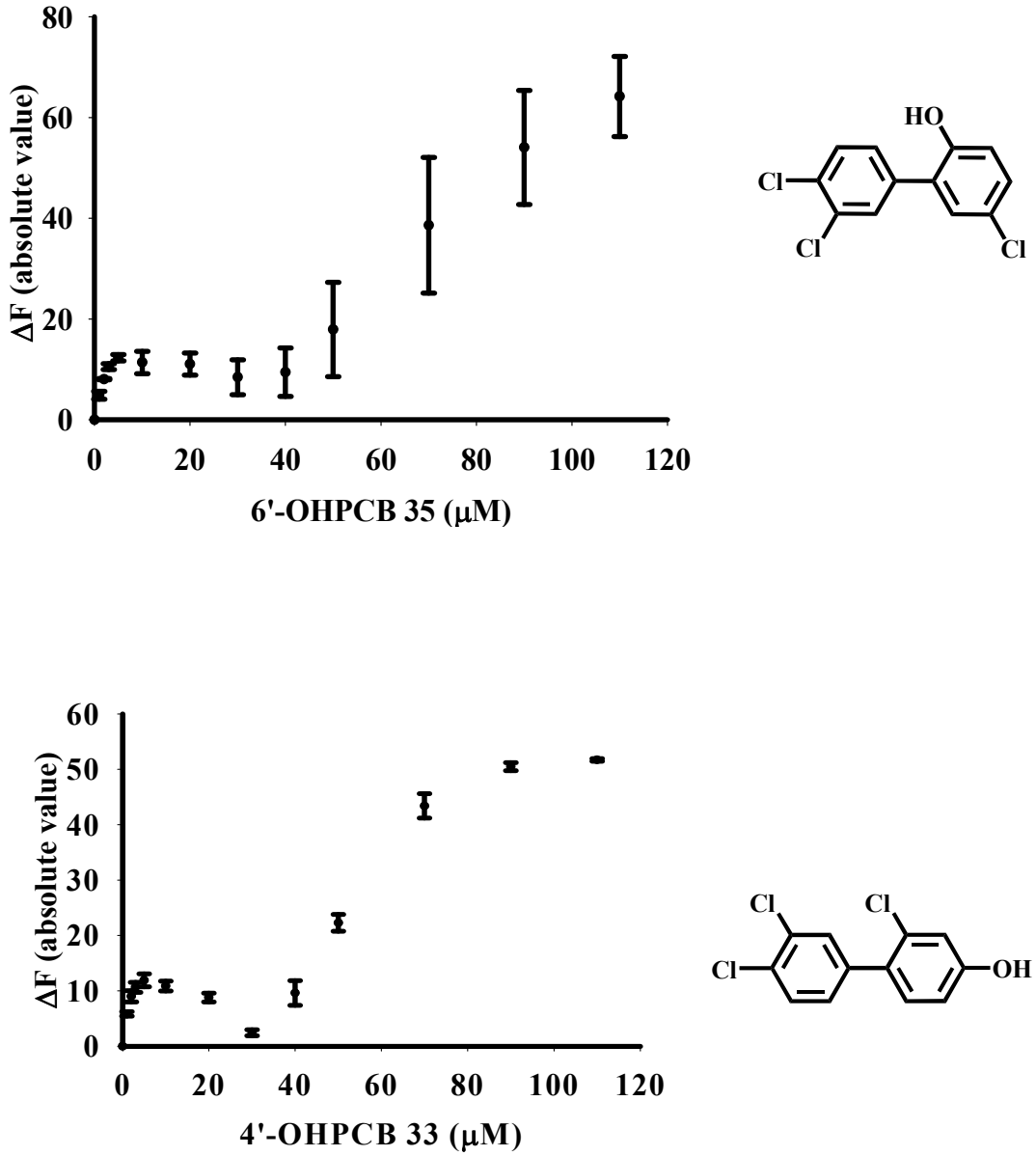

Note: The y-axis represents the absolute value of the decrease in fluorescence of the probe molecule (ANS) at 465 nm (excitation at 380 nm).

Figure 33. Binding 6'-OHPCB 35 and 4'-OHPCB 33 to hSULT2A1. A plot of the absolute value of the fluorescence change versus OHPCBs concentration is shown. Assays were carried out with a saturating concentration of ANS (40 μM). Data points are the mean ± standard error of triplicate determinations.

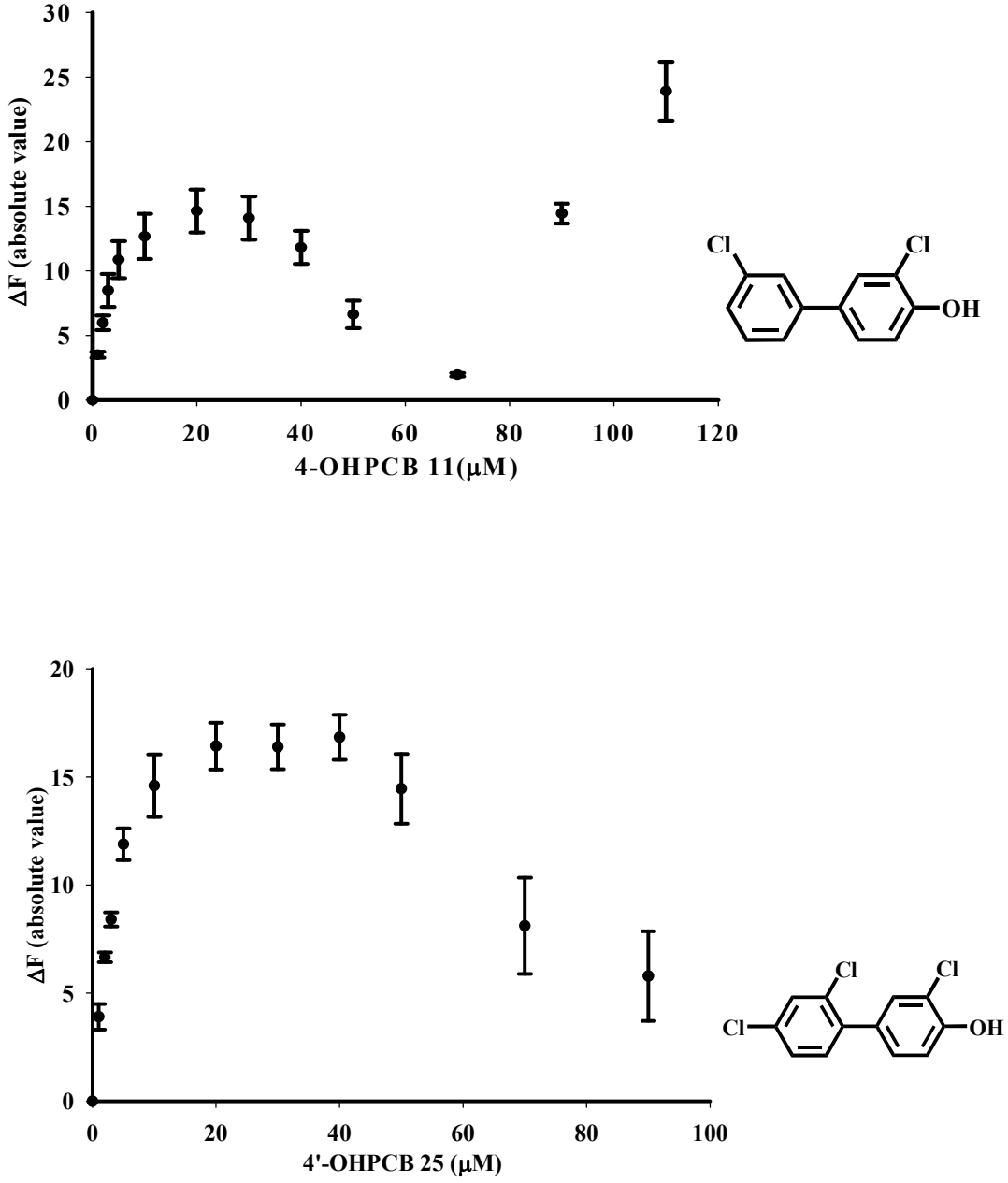

Note: The y-axis represents the absolute value of the decrease in fluorescence of the probe molecule (ANS) at 465 nm (excitation at 380 nm).

Figure 34. Binding 4-OHPCB 11 and 4'-OHPCB 25 to hSULT2A1. A plot of the absolute value of the fluorescence change versus OHPCBs concentration is shown. Assays were carried out with a saturating concentration of ANS (40 μM). Data points are the mean ± standard error of triplicate determinations.

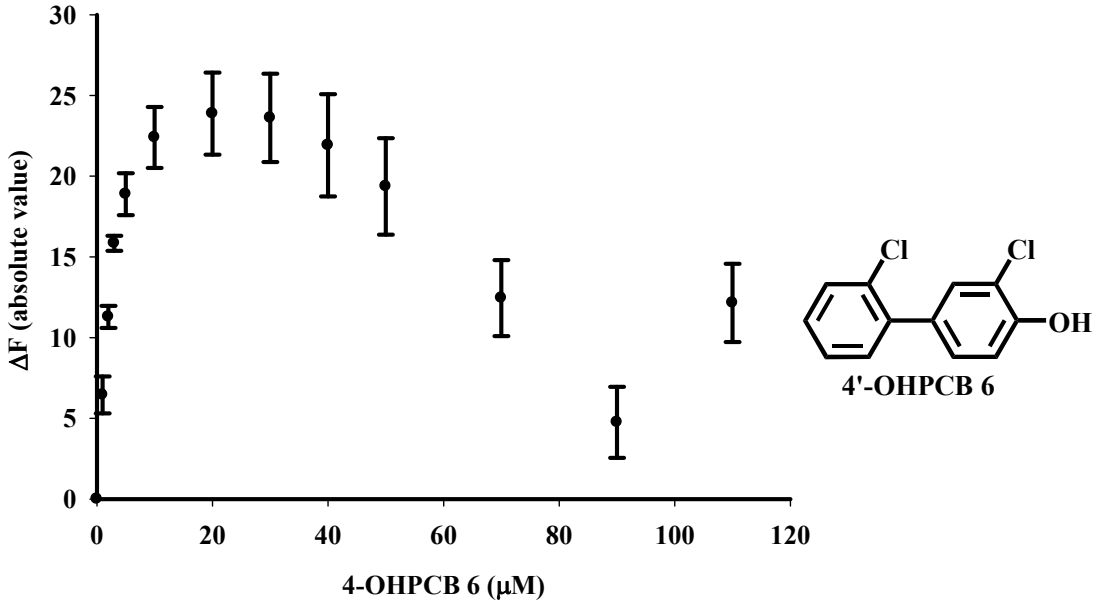

Note: The y-axis represents the absolute value of the decrease in fluorescence of the probe molecule (ANS) at 465 nm (excitation at 380 nm).

Figure 35. Binding 4'-OHPCB 6 to hSULT2A1. A plot of the absolute value of the fluorescence change versus OHPCBs concentration is shown. Assays were carried out with a saturating concentration of ANS (40 μM). Data points are the mean ± standard error of triplicate determinations.

Since the OHPCBs tested showed inhibition of DHEA sulfation, and many were alternate substrates (see above), this implies that they were acting at the active site of the enzyme. Therefore, the initial displacement of ANS observed during the titration studies was most likely from the active site of hSULT2A1 and not from an allosteric site of the enzyme. Dissociation constants (K_d values) were derived for some of the OHPCBs, and these are seen in Table 8. However with others, it was not possible to determine valid K_d values due to binding interaction that were not modeled by simple one-site or two-site binding equations. In fact, for several OHPCBs, an increase in fluorescence was seen

following the usual decrease in fluorescence, and this was then followed by another decrease in fluorescence intensity at higher concentrations of the OHPCBs.

Table 8. K_d values for six hydroxylated polychlorinated biphenyls (OHPCBs)

OHPCBs	K_d (μM)
4'-hydroxy-4-monochlorobiphenyl (4'-OHPCB 3)	3.48 ± 1.03
4-hydroxy-3,5-dichlorobiphenyl (4-OHPCB 14)	2.55 ± 0.63
4-hydroxy-3,3'5'-tricrobiphenyl (4-OHPCB 36)	2.46 ± 0.43
4-hydroxy-2',3,5-trichorobiphenyl (4-OHPCB 34)	2.21 ± 0.44
4'-hydroxy-2,3',4,5'-tetrachlorobiphenyl (4'-OHPCB 68)	2.26 ± 0.33
3',4'-dihydroxy-4-monochlorobiphenyl (3',4'-diOHPCB 3)	1.17 ± 1.11 (K_{d1}) 41.9 ± 74.8 (K_{d2})

Note: The binding data for 3', 4'-diOHPCB 3 fit to a two-site, nonspecific binding curve, others fit to a one-site nonspecific binding curve

In order to rule out the possibility of an interaction between ANS and OHPCBs, an experiment was carried out with no enzyme, but with 40 μM ANS present. Titration was then carried out with 6'-OHPCB 35 (one of the OHPCB that showed the unique changes in fluorescence). The result showed that there was no direct interaction between 6'-OHPCB 35 and ANS (Figure 36), because an increase in fluorescence with increasing concentration of 6'-OHPCB 35 was not observed under these conditions.

Further explanations for the multiphasic binding observed with some of the OHPCBs were explored. The initial binding in all cases would be the displacement of ANS bound to the hydrophobic active site of hSULT2A1 due to the fact that upon titration with OHPCBs a decrease in fluorescence would be seen as ANS moves from the active site to the aqueous environment. Further titration with higher concentrations of OHPCBs, might cause a conformational change of the hSULT2A1 where ANS would be

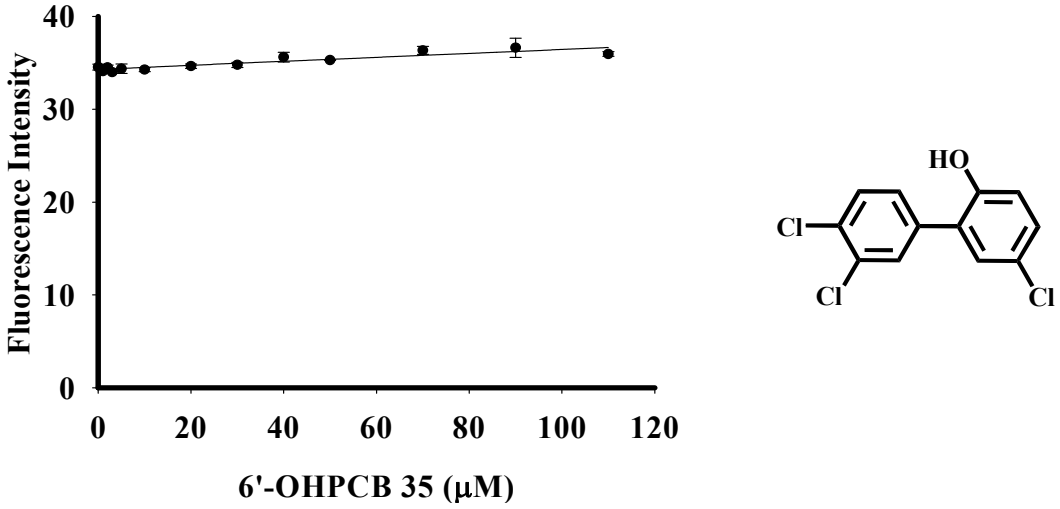

Figure 36. Fluorescence intensity of 40 μM ANS following addition of increasing concentrations of 6'-OHPCB 35 in the absence of enzyme.

able to bind to other sites, and an increase in fluorescence would be observed. As even higher concentrations of OHPCB were reached, ANS might be displaced once more as additional OHPCB molecules bound to the enzyme. A schematic description of this process is seen in Figure 37.

Another explanation for this multiphasic binding seen with some OHPCBs could be as a result of pi-pi interactions. First there might be displacement of ANS by OHPCB from the active site, then binding of ANS to the enzyme-OHPCB complex resulting in pi-pi interactions between the OHPCB and ANS. This might be followed by another molecule of OHPCB coming in to displace ANS resulting in two OHPCB molecules bound simultaneously at the active site.

Additional explanations of the multiphasic binding observed with some OHPCBs would include differential binding to enzyme-substrate and/or enzyme-product complexes such as E-DHEA and E-PAP. The same binding profiles obtained for those

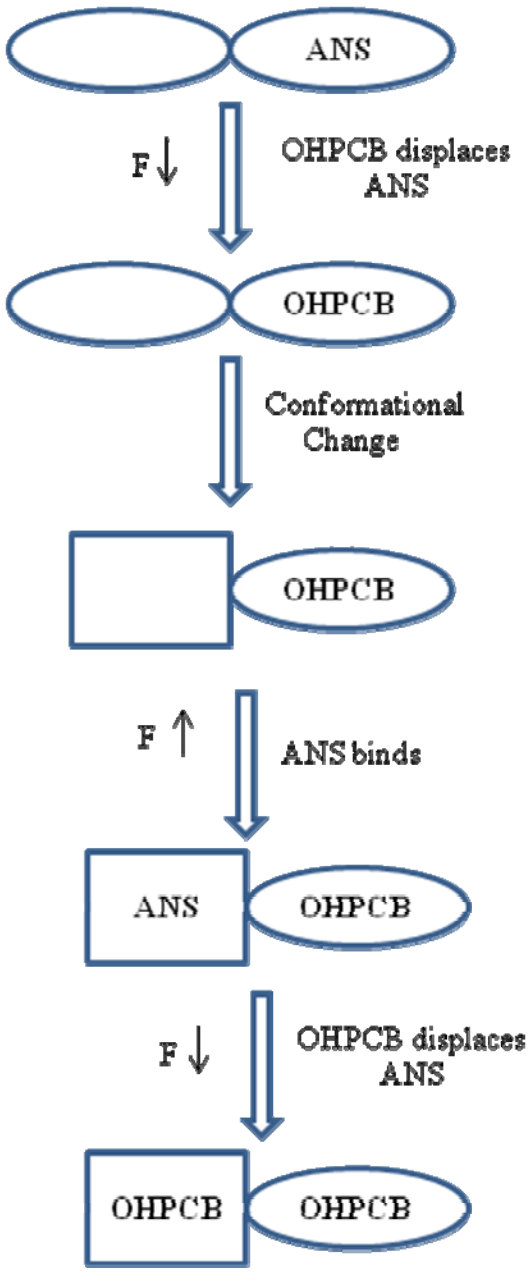

Figure 37. Cartoon representation of the potential mechanism for binding of OHPCBs to hSULT2A1. F is fluorescence intensity, ANS is the probe molecule.

OHPCBs showing multiphasic binding to the free enzyme were also obtained for E-DHEA and E-PAP complexes (Figure 38). Reasonable K_d values were not obtained for these PCB metabolites.

The binding of two OHPCBs (4-OHPCB 14 and 4-OHPCB 34) suggests that binding to E-PAP complex is similar to binding to the free enzyme based on the K_d values obtained, however the total fluorescence intensity is different (Figure 39). The K_d value for binding to E-PAP complex is 2.21 ± 0.50 μM for 4-OHPCB 14 (compared to K_d = 2.55 ± 0.63 μM for binding to free enzyme) and 3.20 ± 0.31 μM for 4-OHPCB 34 (compared to K_d = 2.07 ± 0.30 μM for binding to the free enzyme).

As seen in Figure 39, in the presence of PAP there is more displacement of ANS than in the absence of PAP. This could be explained based on the structure of the enzyme. hSULT2A1, like other sulfotransferases, is a homodimer with two DHEA binding sites and two PAP binding sites. Therefore, in the E-PAP conformation, there could be a conformational change that allows ANS to be displaced by OHPCBs from the two subunits of the hSULT2A1 dimer resulting in the increase in the total fluorescence intensity observed. Moreover, in the first crystal structure solved for hSULT2A1 with bound PAP, the authors showed that "a possible dimer-directed conformational alteration may regulate the activity of hSULT2A1" (*150*).

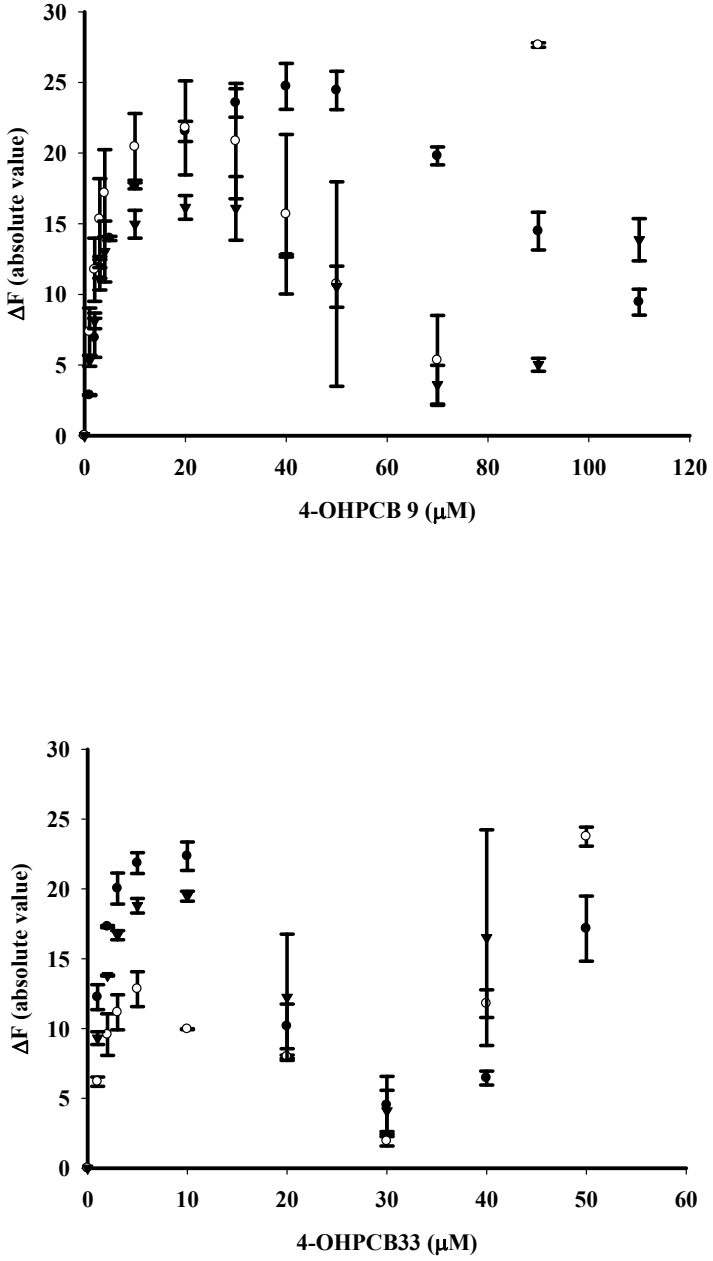

Figure 38. Binding of OHPCB 9 and OHPCB 33 to free enzyme, E-PAP, and E-DHEA complexes. Assays done in the presence of (▼) enzyme only, (●) enzyme and PAP (200 μM), (○) enzyme and DHEA (1 μM). Plots of the absolute value of the fluorescence change versus OHPCBs concentration are shown. Assays were carried out with a saturating concentration of ANS (40 μM). Data points are the mean ± standard error of triplicate determinations.

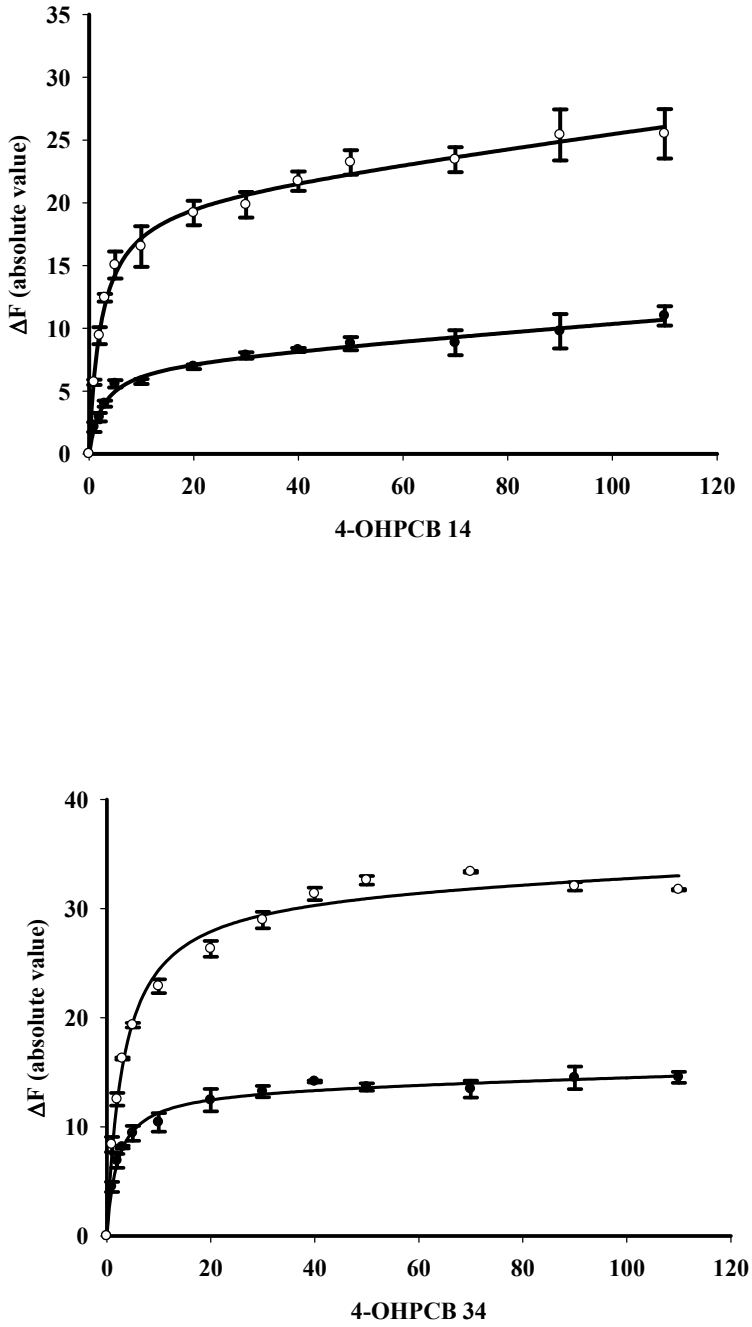

Figure 39. Comparison of binding of 4-OHPCB 14 and 4-OHPCB 34 to different forms of the enzyme (hSULT2A1). Assays done in the presence of (●) free enzyme, and (○) E-PAP complex. Plots of the absolute value of the fluorescence change versus OHPCBs concentration are shown. Assays were carried out with a saturating concentration of ANS (40 μM) and a saturating concentration of PAP (200 μM). Data points are the mean ± standard error of triplicate determinations.

Modeling of Substrate and Inhibition Interactions with hSULT2A1

From the ANS-displacement experiments, 4'-OHPCB 9 and 4'OHPCB 33 showed similar binding patterns with the free enzyme, and with the enzyme-substrate complexes (E-DHEA and E-PAP). Although the K_d values for the binding of 4-OHPCB 14 and 4-OHPCB 34 to the E-PAP complex were similar to that of the free enzyme, the decrease in fluorescence intensity upon displacement of ANS was different. In order to gain better understanding of how OHPCBs bind to hSULT2A1 and to explain what we observed in the ANS-displacement studies, molecular docking experiments were carried out using two crystal structures: hSULT2A1 with bound DHEA (1J99) (*158*) and hSULT2A1 with bound PAP(1EFH) (*150*). The bound DHEA and PAP molecules were removed from the crystal structures before docking studies were carried out and then redocked (cognate docking) into the crystal structures. From among those with multiphasic binding to hSULT2A1 two OHPCBs (4'-OHPCB 9 and 4'-OHPCB 33) were selected, and two OHPCBs (4-OHPCB 14 and 4-OHPCB 34) that displayed classical single-site binding characteristics were also used in the docking experiments. These experiments were carried out using Surflex-Dock in Sybyl 8.0 (see detailed description of methods in chapter V). In this program, compounds are drawn and placed in different molecular areas within the same file and saved as a multimol2 format. The program then docks one compound at a time into the active site of hSULT2A1, until all the compounds are docked and the best 10 poses obtained. The best total score conformers of each of the docked ligands (ANS, OHPCBs, DHEA, and PAP) were selected based on a consensus score of 3 to 5.

When ANS, the fluorescent probe molecule, was docked into hSULT2A1 using the crystal structure which originally had DHEA bound at the active site (PDB code, 1J99), ANS docked at the PAP binding site (Figure 40). However, 4'-OHPCB 9, 4'-OHPCB 33, 4-OHPCB 14 and 4-OHPCB 34 docked at a different site (Figures 41-42).

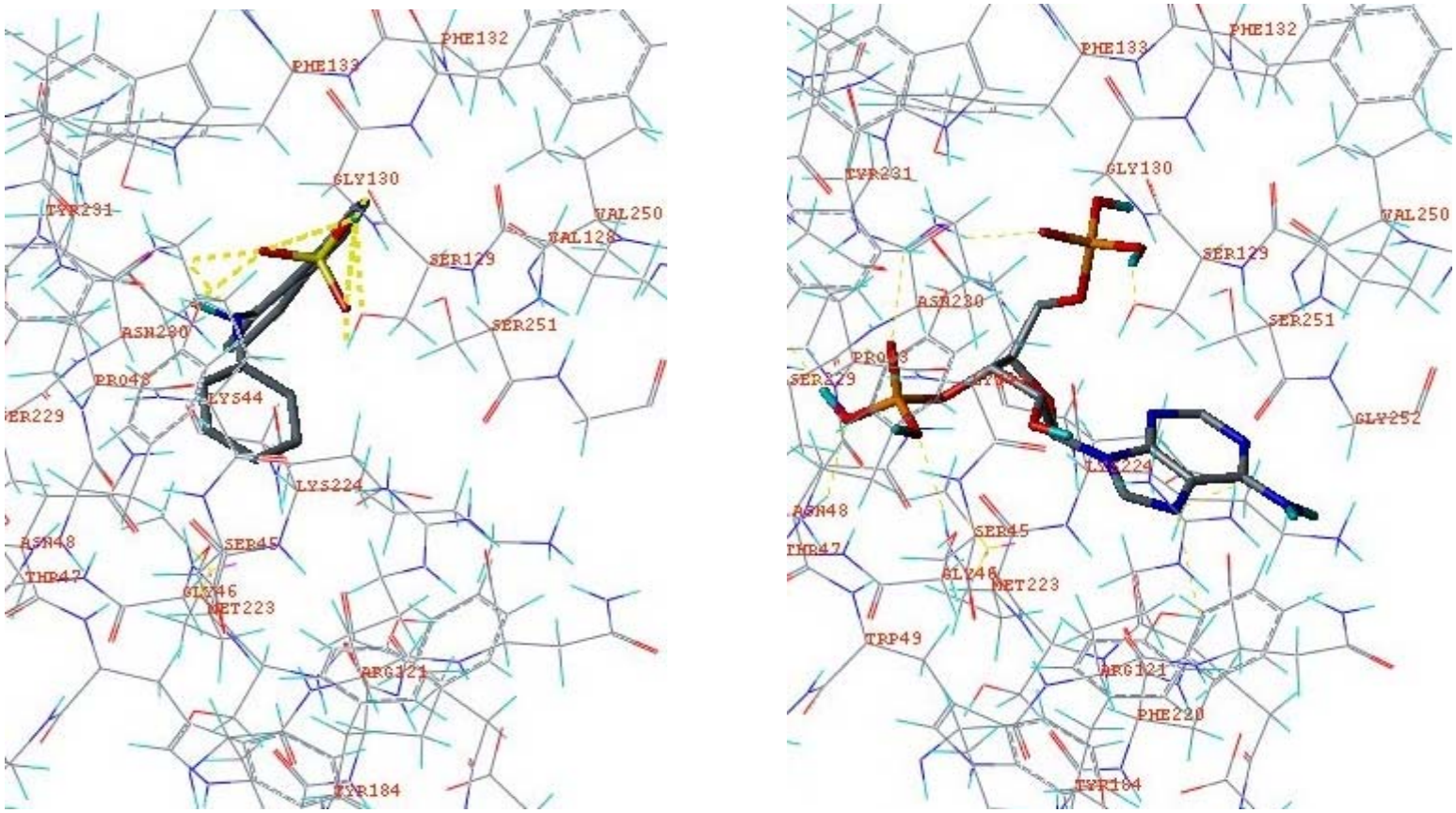

Figure 40. Binding interactions of ANS (left) and PAP (right) with hSULT2A1. ANS binds at the same site as PAP. Hydrogen bonding interactions (yellow dashed lines) and key hSULT2A1 residues interacting with the ligands at the active site are shown. Total score of 3.78 based on a consensus score of 4 for binding of ANS, and total score of 7.80 based on a consensus score of 5 for binding of PAP were obtained. (crystal structure: hSULT2A1 in the conformation observed with DHEA bound (1J99)).

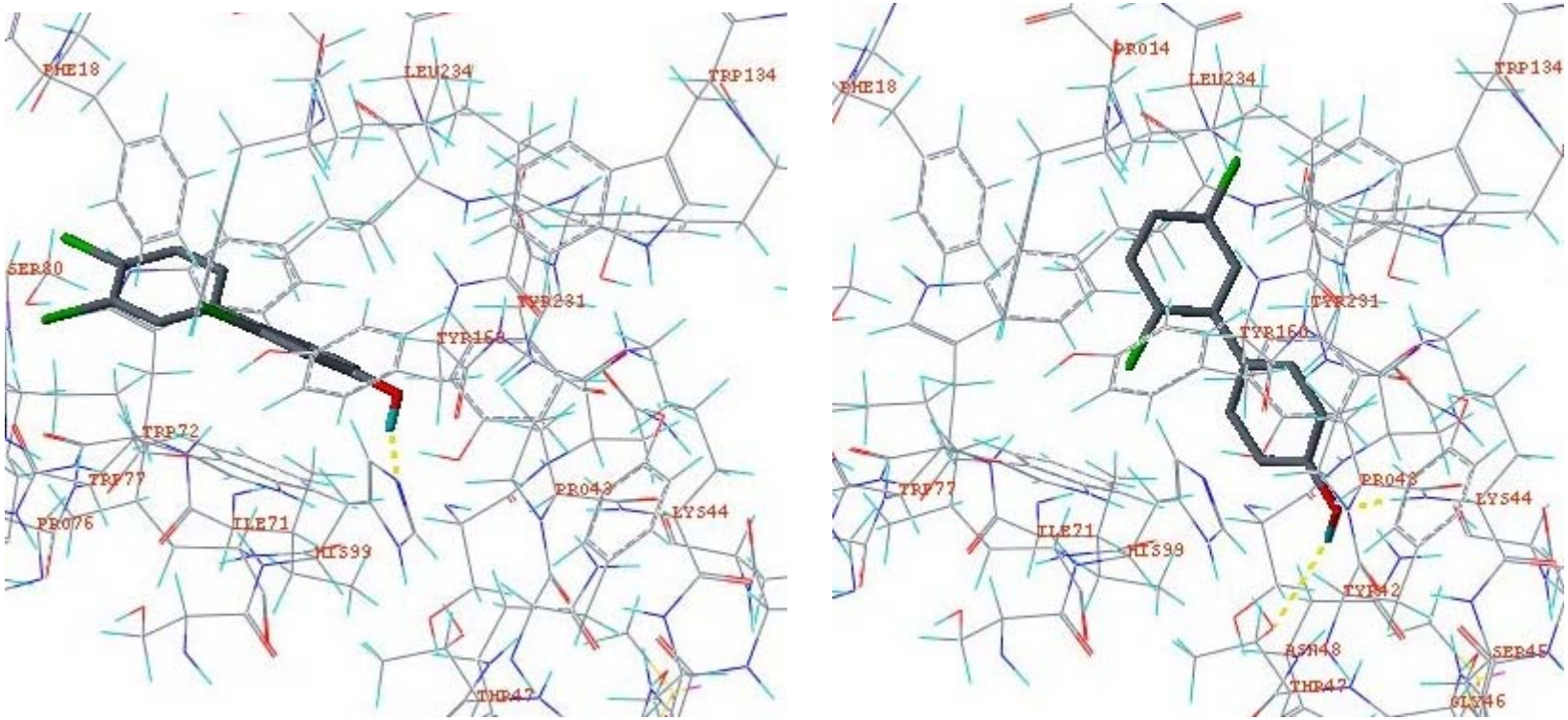

Figure 41. Binding interactions of OHPCBs with hSULT2A1. 4'-OHPCB 33 (left) and 4'-OHPCB 9 (right) bind at the DHEA site. Hydrogen bonding interactions (yellow dashed lines) and key hSULT2A1 residues interacting with the ligands at the active site are shown. Total score of 3.82 based on a consensus score of 5 for binding of 4'-OHPCB 33, and total score of 4.14 based on a consensus score of 5 for binding of 4'-OHPCB 9 were obtained. (crystal structure: hSULT2A1 in the conformation observed with DHEA bound (1J99)).

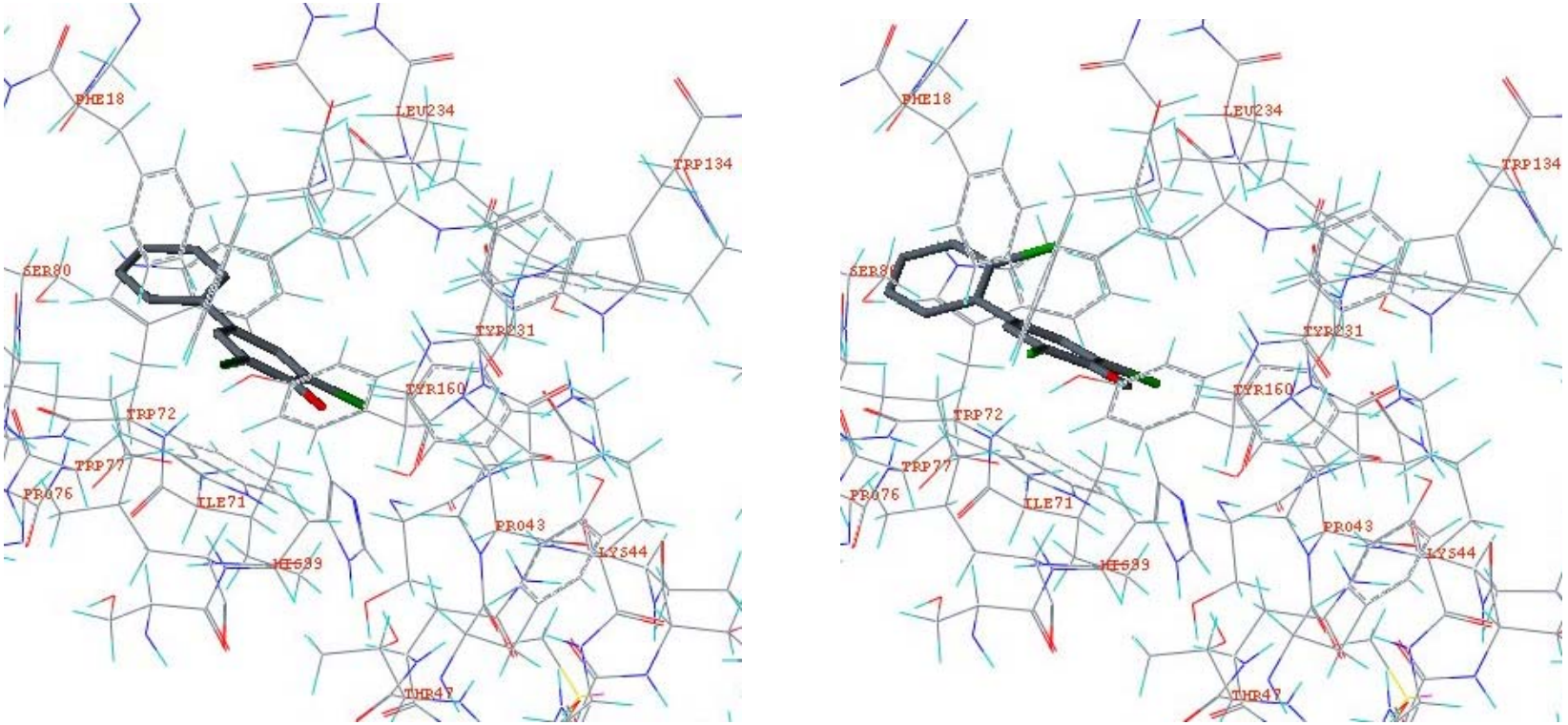

Figure 42. Binding interactions of OHPCBs with hSULT2A1. 4-OHPCB 14 (left) and 4-OHPCB 34 (right) bind at the DHEA site. Key hSULT2A1 residues interacting with the ligands at the active site are shown. Total score of 2.82 based on a consensus score of 2 for binding of 4-OHPCB 14 and a total score of 3.01 based on a consensus score of 5 for binding of 4-OHPCB 34 were obtained. (crystal structure: hSULT2A1 in the conformation observed with DHEA bound (1J99)).

In order to know where these compounds bind (i.e. whether at the DHEA site or at an allosteric site), amino acid residues appearing at a 5Å distance around each docked ligand were labeled and compared to the residues appearing at a 5Å distance around the bound substrate, DHEA (i.e. before extraction of the DHEA) in the original crystal structure of hSULT2A1 (PDB code, 1J99). The residues around the ligands and DHEA were similar. In addition, the extracted DHEA molecule that was docked, bound at the same site as the OHPCBs. Thus the OHPCBs bind at the DHEA site. 4'-OHPCB 9, 4-OHPCB 14, 4'-OHPCB 33 and 4-OHPCB 34 as well as ANS, PAP and DHEA were docked into the crystal structure that had been obtained for hSULT2A1 in complex with PAP (PDB code, IEFH), and all compounds were shown to bind at the DHEA site (Figures 43 to 47). OHPCBs bound similarly to different conformations of the enzyme. The results from these docking experiment support what was seen in the ANS-displacement studies and in the mode of inhibition studies which showed that these compounds are noncompetitive inhibitors of DHEA sulfation that bind at the active site of hSULT2A1.

The crystal structure of hSULT2A1 suggests that the DHEA-binding site might be large enough to accommodate two molecules of OHPCB at the same time. However, there are no crystal structures to support this for hSULT2A1, even though an analogous binding of two substrate molecules has been seen with a family 1 enzyme (i.e. two molecules of p-nitrophenol can occupy the active site of hSULT1A1) (*156*). Since it has been shown that DHEA can bind to hSULT2A1 in two different binding orientations (*158*), we sought to dock two molecules of OHPCB simultaneously into the active site of hSULT2A1. This task was difficult as there are no docking programs available that can dock two ligands simultaneously into the active site of an enzyme. Nevertheless, we tried using Surflex-dock to approximate docking of two molecules of OHPCB simultaneously at the active site of hSULT2A1. This was done by docking one molecule of 4'-OHPCB 33 in the protein in both conformations (crystal structure of hSULT2A1 obtained in presence of DHEA; 1J99, and crystal structure of hSULT2A1 obtained in the presence

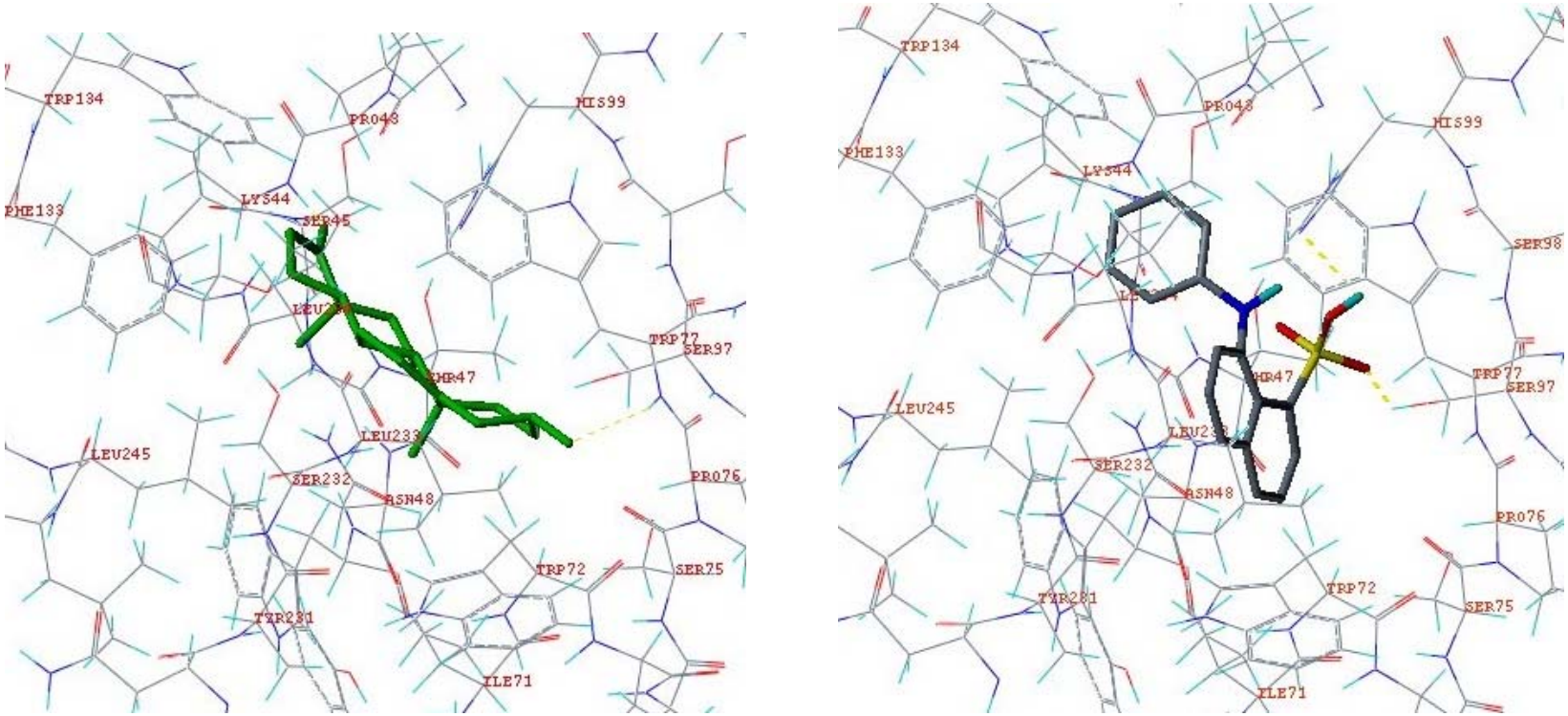

Figure 43. Binding interactions of DHEA (left) and ANS (right) with hSULT2A1. ANS binds at the same site as DHEA. Hydrogen bonding interactions (yellow dashed lines) and key hSULT2A1 residues interacting with the ligands at the active site are shown. Total score of 3.96 based on a consensus score of 3 for binding of DHEA, and total score of 4.22 based on a consensus score of 3 for binding of ANS were obtained. (crystal structure: hSULT2A1 in the conformation observed with PAP bound (1EFH)).

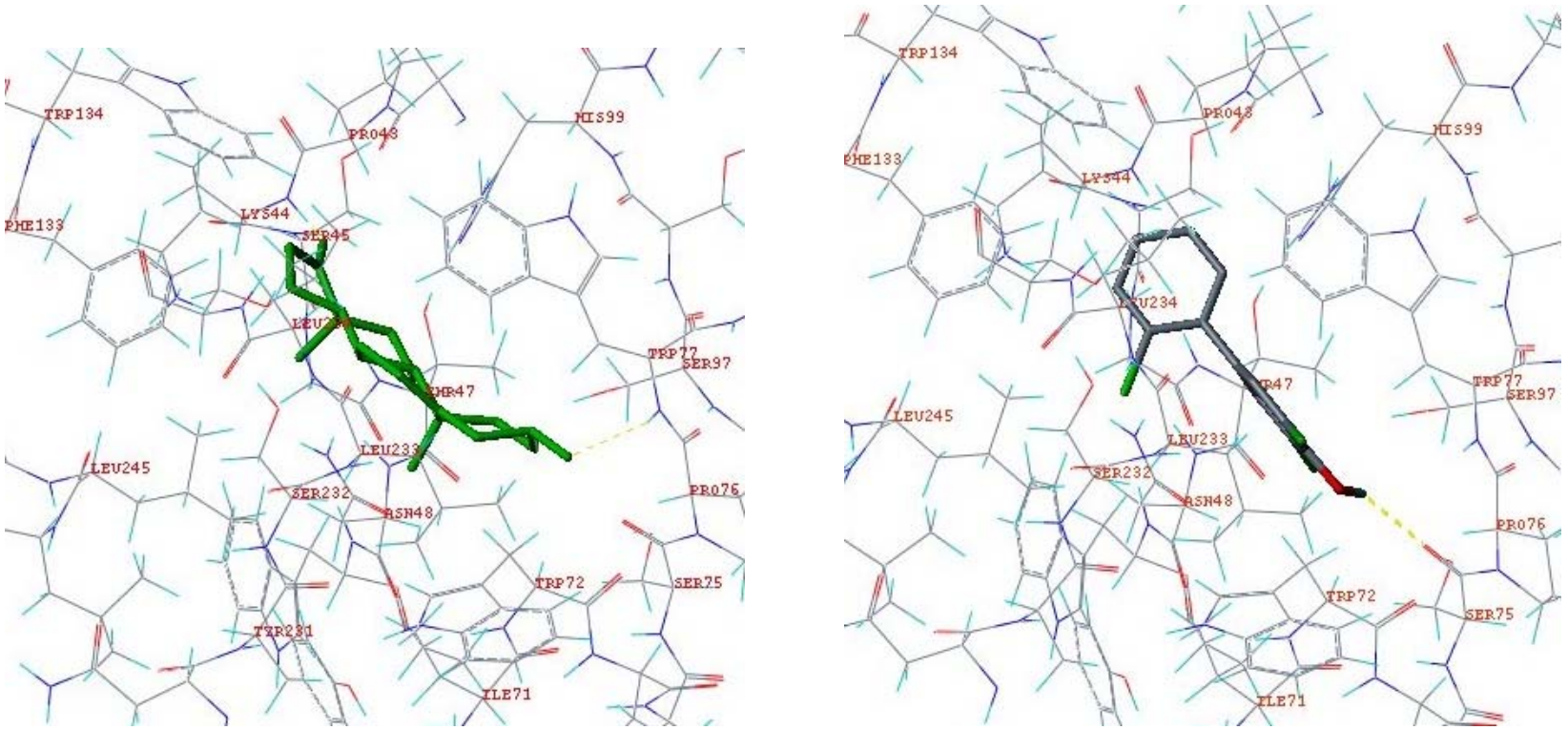

Figure 44. Binding interactions of OHPCBs with hSULT2A1. DHEA (left) and 4-OHPCB 34 (right) bind at the same site. Hydrogen bonding interactions (yellow dashed lines) and key hSULT2A1 residues interacting with the ligands at the active site are shown. Total score of 3.96 based on a consensus score of 3 for binding of DHEA, and total score of 3.63 based on a consensus score of 5 for binding of 4-OHPCB 34 were obtained. (crystal structure: hSULT2A1 in the conformation observed with PAP bound (1EFH)).

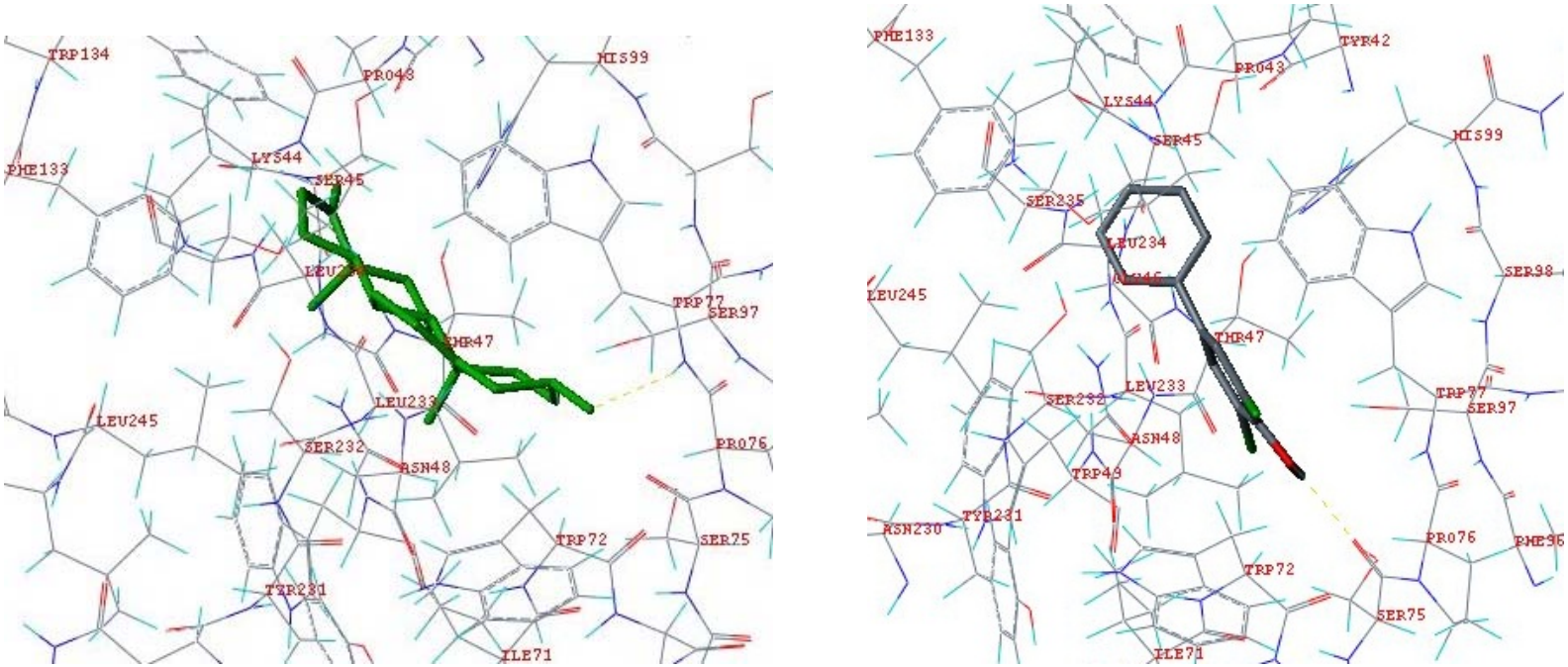

Figure 45. Binding interactions of OHPCBs with hSULT2A1. DHEA (left) and 4-OHPCB 14 (right) bind at the same site. Hydrogen bonding interactions (yellow dashed line) and key hSULT2A1 residues interacting with the ligands at the active site are shown. Total score of 3.96 based on a consensus score of 3 for binding of DHEA, and total score of 3.82 based on a consensus score of 5 for binding of 4-OHPCB 14 were obtained. (crystal structure: hSULT2A1 in the conformation observed with PAP bound (1EFH)).

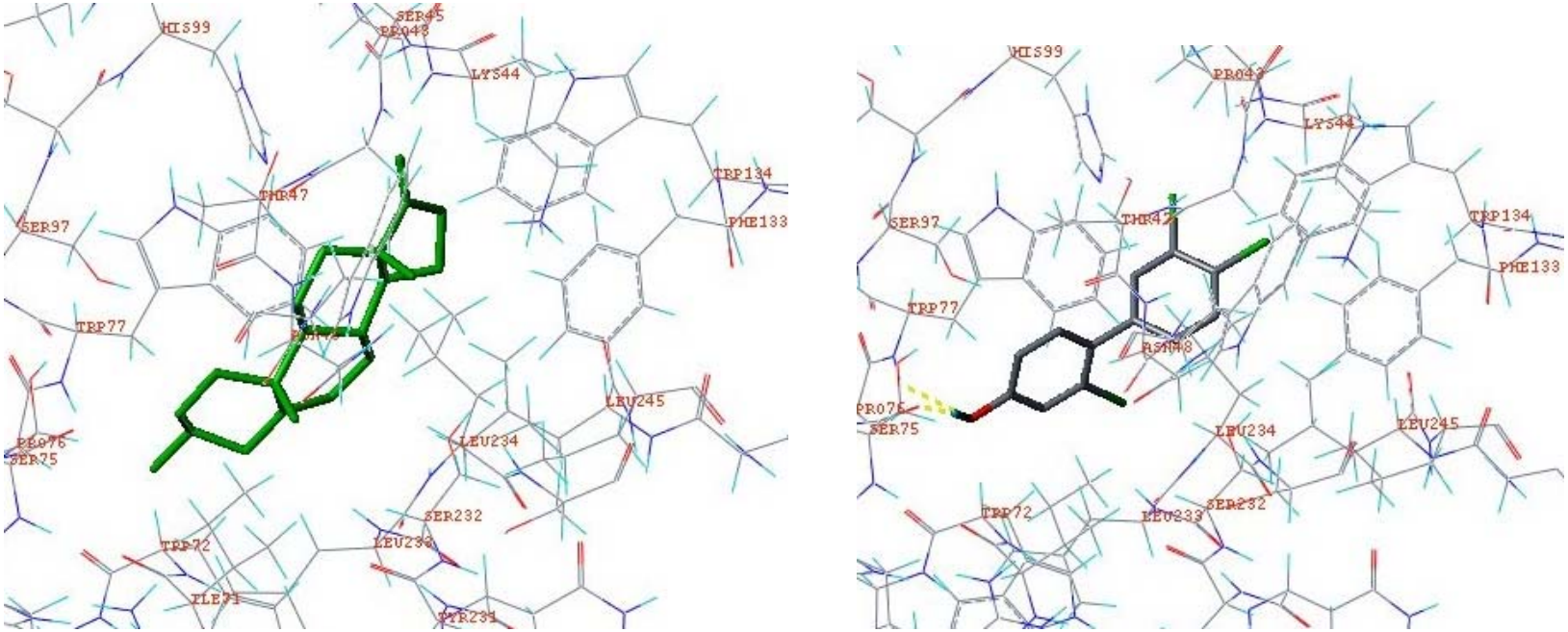

Figure 46. Binding interactions of OHPCBs with hSULT2A1. DHEA (left) and 4'-OHPCB 33 (right) bind at the same site. Hydrogen bonding interactions (yellow dashed lines) and key hSULT2A1 residues interacting with the ligands at the active site are shown. Total score of 3.96 based on a consensus score of 3 for binding of DHEA, and total score of 4.03 based on a consensus score of 5 for binding of 4'-OHPCB 33 were obtained. (crystal structure: hSULT2A1 in the conformation observed with PAP bound (1EFH)).

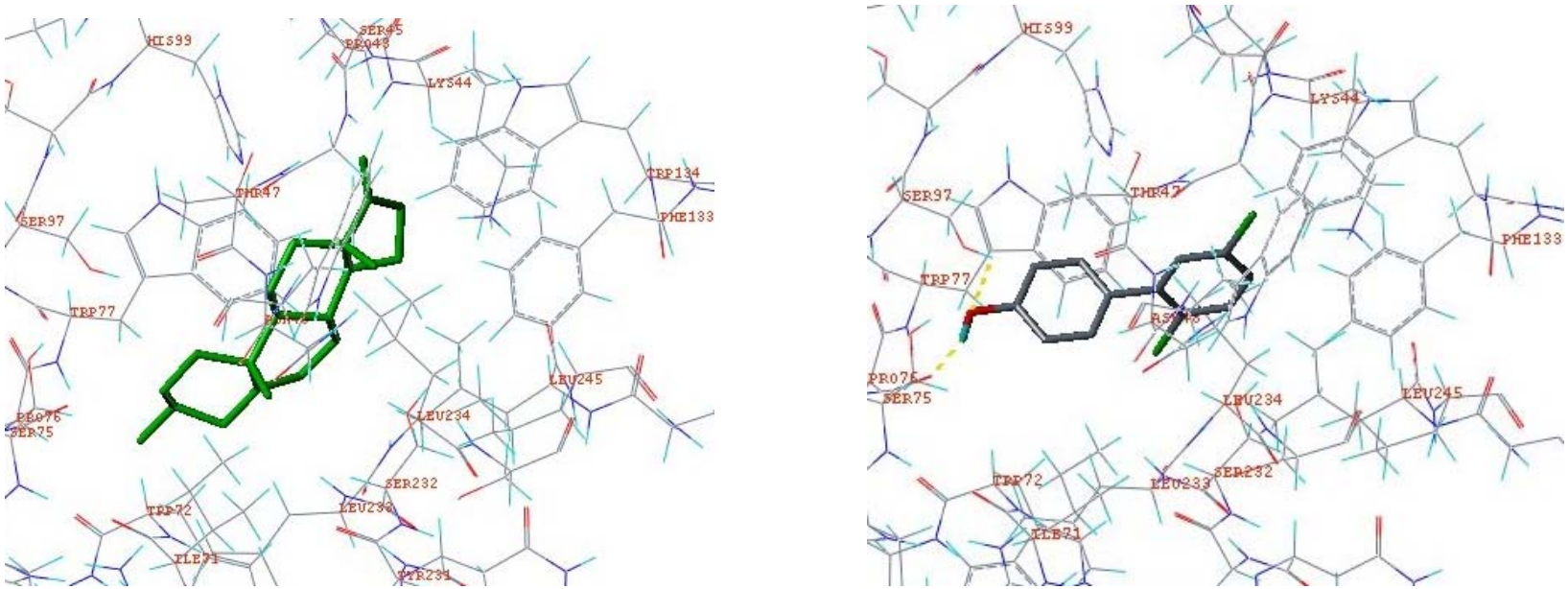

Figure 47. Binding interactions of OHPCBs with hSULT2A1. DHEA (left) and 4'-OHPCB 9 (right) bind at the same site. Hydrogen bonding interactions (yellow dashed lines) and key hSULT2A1 residues interacting with the ligands at the active site are shown. Total score of 3.96 based on a consensus score of 3 for binding of DHEA, and total score of 4.42 based on a consensus score of 4 for binding of 4'-OHPCB 9 were obtained. (crystal structure: hSULT2A1 in the conformation observed with PAP bound (1EFH)).

of PAP; 1EFH) and, after merging this compound onto both protein conformations, we saved them as new protein structure files. The saved protein structures with the merged 4'-OHPCB 33 were then used to dock another molecule of 4'-OHPCB 33. The merged ligand occupied the DHEA binding sites in both conformations and, since the sites were large enough, we hypothesized that another molecule of 4'-OHPCB 33 will also dock at these sites. Although, this could explain the multiphasic binding patterns seen with some of the OHPCBs, it was not the case. The second 4'-OHPCB 33 docked at the PAP-binding sites in both conformations, because the DHEA sites were already fully occupied (Figures 48 to 49).

According to the modeling results and the ANS-displacement assays, ANS bound at the DHEA site in the E-PAP complex, and OHPCBs displaced ANS from the DHEA binding site. From the docking studies, when the enzyme was in the DHEA-bound conformation, ANS bound at the PAP site. Therefore, in the free enzyme, ANS could bind at the PAP site and the DHEA site at the same time, and OHPCBs are able to displace two molecules of ANS. In addition, from the enzyme kinetic data, an OHPCB was a partial competitive inhibitor and three OHPCBs were partial noncompetitive inhibitors meaning that some amount of product could still be formed in the presence of these inhibitors. Eleven OHPCBs were full noncompetitive inhibitors, and they completely blocked enzyme activity, so no product could be formed. The noncompetitive inhibition observed by the OHPCBs is consistent with binding of the inhibitors to both the PAPS and DHEA binding sites, depending upon the enzyme conformation that results from binding either PAPS or DHEA first. This also explains what was observed in the ANS-displacement assays, as some of the OHPCBs showed multiphasic binding patterns.

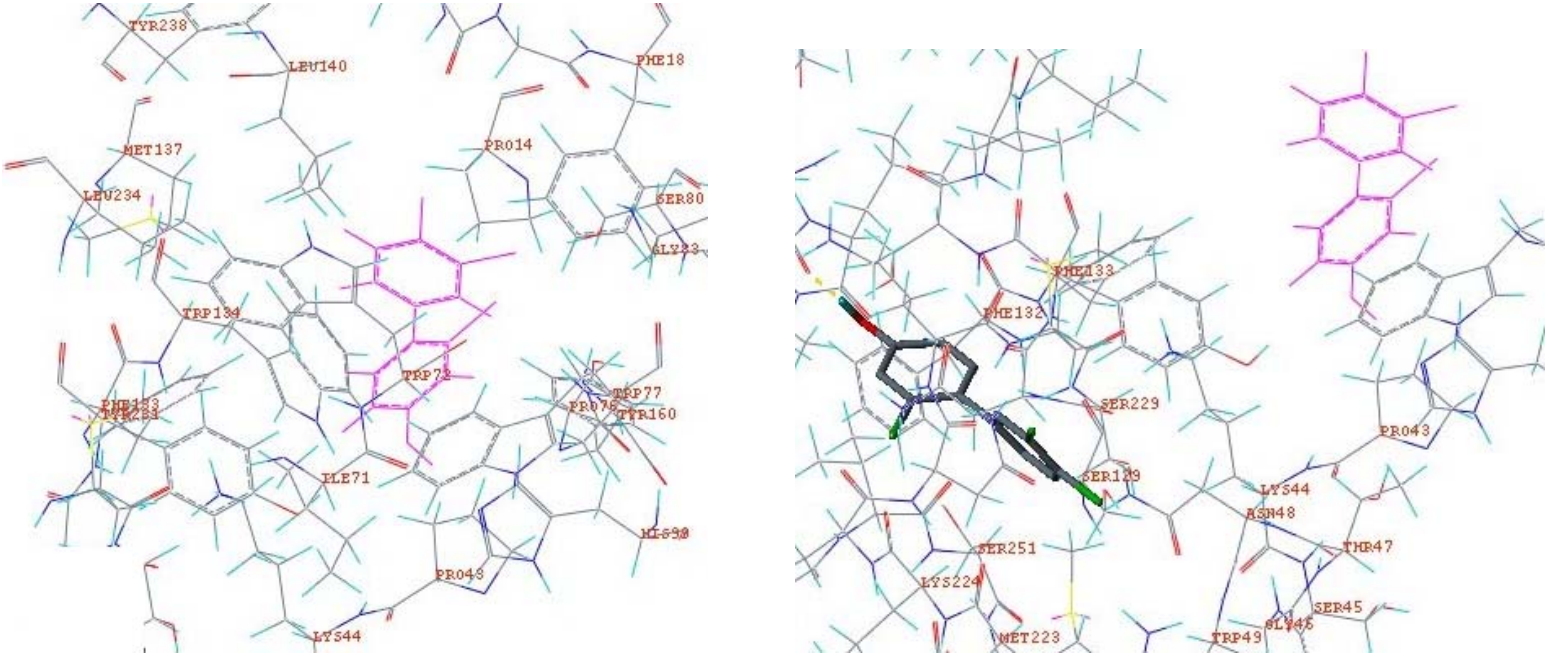

Figure 48. Binding interactions of two molecules of 4'-OHPCB 33. 4'-OHPCB 33 (in magenta with hydrogen atoms shown) was docked in hSULT2A1 in the DHEA conformation (1J99), merged and saved as a new protein structure file. A second 4'-OHPCB 33 was docked into the protein that was merged with 4'-OHPCB33. The first 4'-OHPCB 33 occupied the DHEA binding site and amino acid residues around it were manually labeled (left), and the second 4'-OHPCB33 docked at the PAP binding site and amino acid residues were manually labeled (right). Total score of 2.84 based on a consensus score of 3 for binding of the second 4'-OHPCB 33 was obtained.

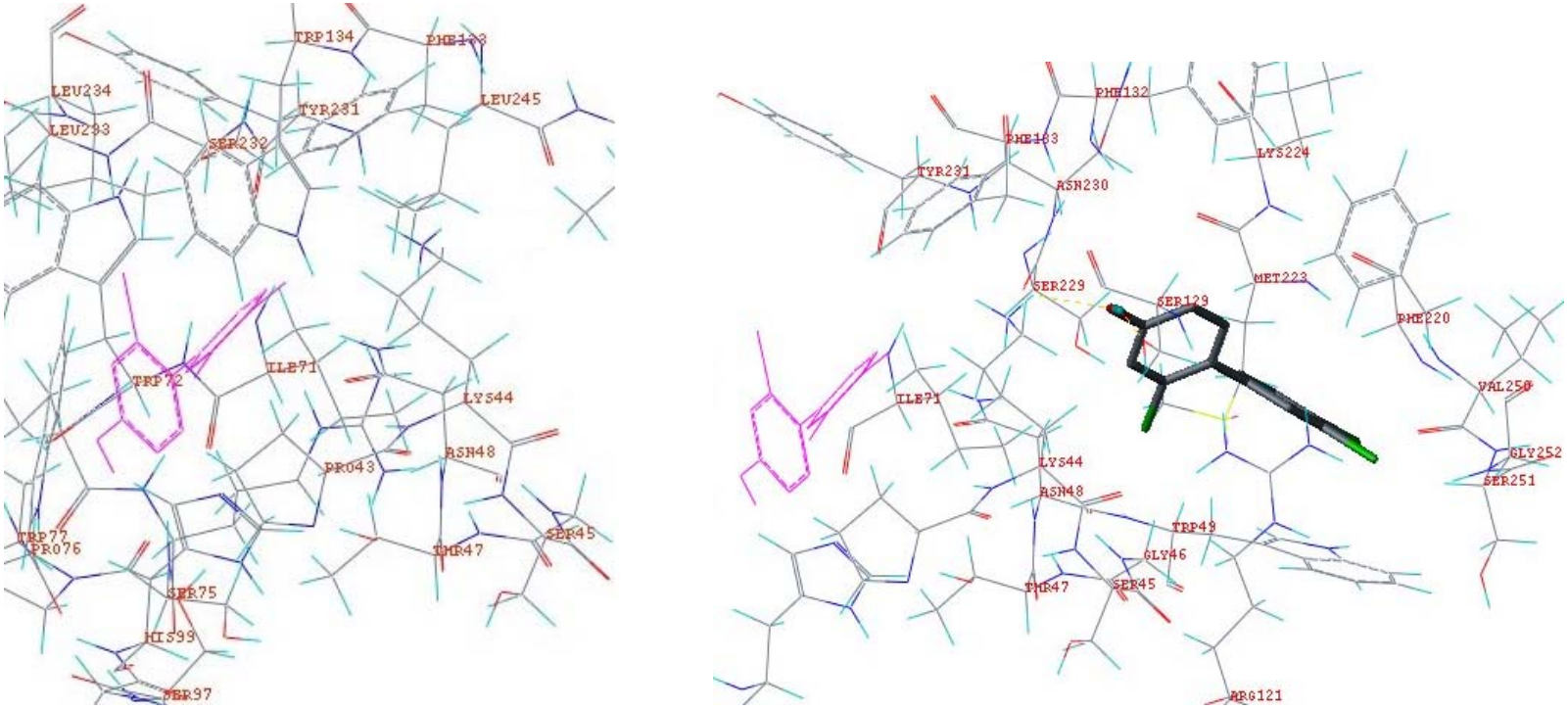

Figure 49. Binding interactions of two molecules of 4'-OHPCB 33. 4'-OHPCB 33 (in magenta) was docked in hSULT2A1 in the PAP conformation (1EFH), merged and saved as a new protein structure file. A second 4'-OHPCB 33 was docked into the protein that was merged with 4'-OHPCB33. The first 4'-OHPCB 33 occupied the DHEA binding site and amino acid residues around it were manually labeled (left), and the second 4'-OHPCB33 docked at the PAP binding site and amino acid residues around it were manually labeled (right). Total score of 3.85 based on a consensus score of 3 for binding of the second 4'-OHPCB 33 was obtained.

CHAPTER IV

CONCLUSIONS

We live in a world of constant exposure to environmental pollutants. Some of these pollutants are industrial chemicals such as the polychlorinated biphenyls (PCBs). Some PCBs and their hydroxylated metabolites (OHPCBs) have been shown to be retained in the serum and plasma of humans and animals, and to cause adverse health effects. For example, they mimic endogenous hormones and disrupt endocrine function *(85, 142)*. Toxicity of PCBs can also be a result of their binding to drug metabolizing enzymes with subsequent formation of reactive metabolites that can then interact with DNA and proteins leading to carcinogenesis *(70)*.

The focus of this dissertation is on the hydroxylated metabolites of lower chlorinated PCBs, whose parent compounds have been found in urban and indoor air, and their interaction with the drug metabolizing enzymes known as sulfotransferases. Exposure to lower chlorinated PCBs through inhalation is a potential route of toxicity to humans. The number of chlorine atoms and the positioning of those atoms are determinants of the toxicity of PCBs and their hydroxy metabolites (*210*). Assessing the toxicity of these compounds on the basis of their structural characteristics therefore becomes highly important. We have developed a 3D-QSAR model to study the reversible reaction of PCB hydroxylated metabolites (OHPCBs) with hSULT2A1, an enzyme known to be important in metabolism of hydroxysteroids, bile acids and xenobiotics. This model may assist in predicting which lower chlorinated PCB congeners would potentially pose a threat to human health through mechanisms involving interactions with hSULT2A1.

In order to develop this 3D-QSAR model, it was first necessary to determine inhibition constants for OHPCBs in the hSULT2A1-catalyzed sulfation of DHEA. The inhibition studies showed that all 15 hydroxylated PCB metabolites we tested disrupted the activity of the enzyme (hSULT2A1) catalyzing the sulfation of DHEA. However,

those OHPCBs with the 3, 5-dichloro-4-hydroxy substitutions proved to be the most potent inhibitors. We then investigated the 15 OHPCBs as potential substrates for the enzyme and found out that seven of these OHPCBs were substrates, and OHPCBs that possess the 3, 5-dichloro-4-hydroxy substitution pattern were the best substrates for hSULT2A1. OHPCBs as alternate substrates can compete with DHEA for the active site of hSULT2A1, and this can ultimately lead to inhibition of DHEA sulfation.

Since we knew these compounds inhibit DHEA sulfation, and we knew which of the OHPCBs served as alternate substrates, we proceeded to develop our 3D-QSAR model. The model had good predictive power with a q^2 value of 0.697. This proves that the model is useful, and it can provide experimentally testable predictions of activity of other hydroxylated PCBs. The model highlighted structural requirements that may be important in the toxicity of these compounds. For example, the 3, 5-dichloro-4-hydroxy-substitution pattern with an ortho chlorine substitution at the ring junction seems to be very important, as OHPCBs having this substitution pattern had the highest inhibitory effect on the sulfation of DHEA catalyzed by hSULT2A1. Moreover, these OHPCBs were the best substrates for hSULT2A1. The knowledge gained from the methodology for developing this model can be extended to other models based on OHPCB metabolites that are similar in structure and chemical properties. Such models may be useful in predicting interactions of OHPCBs with other isoforms of sulfotransferases in humans.

Sulfation of OHPCBs to their corresponding sulfates may lead to their metabolic excretion, or it might lead to their retention in the body. Some PCB sulfates may retain significant lipophilic properties based on their calculated octanol/water partition coefficients (*80*), and they may not be readily eliminated. Furthermore, there is evidence of increased toxicity with sulfates of other compounds. For example, indoxyl sulfate, a known circulating uremic toxin, not only promotes progression of glomerular necrosis, but also leads to renal failure and its concentration in uremic patients is exceedingly high (*211-212*). The sulfate ester of α-hydroxy tamoxifen is also highly toxic and has been

linked to endometrial cancer in breast cancer patients treated with its parent compound, tamoxifen (*102, 213*).

Conclusions made from the model developed in this dissertation, as with any model, are based on assuming that similar OHPCBs will have similar effects in biological systems of interest. The model that was derived here, although having good predictive power, has some limitations. The model did not include highly chlorinated hydroxy PCB metabolites and/or strictly non-coplanar hydroxy PCB metabolites (i.e. OHPCBs containing two or more ortho chlorine atoms at the ring junction) which may have different structural requirements important for their toxicity. One problem with trying to use this model to predict the activity of highly chlorinated PCB metabolites towards hSULT2A1 is that their activities cannot be experimentally verified with the current methodology due to the solubility limit of higher chlorinated OHPCBs in our test system, as we saw with 4-OHPCB 165.

In addition to the above, we also investigated the mechanism of inhibition and found that all 15 compounds were noncompetitive inhibitors of DHEA sulfation. The noncompetitive nature of these compounds was also seen when we did the binding studies using ANS-displacement assay. Although, some of the OHPCBs tested showed similar binding to the free enzyme, and enzyme-substrate complexes, the decrease in fluorescence intensity upon displacement of ANS was different. Others were also shown to bind similarly with all forms of the enzyme but exhibited multiphasic binding characteristics. To further understand what we had observed in the ANS-displacement studies and the kinetic assays for determining the mechanism of inhibition, we carried out modeling studies on the interaction of OHPCBs with SULT2A1. We used two crystal structures of SULT with different conformations i.e. a crystal structure with bound substrate, DHEA (1J99) *(145)*, and a crystal structure with bound PAP (1EFH) *(137)*, and the results showed that OHPCBs bind similarly to different conformations of the enzyme.

One explanation in relation to OHPCBs binding to active site of the enzyme, and yielding a noncompetitive inhibition pattern could be partly due to the enzyme, hSULT2A1, following a compulsory ordered substrate binding and product release in the presence of PAP or 200 μM PAPS (a saturating concentration of PAPS used in the kinetic assays for mechanism of inhibition). Therefore, the noncompetitive inhibition pattern observed through the active site docking models may be a result of preferential binding to enzyme-product complex (*187*). Another explanation could be that it is a result of the effect of structural rearrangement in SULT2A1 in the presence of PAPS or PAP on the binding and kinetics of the sulfation of substrates which is not seen in the presence of DHEA (*206*). Thus, the different conformations of the enzyme providing noncompetitive inhibition, even though still binding at the active site, depend upon whether or not PAPS or PAP is bound to the sulfotransferase. Binding at the active site is further confirmed by the fact that those OHPCBs that are substrates for sulfation catalyzed by hSULT2A1 also show noncompetitive inhibition patterns.

Future studies should address toxicity of these lower chlorinated PCB metabolites (OHPCB) *in vivo* using animal models. The models can be most useful if the results from these *in vitro* studies can be correlated to the *in vivo* studies. Animal models using rats might not be as informative for SULT2A1, as others in our laboratory have shown that many of the OHPCBs interact differently with rat SULT2A3, the rat homologue of the human SULT2A1 (*214*). Thus, there is a problem with species differences. It is possible that experiments using mouse models will be preferable to validate and extrapolate the *in vitro* assays to the *in vivo* inhibitory effects of the hydroxy PCB metabolites, although the interaction of OHPCBs with the mouse homologue of human SULT2A1 has not yet been studied. Alternatively, humanized mice could be developed and used to study the interaction of these compounds with hSULT2A1 *in vivo*. Additionally, studies should be done *in vivo* to demonstrate what happens when DHEA sulfation catalyzed by hSULT2A1 is blocked by OHPCBs. Finally, a crystal structure of hSULT2A1 in complex

with OHPCB would be useful to further strengthen the conclusion that these compounds indeed bind at the active site while exhibiting noncompetitive inhibition patterns. Examining the effect of OHPCBs on reactions performed in the reverse direction would further prove that these inhibitors are binding at the DHEA-binding site. However, there is no current evidence for any reverse reaction catalyzed by hSULT2A1.

In summary, the research presented in this dissertation has opened multiple new avenues for future work on the roles of sulfotransferases in the metabolism and toxicities of OHPCBs. At the same time it has also provided new insights into the specificities and catalytic function of hSULT2A1, an enzyme that is important in metabolism of both endogenous and xenobiotic molecules.

CHAPTER V

METHODS

Chemicals and reagents

The hydroxylated polychlorinated biphenyls used in this work were provided by Dr. Hans-Joachim Lehmler in the Department of Occupational and Environmental Health at the University of Iowa. 4'-hydroxy-4-monochlorobiphenyl (4'-OHPCB 3), 4'-hydroxy-2, 5-dichlorobiphenyl (4'-OHPCB 9), 4-hydroxy-3, 3'-dichlorobiphenyl (4-OHPCB 11), 4'-hydroxy-3, 4-dichlorobiphenyl (4'-OHPCB 12), 4-hydroxy-3, 5-dichlorobiphenyl (4-OHPCB 14), 4'-hydroxy-2, 3', 4-trichlorobiphenyl (4'-OHPCB 25), 4-hydroxy-2', 3, 5-trichlorobiphenyl (4-OHPCB 34), 6'-hydroxy-3, 3', 4-trichlorobiphenyl (6'-OHPCB 35), 4-hydroxy-3, 3', 5'-trichlorobiphenyl (4-OHPCB 36), 4'-hydroxy-2, 3', 4, 5'-tetrachlorobiphenyl (4'-OHPCB 68), 3', 4'-dihydroxy-2, 3,-dichlorobiphenyl (3',4'-diOHPCB 5) and 3', 4'-dihydroxy-4-monochlorobiphenyl (3',4'-diOHPCB 3) were synthesized as described previously (*215*). The synthesis of three additional 4-hydroxy PCB metabolites, 4'-hydroxy-2' 3, 4-trichlorobiphenyl (4'-OHPCB 33), 4'-hydroxy-2, 3'-dichlorobiphenyl (4'-OHPCB 6), 4- hydroxy-2, 4'-dichlorobiphenyl (4-OHPCB 8), have also been reported (*214*).

Bacto tryptone and yeast extract were purchased from Becton Dickinson, Co. (Sparks, MD). Sodium Chloride (NaCl), chloroform ($CHCl_3$), anhydrous sodium sulfate, and sucrose were purchased from Fisher Scientific (Pittsburgh, PA). Sodium hydroxide (NaOH), glycerol, methylene blue, acetone, potassium phosphate monobasic (KH_2PO_4), 2-mercaptoethanol, phenylmethylsulfonyl fluoride, dehydroepiandrosterone (DHEA), antipain, pepstatin A, 8-anilino-1-naphthalene sulfonic acid (ANS), adenosine 3', 5'-diphosphate (PAP), and 3'-phosphoadenosine 5'-phosphosulfate (PAPS) were from Sigma-Aldrich (St. Louis, MO). PAPS was further purified (> 98% by HPLC) using a previously published procedure (*216*). ^{3}H-DHEA (94.5 Ci/nmol) was obtained from Perkin Elmer Life and Analytical Sciences (Boston, MA). Bovine serum albumin (BSA)

and hydroxyapatite (Bio-Gel HT) were from Bio-Rad Laboratories (Hercules, CA). DE52 was from Whatman (Fairfield IL). Tween 20 was purchased from J.T. Baker Chemicals (Philipsburg, NJ). Isopropyl-1-thio-D-galactopyranoside (IPTG) was from AMRESCO Inc (Solon, OH). Ampicillin, dithiothreitol (DTT), tris (hydroxymethyl)aminomethane hydrochloride (Tris-HCL), and Econo-Safe biodegradable scintillation cocktail were purchased from RPI (Mt. Prospect, IL). All other chemicals were of highest purity and commercially available.

Protein Expression and cell extract preparation

The expression of hSULT2A1 in recombinant *Escherichia coli* BL21 (DE3) cells and preparation of cell extract was carried out with minor modifications of the procedure described previously by Sheng and Duffel, 2003 (*217*). Luria broth (LB) medium (1.6% Bacto Tryptone (v/v), 1% yeast extract, 0.5% NaCl) was prepared in a 2-L flask and adjusted to pH 7.0 using a NaOH solution. The solution was autoclaved before antibiotic was added. 50 µg/µl of antibiotic (i.e. ampicillin) was sterilized with a 0.22 µm millex-GS membrane filter (Millipore Corporation, Bedford, MA) and added to the medium. Using a sterile micropipette tip, cells were inoculated into 3 mL of this LB buffer contained in a 14 mL culture tube and incubated on a reciprocating shaker (210 rpm) at 28^{o}C for 24 h. A 100 µL aliquot of the resulting cell culture was used to inoculate 20 mL of LB medium in each of four 50 mL culture tubes under sterile conditions, and incubation carried out under the same conditions as above. After the 24 h period, a 20 mL aliquot of each cell culture was used to inoculate 400 mL of sterile LB medium in each of four 1 L unbaffled flasks. The cells were incubated at 28^{o}C and 210 rpm for 1 h, and 1 mM IPTG (isopropyl-1-thio-D-galactopyranoside) was then added. The cells were then incubated for an additional 23 h period. After a total of 24 h, the cell culture from each flask was harvested by centrifugation at 10,000 x g for 30 min. The cell pellet of about 19g (wet weight) was suspended in 20 mL ice-cold buffer A (10 mM Tris-HCL buffer,

pH 7.5, containing 0.25M sucrose, 10% (v/v) glycerol, 1 mM phenylmethyl sulfonyl fluoride, 1 μM pepstatin A, 1 mM dithiothreitol and 3.3 μM antipain). Cells were then placed in a plastic beaker on ice and disrupted by sonication with a Branson Digital Sonifier (model 450, Branson Ultrasonics Corp., Danbury, CT). The sonicator was programmed for 10 s periods of sonication with a pulse sequence of 0.2 s on and 0.2 s off at a power setting of 146 Watts. Cooling intervals of 40 s were used between each of 10 sonication periods. The homogenate was centrifuged using a Sorvall® RC26 Plus centrifuge for 30 min at 12,000 x g. After centrifugation, the supernatant (cell extract) was carefully poured into a 50 mL culture tube and stored at -70^{o}C. A fraction of this homogenate was used for the modified Lowry assay for protein content determination (*218*), and the activity of the crude enzyme cell extract was determined with the methylene blue assay.

Purification of recombinant hSULT2A1

The purification of hSULT2A1 has previously been described by Gulcan *et al.,* 2008 (*173*). 10 mL cell extract was applied to a DE52 column (2.5 × 17 cm) that had been equilibrated with buffer B (50 mM Tris-HCL buffer pH 7.5 containing 0.25 M sucrose, 1 mM DTT, 10% (v/v) Glycerol, 0.05% (v/v) Tween 20). Proteins that were not bound to the column were eluted with buffer B. A 250 mL linear gradient of buffer B and buffer B with 0.5 M KCL was used to elute hSULT2A1, and fractions (of 5 mL in each tube) were collected. With the aid of the methylene blue assay, the fractions with the highest sulfotransferase activity were combined (total of 45 mL) and then concentrated using ultrafiltration (YM10 membrane, Millipore Corporation, Bedford MA). Four successive dilutions with buffer C (10 mM potassium phosphate, 0.25 M sucrose, 1 mM DTT and 0.05% (v/v) Tween 20, pH 6.8) followed by ultrafiltration were used to equilibrate the enzyme. The enzyme (3840 units) was then applied to a hydroxyapatite column (2.5 x 9.0 cm dimension) and proteins that did not bind to the column were

removed by washing with buffer C. Enzyme was then eluted with a linear gradient formed between 200 mL of buffer C and 200 mL of buffer C containing 0.4 M potassium phosphate at pH 6.8. Fractions having the highest hSULT2A1 activity were combined, concentrated, and equilibrated with buffer D (30 mM potassium phosphate, 0.25 M sucrose, 1 mM DTT and 0.05% (v/v) Tween 20, pH 6.8) as described above. The enzyme (2780 units) was then applied to a second hydroxyapatite column that had been equilibrated with buffer D, and non-bound proteins were removed by elution with buffer D. A linear gradient of 75 mL buffer D and 75 mL buffer D containing 0.3 M potassium phosphate at pH 6.8 was used for elution of the enzyme. The fractions with the highest activity were combined and concentrated to 13.5 mL by ultrafiltration. The purified SULT2A1 displayed a single band on SDS-PAGE with Coomassie blue staining. The protein content was determined using a previously described procedure (*218*) with bovine serum albumin as standard.

Methylene Blue Assay

During purification, human hydroxysteroid sulfotransferase activity was determined using a previously described assay (*219-220*). The chloroform extraction of an ion-pair formation occurring between methylene blue and DHEA-sulfate (or any other hydrophobic sulfate of interest) is used in this method. Reaction mixtures contained 0.2 mM PAPS, 5 mM 2-mercaptoethanol, 0.25 M sodium acetate at pH 5.5, 0.05 mM DHEA 5% (v/v) acetone. Assays were started by addition of enzyme with appropriate concentrations of cytosolic protein (during the purification process) or purified enzyme at 37^{o}C, and incubated for 15 min for cytosolic protein and 10 min for purified protein. The assays were then terminated by the addition of 0.5 mL of methylene blue immediately followed by addition of 2 mL chloroform. After mixing thoroughly with a vortex mixer for 20 s, the two layers were separated by centrifugation at 2000 x g for 10 min. The lower layer (chloroform) was transferred carefully to tubes containing approximately 50

mg of anhydrous sodium sulfate, mixed with the vortex mixer, and the absorbance read at 651 nm. Enzyme specific activities were expressed as nmoles/min/mg of protein using equation 5.

$$\text{Specific activity} = \frac{(\text{sample } A_{651} - \text{control } A_{651}) \times 10 \text{ nmoles}}{0.3\ A_{651} \text{ units} \times \text{time (min)} \times \text{mg of protein}} \qquad (5)$$

Radiochemical Assays

Inhibition of DHEA sulfation

The effect of OHPCBs on hSULT2A1-catalyzed sulfation of DHEA was assessed by a radiochemical assay method. Assays contained 200 μM PAPS, 1 μM [^{3}H]DHEA, 0.25 M potassium phosphate at pH 7.0, 7.5 mM 2-mercaptoethanol, and varying concentrations of OHPCBs in ethanol. The final concentration of ethanol in each reaction mixture was 2% (v/v). Assays were started by the addition of 0.25 μg hSULT2A1 in a total volume of 200 μL. Assays were incubated for 10 min at 37^{o}C. Reactions were terminated by the addition of 0.8 mL 50 mM KOH, immediately followed by addition of 0.5 mL $CHCl_3$. The reaction mixtures were vortexed thoroughly for 20 s and subjected to centrifugation for 5 min at 3000 rpm to separate the aqueous and organic phases. 100 μL of the aqueous layer containing the DHEA-sulfate was added to 10 mL biodegradable Econo-Safe scintillation cocktail for determination of radioactivity using a Perkin Elmer TriCarb 2900 TR liquid scintillation analyzer. Control experiments (control A and B) with tritiated DHEA were carried out without PAPS and enzyme. In addition, $CHCl_3$ was not added to control A. The rate of sulfation was expressed as nmol of DHEA-sulfate formed per minute per mg of protein using equation 6.

$$\text{Rate of Sulfation} = \frac{\text{DHEA-sulfate formed (nmol)}}{\text{10 min x mg protein}} \quad (6)$$

where:

$$\text{DHEA-sulfate formed (nmol)} = \frac{\text{(cpm measured - control B cpm) x 0.02 nmols x10}}{\text{control A cpm x 0.85}}$$

and 0.02 nmol is the amount of DHEA (in 100 µL of the aqueous phase), 10 represents the fact that only 100 µL of the 1.0 mL aqueous layer is subjected to scintillation analysis, and 0.85 represents the fraction of DHEA-S left in the aqueous phase after extraction with chloroform.

HPLC Assay

In order to determine which of the hydroxy metabolites of polychlorinated biphenyls serve as substrates for hSULT2A1, a previously described HPLC assay was used (*221*). Assay mixtures contained 200 µM PAPS, 0.25 M potassium phosphate at pH 7.0, 7.5 mM 2-mercaptoethanol, OHPCBs in acetone 5% (v/v) and 1 µg of enzyme in a 30 µL total volume. The reaction was started by adding enzyme, incubated for 10 min at 37^{o}C, and terminated by adding 30 µL methanol. After vigorously mixing for 30 s, the sample was placed on ice, and 30 µL of the total 60 µL (reaction mix plus methanol) was then injected into a 20 µL HPLC sample injector loop and chromatography was carried out using an Alltima C-18, (4.6 mm x 250 mm, 5 µm) reversed phase column (Alltech, Deerfield, IL) on a Shimadzu LC-20AT instrument equipped with Shimadzu UV detector. The mobile phase consisted of 100 mM KH_2PO_4, 75 mM NH_4Cl, 340 µL n-octylamine and 12% methanol. The mobile phase was adjusted to pH 5.45 with KOH just before adding methanol. Then the mobile phase was filtered through a 0.45 µm membrane filter. The column was then equilibrated for 2 h in order for the *n*-octylamine to saturate the column. A flow rate of 2.0 mL/min was maintained for all analyses with

detection by absorbance at 254 nm. A linear standard curve relating HPLC peak area to PAP concentration was generated, and the concentration of PAP formed in reaction mixture was calculated using the PAP standard curve. The resulting specific activity was expressed in nmol/min/mg protein using equation 7.

$$\text{Specific activity} = \frac{(PAP_{sample} - PAP_{control}) \times 60\ \mu l}{\text{incubation time (min)} \times \text{mg of protein}} \qquad (7)$$

ANS-displacement studies

Binding of ANS and OHPCBs to hSULT2A1

In order to carry out the binding experiments of the interactions of OHPCBs with hSULT2A1, it was important to determine the saturation concentration of ANS (Figure 50) needed in the binding assays. ANS is a probe that is used for the detection and analysis of the binding of hydrophobic ligands to many proteins (*208*). It binds noncovalently to proteins, and can be displaced by specific substrate or inhibitor. Upon displacement from a hydrophobic region of a protein into a more polar environment, ANS exhibits a decrease in fluorescence.

The binding of ANS to hSULT2A1 was carried out using a Perkin Elmer model LS-55 Luminescence spectrophotometer with a water-thermostated cell holder using a 10 mm path length quartz cuvette having windows on all four sides. The fluorescence excitation and emission wavelengths were set at 380 nm and 465 nm, respectively. The slit widths were set at 5 nm for both emission and excitation beams. The temperature was set at 37^{o}C before titrations were done. Binding was measured in 0.25 M potassium phosphate buffer at pH 7.0, with 7.5 mM mercaptoethanol in a total volume of 1 mL.

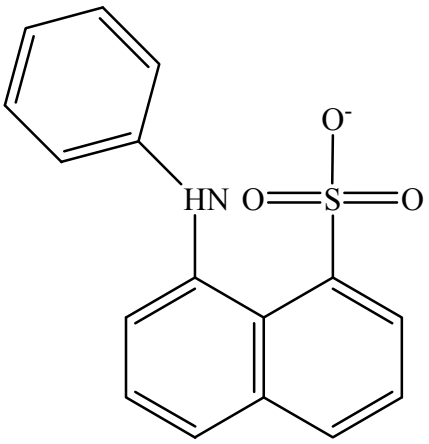

Figure 50. Structure of the probe molecule, 8-anilino-1-naphthalene sulfonate (ANS)

Titration was then followed by ANS with a concentration range of 0-110 μM. A Millex-GS 0.22 μm filter was used to filter all solution before use. ANS was kept in the dark prior to titration due to its sensitivity to light. The phosphate buffer and mercaptoethanol were preincubated for 2 min at 37^{o}C, with or without 3 μg of enzyme, before titrating with ANS. Data were analyzed by using Sigma Plot> pharmacology > simple ligand binding > one site, nonspecific. The increase in fluorescence was plotted against concentration of ANS.

For the binding of OHPCBs, a saturation concentration of 40 μM ANS (see results) was used, and titration was carried out using a range of concentrations of OHPCB(s) that depended on the solubility limit of the given compound. After addition of 3 μg enzyme, the mixture was pre-incubated for 2 min at 37^{o}C. The decrease in fluorescence upon displacement of ANS by OHPCBs was plotted using a scale of absolute value of the change in fluorescence (ΔF) vs. concentration of OHPCB.

Computational Studies

Molecular interactions of OHPCBs with hSULT2A1

In order to understand the molecular interactions between hydroxylated polychlorinated biphenyl (OHPCBs) and hSULT2A1, docking studies were performed using Surflex-Dock in Sybyl 8.0 (Tripos International) on a Linux operating system. Surflex-Dock makes use of a scoring function that is empirically derived, and depends on protein's affinity for the ligand as well as their crystal structures (*222-223*). The Surflex-Dock scoring function positions and orients the probes for optimum interactions with the protein atoms and it includes hydrophobic, polar, repulsive, entropic and solvation terms (*222*). It is a weighted sum of functions that are non-linear with van der Waals surface distances between pairs of proteins and ligand atoms (*222*). Any protein-ligand pairs having a distance greater than 2Å between the van der Waals surfaces are thrown out leaving behind those that are of interest (*222*). Each of these atom pairs of interest is labeled as polar or nonpolar, and is assigned a charge (*222*). Surflex-Dock also makes use of a protomol that serves as a representation of the intended binding sites where ligands are aligned (*224*). The protomol utilizes the steric hydrophobic probe, CH_4, the hydrogen bond probe, C=O, and the hydrogen acceptor probe, N-H (*224*). The protomol is useful in that it directs the ligands during the docking, however the ligands are scored based on the receptor (*224*).

Two x-ray crystal structures of hSULT2A1 were used for docking purposes: hSULT2A1 (1J99) (*158*) in complex with DHEA and hSULT2A1 (1EFH) (*150*) in complex with PAP. The DHEA and PAP molecules were extracted from the DHEA binding site and PAP binding site respectively before docking. The water molecules in the crystal structures were also deleted and hydrogen atoms added and then saved as mol2 files. The ligands (OHPCBs and ANS) were sketched, hydrogens added and energy minimized using the Powell method with Tripos Force field. The termination gradient

was set at 0.05 kcal/mol*Å, maximum iteration at 1000, dielectric constant of 1.0000, and RMS displacement at 0.001. The 3D structures of all the ligands (OHPCBs, ANS, including the extracted molecules, PAP and DHEA) were placed in different molecular areas within the same file and saved as a multimol2 format before docking with Surflex-Dock. The protomol was then generated automatically (threshold of 0.3 with bloat of 1, and threshold of 0.5 with bloat of 0 for the crystal structures of hSULT2A1 in the DHEA-bound conformation and PAP-bound conformation, respectively) and the ligands docked one at a time into the binding site of the receptor, hSULT2A1, with the Surflex-Dock default settings (except additional starting conformation of 100 per molecule). After each Surflex-Dock run, the ten best docked conformers or poses are sorted in a molecular spreadsheet and they represent binding affinities in $-\log_{10}(K_d)$ based on surflex-dock scoring function (crash score (also pK_d units), polar score, D-score, PMF-score, G-score, ChemSco and CScore). The best total score conformer with the best consensus score (CScore) ranging from 3 to 5 were selected for each of the docked ligands (OHPCBs, PAP, ANS, and DHEA). The scores are combined to form the consensus score which is more robust and accurate than any of the scoring functions for analyzing molecular interaction (*225*).

CoMFA of hSULT2A1 and OHPCBs

Comparative Molecular Field Analysis has been used to relate structures of hydroxylated polychlorinated biphenyl to their chemical and biological function using a method previously described (*226*).

Fifteen metabolites of polychlorinated biphenyls were used as a training set to build a QSAR model. Structures of all the compounds were drawn using Sybyl 8.0. (Tripos Inc., 2008) and saved in MOL2 format. To optimize the geometry, Gasteiger-Huckle charges were assigned and molecules were relaxed using the Tripos force field in Sybyl 8.0 with gradient convergence criterion set at 0.05 kcal/(Åmol). The molecules

were aligned based on a common core or substructure (i.e. biphenyl ring) using one of the most active compounds (4-OHPCB 68) as template in Sybyl 8.0. The negative log of the IC_{50} values on a M^{-1} scale (i.e. pIC_{50} scale) were derived and used as the dependent variables in the CoMFA analysis. For external validation purposes, three compounds were randomly selected as a test set out of the 15 compounds, and the remaining 12 compounds used to generate another CoMFA model.

The aligned training set molecules were put in a 3-dimensional cubic lattice with a grid spacing of 2 Å and an extension of 4 Å units beyond the aligned molecules in X, Y, and Z directions in order to derive the CoMFA steric and electrostatic fields. The steric field in CoMFA was calculated according to Lennard-Jones potential, and electrostatic field was calculated by Coulomb Potential. The descriptive fields were calculated separately for each individual molecule, with an sp^3 carbon probe atom having a net charge of +1 and energy cut-off value of 30 kcal/mol for each field.

The partial least squares analysis of the data placed in the molecular spread sheet (MSS) was used to derive the CoMFA models. The CoMFA column served as the independent variable while the pIC_{50} values served as the dependent variable in the PLS analysis. Both models were examined using leave-one-out (LOO) cross validation and non-cross-validation analyses. In the LOO cross validation analysis, a model is derived from the data set with one less compound (assuming this is compound A) and the resulting model is used to predict the activity of that compound A that was removed. The LOO cross validation PLS is done to determine the optimum number of components (which is analogous to the highest q^2 value and lowest PRESS value). During the PLS cross validation, the q^2 (which is the predictive power of the model) increases while the PRESS decreases. The PRESS and q^2 (defined in equation 8) are very important in deriving the optimum number of components and help to eliminate noise or over-fitting of the data.

$$q^2 = 1.0 - \frac{\Sigma (Y_{pred} - Y_{actual})^2}{\Sigma (Y_{actual} - Y_{mean})^2} \quad (8)$$

Where the numerator is PRESS, Y_{pred} is a predictive value, Y_{actual} is an experimental value, Y_{mean} is the best estimate of the mean of all values that might be predicted, and Summations (Σ) are over the same set of Y.

The optimum number of components is then used in the non-cross validation process to derive the conventional correlation coefficient (r^2) in the final model. The r^2 is the fit of the dataset activity to the model. The graphical representation (contour maps) and a plot of actual vs. predicted activity are generated at the end of the PLS analysis.

REFERENCES

(1) Ross, G. (2004) The public health implications of polychlorinated biphenyls (PCBs) in the environment. *Ecotoxicol Environ Saf*, *59*, 275-291.

(2) Erickson, M. D. (2001) Introduction: PCB Properties, uses, occurence, and regulatory history, In *PCBs, Recent Advances in Environmental Toxicology and Health Effects* (Robertson, L. W., and Hansen, L. G., Eds.) pp xi-xxx, The University Press of Kentucky, Lexington, K.Y.

(3) Cartwright, H. M. (2002) Investigation of Structure-Biodegradability Relationships in Polychlorinated Biphenyls Using Self-Organising Maps. *Neural Computing & Applic*, *11*, 30-36.

(4) Safe, S. (1984) Polychlorinated biphenyls (PCBs) and polybrominated biphenyls (PBBs): biochemistry, toxicology, and mechanism of action. *Crit Rev Toxicol*, *13*, 319-395.

(5) Safe, S. (1992) Toxicology, Structure-Function Relationship, Human and Environmental Health Impacts of Polychlorinated Biphenyls: Progress and Problems. *Environ Health Perspect*, *100*, 259-268.

(6) Rudel, R. A., Seryak, L. M., and Brody, J. G. (2008) PCB-containing wood floor finish is a likely source of elevated PCBs in residents' blood, household air and dust: a case study of exposure. *Environ Health*, *7*, 2.

(7) Holoubek, I., Kocan, A., Holoubkova, I., Kohoutek, J., and Falandysz, J. (2001) Polychlorinated Biphenyl (PCB) Contaminated Sites Worldwide: The case of Central and Eastern European Countries, In *PCB, Recent Advances in Environmental Toxicology and Health Effects* (Robertson, L. W., and Hansen, L. G., Eds.) pp 81-83, The University Press of Kentucky, Lexington, K.Y.

(8) Safe, S. H. (1994) Polychlorinated biphenyls (PCBs): environmental impact, biochemical and toxic responses, and implications for risk assessment. *Crit Rev Toxicol*, *24*, 87-149.

(9) Hansen, L. G. (1998) Stepping backward to improve assessment of PCB congener toxicities. *Environ Health Perspect*, *106 Suppl. 1*, 171-189.

(10) Safe, S., Safe, L., and Mullin, M. (1985) Polychlorinated biphenyls (PCBs)-congener-specific analysis of a commercial mixture and a human milk extract. *J Agric Food Chem*, *33*, 24-28.

(11) Wang, S. L., Chang, Y. C., Chao, H. R., Li, C. M., Li, L. A., Lin, L. Y., and Papke, O. (2006) Body burdens of polychlorinated dibenzo-p-dioxins, dibenzofurans, and biphenyls and their relations to estrogen metabolism in pregnant women. *Environ Health Perspect*, *114*, 740-745.

(12) Jensen, S. (1966) Report of a New Chemical Hazard. *New Sci*, *32*, 612.

(13) Hsu, S. T., Ma, C. I., Hsu, S. K. H., Wu, S. S., Hsu, N. H. M., Yeh, C. C., and Wu, S. B. (1985) Discovery and epidemiology of PCB poisoning in Taiwan: A four-year followup. *Environ Health Perspect*, *59*, 5-10.

(14) Guo, Y. L., Lambert, G. H., Hsu, C. C., and Hsu, M. M. (2004) Yucheng: health effects of prenatal exposure to polychlorinated biphenyls and dibenzofurans. *Int Arch Occup Environ Health*, *77*, 153-158.

(15) Hara, I. (1985) Health status and PCBs in blood of workers exposed to PCBs and of their children. *Environ Health Perspect*, *59*, 85-90.

(16) Takamatsu, M., Oki, M., Maeda, K., Inoue, Y., Hirayama, H., and Yoshizuka, K. (1985) Surveys of workers occupationally exposed to PCBs and of yusho patients. *Environ Health Perspect*, *59*, 91-97.

(17) Kontsas, H., Pekari, K., Riala, R., Back, B., Rantio, T., and Priha, E. (2004) Worker exposure to polychlorinated biphenyls in elastic polysulphide sealant renovation. *Ann Occup Hyg*, *48*, 51-55.

(18) Gioia, R., Nizzetto, L., Lohmann, R., Dachs, J., Temme, C., and Jones, K. C. (2008) Polychlorinated biphenyls (PCBs) in air and seawater of the Atlantic Ocean: sources, trends and processes. *Environ Sci Technol*, *42*, 1416-1422.

(19) Jamshidi, A., Hunter, S., Hazrati, S., and Harrad, S. (2007) Concentrations and chiral signatures of polychlorinated biphenyls in outdoor and indoor air and soil in a major U.K. conurbation. *Environ Sci Technol*, *41*, 2153-2158.

(20) Robson, M., and Harrad, S. (2004) Chiral PCB signatures in air and soil: implications for atmospheric source apportionment. *Environ Sci Technol*, *38*, 1662-1666.

(21) Herrick, R. F. (2010) PCBs in School-Persistent Chemicals, Persistent Problem. *New Solutions*, *20*, 115-126.

(22) Herrick, R. F., McClean, M. D., Meeker, J. D., Baxter, L. K., and Weymouth, G. A. (2004) An unrecognized source of PCB contamination in schools and other buildings. *Environ Health Perspect*, *112*, 1051-1053.

(23) Gabrio, T., Piechotowski, I., Wallenhorst, T., Klett, M., Cott, L., Friebel, P., Link, B., and Schwenk, M. (2000) PCB-blood levels in teachers, working in PCB-contaminated schools. *Chemosphere*, *40*, 1055-1062.

(24) Weintraub, M., and Birnbaum, L. S. (2008) Catfish consumption as a contributor to elevated PCB levels in a non-Hispanic black subpopulation. *Environ Res*, *107*, 412-417.

(25) Jacobson, J. L., and Jacobson, S. W. (1996) Intellectual impairment in children exposed to polychlorinated biphenyls in utero. *N Engl J Med*, *335*, 783-789.

(26) Rogan, W. J., and Gladen, B. C. (1992) Neurotoxicology of PCBs and related compounds. *Neurotoxicology*, *13*, 27-35.

(27) Koopman-Esseboom, C., Weisglas-Kuperus, N., de Ridder, M. A., Van der Paauw, C. G., Tuinstra, L. G., and Sauer, P. J. (1996) Effects of polychlorinated biphenyl/dioxin exposure and feeding type on infants' mental and psychomotor development. *Pediatrics*, *97*, 700-706.

(28) Silberhorn, E., Glauert, H. P., and Robertson, L. W. (1990) Carcinogenicity of polyhalogenated biphenyls: PCBs and PBBs. *Crit Rev in Toxicol*, *20*, 439-496.

(29) Bosetti, C., Negri, E., Fattore, E., and La Vecchia, C. (2003) Occupational exposure to polychlorinated biphenyls and cancer risk. *Eur J Cancer Prev*, *12*, 251-255.

(30) Glauert, H. P., Tharappel, J. C., Lu, Z., Stemm, D., Banerjee, S., Chan, L. S., Lee, E. Y., Lehmler, H. J., Robertson, L. W., and Spear, B. T. (2008) Role of Oxidative Stress in the Promoting Activities of PCBs. *Environ Toxicol Pharmacol*, *25*, 247-250.

(31) Oakley, G. G., Devanaboyina, U., Robertson, L. W., and Gupta, R. C. (1996) Oxidative DNA damage induced by activation of polychlorinated biphenyls (PCBs): implications for PCB-induced oxidative stress in breast cancer. *Chem Res Toxicol*, *9*, 1285-1292.

(32) Wen, S., Yang, F. X., Gong, Y., Zhang, X. L., Hui, Y., Li, J. G., Liu, A. L., Wu, Y. N., Lu, W. Q., and Xu, Y. (2008) Elevated levels of urinary 8-hydroxy-2'-deoxyguanosine in male electrical and electronic equipment dismantling workers exposed to high concentrations of polychlorinated dibenzo-p-dioxins and dibenzofurans, polybrominated diphenyl ethers, and polychlorinated biphenyls. *Environ Sci Technol*, *42*, 4202-4207.

(33) Fadhel, Z., Lu, Z., Robertson, L. W., and Glauert, H. P. (2002) Effect of 3,3',4,4'-tetrachlorobiphenyl and 2,2',4,4',5,5'-hexachlorobiphenyl on the induction of hepatic lipid peroxidation and cytochrome P-450 associated enzyme activities in rats. *Toxicology*, *175*, 15-25.

(34) Morse, D. C., Groen, D., Veerman, M., van Amerongen, C. J., Koeter, H. B., Smits van Prooije, A. E., Visser, T. J., Koeman, J. H., and Brouwer, A. (1993) Interference of polychlorinated biphenyls in hepatic and brain thyroid hormone metabolism in fetal and neonatal rats. *Toxicol Appl Pharmacol*, *122*, 27-33.

(35) Chauhan, K. R., Kodavanti P. R. S., and McKinney, J. D. (2000) Assessing the role of ortho-substitution on polychlorinated biphenyl binding to transthyretin, a thyroxine transport protein. *Toxicol Appl Pharmacol*, *162*, 10-21.

(36) Brouwer, A., and van den Berg, K. J. (1986) Binding of a metabolite of 3,4,3',4'-tetrachlorobiphenyl to transthyretin reduces serum vitamin A transport by inhibiting the formation of the protein complex carrying both retinol and thyroxin. *Toxicol Appl Pharmacol*, *85*, 301-312.

(37) Lans, M. C., Klasson-Wehler, E., Willemsen, M., Meussen, E., Safe, S., and Brouwer, A. (1993) Structure-dependent, competitive interaction of hydroxy-polychlorobiphenyls, -dibenzo-p-dioxins and -dibenzofurans with human transthyretin. *Chem Biol Interact*, *88*, 7-21.

(38) Waring, R. H., Ayers, S., Gescher, A. J., Glatt, H. R., Meinl, W., Jarratt, P., Kirk, C. J., Pettitt, T., Rea, D., and Harris, R. M. (2008) Phytoestrogens and xenoestrogens: the contribution of diet and environment to endocrine disruption. *J Steroid Biochem Mol Biol*, *108*, 213-220.

(39) Fischer, L. J., Zhou, H. R., and Wagner, M. A. (1996) Polychlorinated biphenyls release insulin from RINm5F cells. *Life Sci*, *59*, 2041-2049.

(40) Bae, J., Peters-Golden, M., and Loch-Caruso, R. (1999) Stimulation of pregnant rat uterine contraction by the polychlorinated biphenyl (PCB) mixture aroclor 1242 may be mediated by arachidonic acid release through activation of phospholipase A2 enzymes. *J Pharmacol Exp Ther*, *289*, 1112-1120.

(41) Khan, M. A., Lichtensteiger, C. A., Faroon, O., Mumtaz, M., Schaeffer, D. J., and Hansen, L. G. (2002) The hypothalamo-pituitary-thyroid (HPT) axis: a target of nonpersistent ortho-substituted PCB congeners. *Toxicol Sci*, *65*, 52-61.

(42) Lind, P. M., Eriksen, E. F., Sahlin, L., Edlund, M., and Orberg, J. (1999) Effects of the antiestrogenic environmental pollutant 3,3',4,4', 5-pentachlorobiphenyl (PCB #126) in rat bone and uterus: diverging effects in ovariectomized and intact animals. *Toxicol Appl Pharmacol*, *154*, 236-244.

(43) Harris, R., Turan, N., Kirk, C., Ramsden, D., and Waring, R. (2007) Effects of endocrine disruptors on dehydroepiandrosterone sulfotransferase and enzymes involved in PAPS synthesis: genomic and nongenomic pathways. *Environ Health Perspect*, *115 Suppl 1*, 51-54.

(44) Pessah, I. N., Hansen, L. G., Albertson, T. E., Garner, C. E., Ta, T. A., Do, Z., Kim, K. H., and Wong, P. W. (2006) Structure-activity relationship for noncoplanar polychlorinated biphenyl congeners toward the ryanodine receptor-Ca2+ channel complex type 1 (RyR1). *Chem Res Toxicol*, *19*, 92-101.

(45) Safe, S. (2001) Molecular biology of the Ah receptor and its role in carcinogenesis. *Toxicol Lett*, *120*, 1-7.

(46) Van den Berg, M., Birnbaum, L., Bosveld, A.T.C., Brunström, B., Cook, P., Feeley, M., Giesy, J.P., Hanberg, A., Hasegawa, R., Kennedy, S.W., Kubiak, T., Larsen, J.C., van Leeuwen, F.X.R., Liem, A.K.D., Nolt, C., Peterson, R.E., Poellinger, L., Safe, S., Schrenk, D., Tillitt, D., Tysklind, M., Younes, M., Waern, F., Zacharewski, T. (1998) Toxic Equivalency Factors (TEFs) for PCBs, PCDDs, PCDFs for Humans and Wildlife. *Environ Health Perspect*, *106*, 775-792.

(47) Parkinson, A., Cockerline, R., and Safe, S. (1980) Polychlorinated biphenyl isomers and congeners as inducers of both 3-methylcholanthrene- and phenobarbitone-type microsomal enzyme activity. *Chem Biol Interact*, *29*, 277-289.

(48) Parkinson, A., Robertson, L., Safe, L., and Safe, S. (1980) Polychlorinated biphenyls as inducers of hepatic microsomal enzymes: structure-activity rules. *Chem Biol Interact*, *30*, 271-285.

(49) Fisher, J. W., Campbell, J., Muralidhara, S., Bruckner, J. V., Ferguson, D., Mumtaz, M., Harmon, B., Hedge, J. M., Crofton, K. M., Kim, H., and Almekinder, T. L. (2006) Effect of PCB 126 on hepatic metabolism of thyroxine and perturbations in the hypothalamic-pituitary-thyroid axis in the rat. *Toxicol Sci*, *90*, 87-95.

(50) Bandiera, S., Safe, S., and Okey, A. B. (1982) Binding of polychlorinated biphenyls classified as either phenobarbitone-, 3-methylcholanthrene-, or mixed-type inducers to cytosolic Ah receptor. *Chem Biol Interact*, *39*, 259-277.

(51) Humphrey, H. E., Gardiner, J. C., Pandya, J. R., Sweeney, A. M., Gasior, D. M., McCaffrey, R. J., and Schantz, S. L. (2000) PCB congener profile in the serum of humans consuming Great Lakes fish. *Environ Health Perspect*, *108*, 167-172.

(52) Corrigan, F. M., Murray, L., Wyatt, C. L., and Shore, R. F. (1998) Diorthosubstituted polychlorinated biphenyls in caudate nucleus in Parkinson's disease. *Exp Neurol*, *150*, 339-342.

(53) Tilson, H. A., and Kodavanti, P. R. (1998) The neurotoxicity of polychlorinated biphenyls. *Neurotoxicology*, *19*, 517-525.

(54) Mariussen, E., and Fonnum, F. (2001) The effect of polychlorinated biphenyls on the high affinity uptake of the neurotransmitters, dopamine, serotonin, glutamate and GABA, into rat brain synaptosomes. *Toxicology*, *159*, 11-21.

(55) Berberian, I., Chen, L. C., Robinson, F. R., Glauert, H. P., Chow, C. K., and Robertson, L. W. (1995) Effect of dietary retinyl palmitate on the promotion of altered hepatic foci by 3,3',4,4'-tetrachlorobiphenyl and 2,2',4,4',5,5'-hexachlorobiphenyl in rats initiated with diethylnitrosamine. *Carcinogenesis*, *16*, 393-398.

(56) Brouwer, A., Longnecker, M. P., Birnbaum, L. S., Cogliano, J., Kostyniak, P., Moore, J., Schantz, S., and Winneke, G. (1999) Characterization of potential endocrine-related health effects at low-dose levels of exposure to PCBs. *Environ Health Perspect*, *107 Suppl 4*, 639-649.

(57) Tan, Y., Chen, C. H., Lawrence, D., and Carpenter, D. O. (2004) Ortho-substituted PCBs kill cells by altering membrane structure. *Toxicol Sci*, *80*, 54-59.

(58) Nishihara, Y., and Utsumi, K. (1986) 2,5,2',5'-Tetrachlorobiphenyl impairs the bioenergetic functions of isolated rat liver mitochondria. *Biochem Pharmacol*, *35*, 3335-3339.

(59) Uraki, Y., Suzuki, S., Yasuhara, A., and Shibamoto, T. (2004) Determining sources of atmospheric polychlorinated biphenyls based on their fracturing concentrations and congener compositions. *J Environ Sci Health A Tox Hazard Subst Environ Eng*, *39*, 2755-2772.

(60) Imsilp, K., Schaeffer, D. J., and Hansen, L. G. (2005) PCB disposition and different biological effects in rats following direct soil exposure versus PCBs off-gassed from the soil. *Toxicol Environ Chem*, *87*, 267-285.

(61) Hu, D., Lehmler, H. J., Martinez, A., Wang, K., and Hornbuckle, K. C. (2010) Atmospheric PCB congeners across Chicago. *Atmos Environ*, *44*, 1550-1557.

(62) Palmer, P. M., Belanger, E. E., Wilson, L. R., Hwang, S. A., Narang, R. S., Gomez, M. I., Cayo, M. R., Durocher, L. A., and Fitzgerald, E. F. (2008) Outdoor air PCB concentrations in three communities along the Upper Hudson River, New York. *Arch Environ Contam Toxicol*, *54*, 363-371.

(63) Hansen, L. G., and O'Keefe, P. W. (1996) Polychlorinated dibenzofurans and dibenzo-p-dioxins in subsurface soil, superficial dust, and air extracts from a contaminated landfill. *Arch Environ Contam Toxicol*, *31*, 271-276.

(64) Hornbuckle, K. C., and Green, M. L. (2003) The impact of an urban-industrial region on the magnitude and variability of persistent organic pollutant deposition to Lake Michigan. *Ambio*, *32*, 406-411.

(65) Martinez, A., Wang, K., and Hornbuckle, K. C. (2010) Fate of PCB Congeners in an Industrial Harbor of Lake Michigan. *Environ Sci Technol*, *44*, 2803-2808.

(66) Persoon, C., and Hornbuckle, K. C. (2009) Calculation of passive sampling rates from both native PCBs and depuration compounds in indoor and outdoor environments. *Chemosphere*, *74*, 917-923.

(67) Persoon, C., Peters, T. M., Kumar, N., and Hornbuckle, K. C. (2010) Spatial Distribution of Airborne Polychlorinated Biphenyls in Cleveland, Ohio and Chicago, Illinois. *Environ Sci Technol*, *44*, 2797-2802.

(68) Rudel, R. A., and Perovich, L. J. (2009) Endocrine disrupting chemicals in indoor and outdoor air. *Atmos Environ*, *43*, 170-181.

(69) Menichini, E., Iacovella, N., Monfredini, F., and Turrio-Baldassarri, L. (2007) Relationship between indoor and outdoor air pollution by carcinogenic PAHs and PCBs. *Atmos Environ*, *41*, 9518-9529.

(70) Currado, G. M., and Harrad, S. (1998) Comparison of Polychlorinated Biphenyl Concentrations in Indoor and Outdoor Air and the Potential Significance of Inhalation as a Human Exposure Pathway. *Environ Sci Technol*, *32*, 3043-3047.

(71) Ludewig, G., Lehmann, L., Esch, H., and Robertson, L. W. (2008) Metabolic Activation of PCBs to Carcinogens in Vivo - A Review. *Environ Toxicol Pharmacol*, *25*, 241-246.

(72) Routti, H., Letcher, R. J., Arukwe, A., Van Bavel, B., Yoccoz, N. G., Chu, S., and Gabrielsen, G. W. (2008) Biotransformation of PCBs in relation to phase I and II xenobiotic-metabolizing enzyme activities in ringed seals (Phoca hispida) from Svalbard and the Baltic Sea. *Environ Sci Technol*, *42*, 8952-8958.

(73) Sandau, C. D., Ayotte, P., Dewailly, E., Duffe, J., and Norstrom, R. J. (2000) Analysis of hydroxylated metabolites of PCBs (OH-PCBs) and other chlorinated phenolic compounds in whole blood from Canadian inuit. *Environ Health Perspect*, *108*, 611-616.

(74) Bergman, A., Klasson-Wehler, E., and Kuroki, H. (1994) Selective retention of hydroxylated PCB metabolites in blood. *Environ Health Perspect*, *102*, 464-469.

(75) Hovander, L., Malmberg, T., Athanasiadou, M., Athanassiadis, I., Rahm, S., and Bergman, Å. (2002) Identification of hydroxylated PCB metabolites and other phenolic halogenated pollutants in human blood plasma. *Arch Environ Contam Toxicol*, *42*, 105-117.

(76) Narasimhan, T. R., Kim, H. L., and Safe, S. H. (1991) Effects of hydroxylated polychlorinated biphenyls on mouse liver mitochondrial oxidative phosphorylation. *J Biochem Toxicol*, *6*, 229-236.

(77) Liu, Y., Apak, T. I., Lehmler, H. J., Robertson, L. W., and Duffel, M. W. (2006) Hydroxylated polychlorinated biphenyls are substrates and inhibitors of human hydroxysteroid sulfotransferase SULT2A1. *Chem Res Toxicol*, *19*, 1420-1425.

(78) Sacco, J. C., and James, M. O. (2005) Sulfonation of environmental chemicals and their metabolites in the polar bear (Ursus maritimus). *Drug Metab Dispos*, *33*, 1341-1348.

(79) Sacco, J. C., Lehmler, H. J., Robertson, L. W., Li, W., and James, M. O. (2008) Glucuronidation of polychlorinated biphenylols and UDP-glucuronic acid concentrations in channel catfish liver and intestine. *Drug Metab Dispos*, *36*, 623-630.

(80) James, M. O. (2001) Polychlorinated Biphenyls: Metabolism and Metabolites, In *PCBs, Recent Advances in Environmental Toxicology and Health Effects* (Robertson, L. W., and Hansen, L. G., Eds.) pp 35-46, The University Press of Kentucky, Lexington, K.Y.

(81) Letcher, R. J., Klassen-Wehler, E., and Bergman, A. (2000) Methylsulfone and Hydroxylated Metabolites of Polychlorinated Biphenyls. In *New Types of Persistent Halogenated Compound* (Paasivirta, J., Ed.) pp 317-357, Berling Springer-Verlag.

(82) Goto, M., Hattori, K., and Sugahara, K. (1975) Metabolism of pentachloro- and hexachlorobiphenyls in rat *Chemosphere*, *3*, 177-180.

(83) Koga, N., Beppu, M., Ishida, C., and Yoshimura, H. (1989) Further studies on metabolism in vivo of 3,4,3',4'-tetrachlorobiphenyl in rats: identification of minor metabolites in rat faeces. *Xenobiotica*, *19*, 1307-1318.

(84) Chen, P. R., McKinney, J. D., and Matthews, H. B. (1976) Metabolism of 2,4,5,2',5'-pentachlorobiphenyl in the rat. Qualitative and quantitative aspects. *Drug Metab Dispos*, *4*, 362-367.

(85) Sundstrom, G., Jansson, B., and Jensen, S. (1975) Structure of phenolic metabolites of p,p'-DDE in rat, wild seal and guillemot. *Nature*, *255*, 627-628.

(86) Srinivasan, A., Robertson, L. W., and Ludewig, G. (2002) Sulfhydryl binding and topoisomerase inhibition by PCB metabolites. *Chem Res Toxicol*, *15*, 497-505.

(87) Wang, J. C. (1996) DNA topoisomerases. *Annu Rev Biochem*, *65*, 635-692.

(88) Amaro, A. R., Oakley, G. G., Bauer, U., Spielmann, H. P., and Robertson, L. W. (1996) Metabolic activation of PCBs to quinones: reactivity toward nitrogen and sulfur nucleophiles and influence of superoxide dismutase. *Chem Res Toxicol*, *9*, 623-629.

(89) McLean, M. R., Robertson, L. W., and Gupta, R. C. (1996) Detection of PCB adducts by the 32P-postlabeling technique. *Chem Res Toxicol*, *9*, 165-171.

(90) Oakley, G. G., Devanaboyina, U., Robertson, L. W., and Gupta, R. C. (1996) Oxidative DNA damage induced by activation of polychlorinated biphenyls (PCBs): implications for PCB-induced oxidative stress in breast cancer. *Chem Res Toxicol*, *9*, 1285-1292.

(91) Park, J. S., Bergman, A., Linderholm, L., Athanasiadou, M., Kocan, A., Petrik, J., Drobna, B., Trnovec, T., Charles, M. J., and Hertz-Picciotto, I. (2008) Placental transfer of polychlorinated biphenyls, their hydroxylated metabolites and pentachlorophenol in pregnant women from eastern Slovakia. *Chemosphere*, *70*, 1676-1684.

(92) Porterfield, S. P. (1994) Vulnerability of the developing brain to thyroid abnormalities: environmental insults to the thyroid system. *Environ Health Perspect*, *102 Suppl 2*, 125-130.

(93) Peterson, R. E., Theobald, H. M., and Kimmel, G. L. (1993) Developmental and reproductive toxicity of dioxins and related compounds: cross-species comparisons. *Crit Rev Toxicol*, *23*, 283-335.

(94) Schuur, A. G., Brouwer, A., Bergman, A., Coughtrie, M. W., and Visser, T. J. (1998) Inhibition of thyroid hormone sulfation by hydroxylated metabolites of polychlorinated biphenyls. *Chem Biol Interact*, *109*, 293-297.

(95) Korach, K. S., Sarver, P., Chae, K., McLachlan, J. A., and McKinney, J. D. (1988) Estrogen receptor-binding activity of polychlorinated hydroxybiphenyls: conformationally restricted structural probes. *Mol Pharmacol*, *33*, 120-126.

(96) Connor, K., Ramamoorthy, K., Moore, M., Mustain, M., Chen, I., Safe, S., Zacharewski, T., Gillesby, B., Joyeux, A., and Balaguer, P. (1997) Hydroxylated polychlorinated biphenyls (PCBs) as estrogens and antiestrogens: structure-activity relationships. *Toxicol Appl Pharmacol*, *145*, 111-123.

(97) Kester, M. H., Bulduk, S., Tibboel, D., Meinl, W., Glatt, H., Falany, C. N., Coughtrie, M. W., Bergman, A., Safe, S. H., Kuiper, G. G., Schuur, A. G., Brouwer, A., and Visser, T. J. (2000) Potent inhibition of estrogen sulfotransferase by hydroxylated PCB metabolites: a novel pathway explaining the estrogenic activity of PCBs. *Endocrinology*, *141*, 1897-1900.

(98) Yager, J. D. (2000) Endogenous estrogens as carcinogens through metabolic activation. *J Natl Cancer Inst Monogr*, 67-73.

(99) Gregoraszczuk, E. L., Rak, A., Ludewig, G., Gasinska, A (2008) Effects of estradiol, PCB3, and their hydroxylated metabolites on proliferation, cell cycle, and apoptosis of human breast cancer cells. *Environ Toxicol and Pharmacol*, *25*, 227-233.

(100) Chang, H. J., Shi, R., Rehse, P., and Lin, S. X. (2004) Identifying androsterone (ADT) as a cognate substrate for human dehydroepiandrosterone sulfotransferase (DHEA-ST) important for steroid homeostasis: structure of the enzyme-ADT complex. *J Biol Chem*, *279*, 2689-2696.

(101) Baumann, E. (1876) Ueber sulfosauren im harn., In *Ber Dtsch Chem Ges* p 54.

(102) Apak, T. I., and Duffel, M. W. (2004) Interactions of the stereoisomers of alpha-hydroxytamoxifen with human hydroxysteroid sulfotransferase SULT2A1 and rat hydroxysteroid sulfotransferase STa. *Drug Metab Dispos*, *32*, 1501-1508.

(103) Gamage, N., Barnett, A., Hempel, N., Duggleby, R. G., Windmill, K. F., Martin, J. L., and McManus, M. E. (2006) Human sulfotransferases and their role in chemical metabolism. *Toxicol Sci*, *90*, 5-22.

(104) Klaassen, C. D., and Boles, J. W. (1997) Sulfation and sulfotransferases 5: the importance of 3'-phosphoadenosine 5'-phosphosulfate (PAPS) in the regulation of sulfation. *FASEB J*, *11*, 404-418.

(105) Nowell, S., and Falany, C. N. (2006) Pharmacogenetics of human cytosolic sulfotransferases. *Oncogene*, *25*, 1673-1678.

(106) Falany, C. N. (1997) Enzymology of human cytosolic sulfotransferases. *FASEB J*, *11*, 206-216.

(107) Venkatachalam, K. V. (2003) Human 3'-phosphoadenosine 5'-phosphosulfate (PAPS) synthase: biochemistry, molecular biology and genetic deficiency. *IUBMB Life*, *55*, 1-11.

(108) Robbins, P. W., Lipmann, F. (1956) The enzymatic sequence in the biosynthesis of active sulfate synthesis. *J Am Chem Soc.*, *78*, 6409-6410.

(109) Bandurski, R. S., Wilson, L.G., and Squires, C. L. (1956) The mechanism of "active sulfate" formation. *J Am Chem Soc*, *78*, 6408-6409.

(110) Yasuda, S., Suiko, M., and Liu, M. C. (2005) Oral contraceptives as substrates and inhibitors for human cytosolic SULTs. *J Biochem (Tokyo)*, *137*, 401-406.

(111) Suiko, M., Sakakibara, Y., and Liu, M. C. (2000) Sulfation of environmental estrogen-like chemicals by human cytosolic sulfotransferases. *Biochem Biophys Res Commun*, *267*, 80-84.

(112) Wang, J., Falany, J. L., and Falany, C. N. (1998) Expression and characterization of a novel thyroid hormone-sulfating form of cytosolic sulfotransferase from human liver. *Mol Pharmacol*, *53*, 274-282.

(113) Coughtrie, M. W. H., Bamforth, K. J., Sharp, S., Jones, A. L., Borthwick, E. B., Barker, E. V., Roberts, R. C., Hume, R., and Burchell, A. (1994) Sulfation of endogenous compounds and xenobiotics-interactions and function in health and disease. *Chem Biol Interact*, *92*, 247-256.

(114) Wang, L. Q., and James, M. O. (2006) Inhibition of sulfotransferases by xenobiotics. *Curr Drug Metab*, *7*, 83-104.

(115) Labrie, F., Luu-The, V., Labrie, C., Belanger, A., Simard, J., Lin, S. X., and Pelletier, G. (2003) Endocrine and intracrine sources of androgens in women: inhibition of breast cancer and other roles of androgens and their precursor dehydroepiandrosterone. *Endocr Rev*, *24*, 152-182.

(116) Cowen, A. E., Korman, M. G., Hofmann, A. F., and Cass, O. W. (1975) Metabolism of lethocholate in healthy man. I. Biotransformation and biliary excretion of intravenously administered lithocholate, lithocholylglycine, and their sulfates. *Gastroenterology*, *69*, 59-66.

(117) Hofmann, A. F. (2004) Detoxification of lithocholic acid, a toxic bile acid: relevance to drug hepatotoxicity. *Drug Metab Rev*, *36*, 703-722.

(118) Visser, T. J., van Buuren, J. C. P., Rutgers, M., Rooda, S. J. E., and de Herder, W. W. (1990) The role of sulfation in thyroid hormone metabolism. *Trends Endocrinol Metab*, *1*, 211.

(119) Wang, P. C., Buu, N. T., Kuchel, O., and Genest, J. (1983) Conjugation patterns of endogenous plasma catecholamines in human and rat. *J Lab Clin Med*, *101*, 141-151.

(120) Kuchel, O., Buu, N. T., Racz, K., Leon, A. d., Serri, O., and Kyncl, J. (1986) Role of sulfate conjugation of catecholamines in blood pressure regulation. *Fed Proc*, *45*, 2254-2259.

(121) Wilson, A. A., Wang, J., Koch, P., and Walle, T. (1997) Stereoselective sulphate conjugation of fenoterol by human phenolsulphotransferases. *Xenobiotica*, *27*, 1147-1154.

(122) Pesola, G. R., and Walle, T. (1993) Stereoselective sulfate conjugation of isoproterenol in humans: comparison of hepatic, intestinal, and platelet activity. *Chirality*, *5*, 602-609.

(123) Walle, U. K., Pesola, G. R., and Walle, T. (1993) Stereoselective sulphate conjugation of salbutamol in humans: comparison of hepatic, intestinal and platelet activity. *Br J Clin Pharmacol*, *35*, 413-418.

(124) Walle, T., Walle, U. K., Thornburg, K. R., and Schey, K. L. (1993) Stereoselective sulfation of albuterol in humans. Biosynthesis of the sulfate conjugate by HEP G2 cells. *Drug Metab Dispos*, *21*, 76-80.

(125) Miller, R. P., Roberts, R. J., and Fischer, L. J. (1976) Acetaminophen elimination kinetics in neonates, children, and adults. *Clin Pharmacol Ther*, *19*, 284-294.

(126) Richard, K., Hume, R., Kaptein, E., Stanley, E. L., Visser, T. J., and Coughtrie, M. W. (2001) Sulfation of thyroid hormone and dopamine during human development: ontogeny of phenol sulfotransferases and arylsulfatase in liver, lung, and brain. *J Clin Endocrinol Metab*, *86*, 2734-2742.

(127) Meerman, J. H., van Doorn, A. B., and Mulder, G. J. (1980) Inhibition of sulfate conjugation of N-hydroxy-2-acetylaminofluorene in isolated perfused rat liver and in the rat in vivo by pentachlorophenol and low sulfate. *Cancer Res*, *40*, 3772-3779.

(128) Weisburger, J. H., Yamamoto, R. S., Williams, G. M., Grantham, P. H., Matsushima, T., and Weisburger, E. K. (1972) On the sulfate ester of N-hydroxy-N-2-fluorenylacetamide as a key ultimate hepatocarcinogen in the rat. *Cancer Res*, *32*, 491-500.

(129) Werner, S., Kunz, S., Wolff, T., and Schwarz, L. R. (1996) Steroidal drug cyproterone acetate is activated to DNA-binding metabolites by sulfonation. *Cancer Res*, *56*, 4391-4397.

(130) Armstrong, J. I., and Bertozzi, C. R. (2000) Sulfotransferases as targets for therapeutic intervention. *Curr Opin Drug Discov Devel*, *3*, 502-515.

(131) Tseng, L., Mazella, J., Lee, L. Y., and Stone, M. L. (1983) Estrogen sulfatase and estrogen sulfotransferase in human primary mammary carcinoma. *J Steroid Biochem*, *19*, 1413-1417.

(132) Farzan, M., Mirzabekov, T., Kolchinsky, P., Wyatt, R., Cayabyab, M., Gerard, N. P., Gerard, C., Sodroski, J., and Choe, H. (1999) Tyrosine sulfation of the amino terminus of CCR5 facilitates HIV-1 entry. *Cell*, *96*, 667-676.

(133) Glatt, H. (1997) Bioactivation of mutagens via sulfation. *FASEB J.*, *11*, 314-321.

(134) Mulder, G. J. (1984) Sulfation-Metabolic aspects, In *Progress in Drug Metabolism. Vol. 8* (Bridges, J. W., and Chasseaud, L. F., Eds.) pp 35-100, Taylor and Francis, London.

(135) Buhl, A. E., Waldon, D.J., Baker, C.A., Johnson, G.A. (1990) Minoxidil sulfate is the active metabolite that stimulates hair follicles. *AACN Clin Issues*, *95*, 553-557.

(136) Thomas, R. C., and Harpootlian, H. (1975) Metabolism of minoxidil, a new hypotensive agent II: biotransformation following oral administration to rats, dogs, and monkeys. *J Pharm Sci*, *64*, 1366-1371.

(137) Meisheri, K. D., Cipkus, L. A., and Taylor, C. J. (1988) Mechanism of action of minoxidil sulfate-induced vasodilatation: a role for increased K+ permeability. *J Pharmacol Exp Ther*, *245*, 751-760.

(138) Johnson, G. A., Barsuhn, K. J., and McCall, J. M. (1982) Sulfation of minoxidil by liver sulfotransferase. *Biochem Pharmacol*, *31*, 2949-2954.

(139) Falany, C. N. (1991) Molecular enzymology of human liver cytosolic sulfotransferases. *Trends in Pharmacol Sci*, *12*, 255-259.

(140) Leilich, G., Knauf, H., Mutschler, E., and Volger, K. D. (1980) Influence of triamterene and hydroxytriamterene sulfuric acid ester on diuresis and saluresis in rats after oral and intravenous application. *Arzneimittelforschung*, *30*, 949-953.

(141) Zuckerman, A., Bolan, E., de Paulis, T., Schmidt, D., Spector, S., and Pasternak, G. W. (1999) Pharmacological characterization of morphine-6-sulfate and codeine-6-sulfate. *Brain Res*, *842*, 1-5.

(142) Garay, R. P., Rosati, C., Fanous, K., Allard, M., Morin, E., Lamiable, D., and Vistelle, R. (1995) Evidence for (+)-cicletanine sulfate as an active natriuretic metabolite of cicletanine in the rat. *Eur J Pharmacol*, *274*, 175-180.

(143) Kim, M. S., Shigenaga, J., Moser, A., Grunfeld, C., and Feingold, K. R. (2004) Suppression of DHEA sulfotransferase (Sult2A1) during the acute-phase response. *Am J Physiol Endocrinol Metab*, *287*, E731-738.

(144) Sheng, J. J., and Duffel, M. W. (2001) Bacterial expression, purification, and characterization of rat hydroxysteroid sulfotransferase STa. *Protein Expression & Purification*, *21*, 235-242.

(145) Allali-Hassani, A., Pan, P. W., Dombrovski, L., Najmanovich, R., Tempel, W., Dong, A., Loppnau, P., Martin, F., Thornton, J., Edwards, A. M., Bochkarev, A., Plotnikov, A. N., Vedadi, M., and Arrowsmith, C. H. (2007) Structural and chemical profiling of the human cytosolic sulfotransferases. *PLoS Biol*, *5*, e97.

(146) Falany, C. N., Xie, X., Wang, J., Ferrer, J., and Falany, J. L. (2000) Molecular cloning and expression of novel sulphotransferase-like cDNAs from human and rat brain. *Biochem J*, *346*, 857-864.

(147) Freimuth, R. R., Wiepert, M., Chute, C. G., Wieben, E. D., and Weinshilboum, R. M. (2004) Human cytosolic sulfotransferase database mining: identification of seven novel genes and pseudogenes. *Pharmacogenomics J*, *4*, 54-65.

(148) Nagata, K., and Yamazoe, Y. (2000) Pharmacogenetics of sulfotransferase. *Ann Rev Pharmacol Toxicol*, *40*, 159-176.

(149) Blanchard, R. L., Freimuth, R. R., Buck, J., Weinshilboum, R. M., and Coughtrie, M. W. (2004) A proposed nomenclature system for the cytosolic sulfotransferase (SULT) superfamily. *Pharmacogenetics*, *14*, 199-211.

(150) Pedersen, L. C., Petrotchenko, E. V., and Negishi, M. (2000) Crystal structure of SULT2A3, human hydroxysteroid sulfotransferase. *FEBS Lett*, *475*, 61-64.

(151) Kakuta, Y., Pedersen, L. C., Chae, K., Song, W. C., Leblanc, D., London, R., Carter, C. W., and Negishi, M. (1998) Mouse steroid sulfotransferases: substrate specificity and preliminary X-ray crystallographic analysis. *Biochem Pharmacol*, *55*, 313-317.

(152) Kiehlbauch, C. C., Lam, Y. F., and Ringer, D. P. (1995) Homodimeric and heterodimeric aryl sulfotransferases catalyze the sulfuric acid esterification of *N*-hydroxy-2-acetylaminofluorene. *J Biol Chem*, *270*, 18941-18947.

(153) Kakuta, Y., Pedersen, L. G., Carter, C. W., Negishi, M., and Pedersen, L. C. (1997) Crystal structure of estrogen sulphotransferase. *Nat Struct Biol*, *4*, 904-908.

(154) Pedersen, L. C., Petrotchenko, E., Shevtsov, S., and Negishi, M. (2002) Crystal structure of the human estrogen sulfotransferase-PAPS complex: Evidence for catalytic role of Ser137 in the sulfuryl transfer reaction. *J Biol Chem*, *277*, 17928-17932.

(155) Lu, J. H., Li, H. T., Liu, M. C., Zhang, J. P., Li, M., An, X. M., and Chang, W. R. (2005) Crystal structure of human sulfotransferase SULT1A3 in complex with dopamine and 3'-phosphoadenosine 5'-phosphate. *Biochem Biophys Res Commun*, *335*, 417-423.

(156) Gamage, N. U., Duggleby, R. G., Barnett, A. C., Tresillian, M., Latham, C. F., Liyou, N. E., McManus, M. E., and Martin, J. L. (2003) Structure of a human carcinogen-converting enzyme, SULT1A1. Structural and kinetic implications of substrate inhibition. *J Biol Chem*, *278*, 7655-7662.

(157) Shevtsov, S., Petrotchenko, E. V., Pedersen, L. C., and Negishi, M. (2003) Crystallographic analysis of a hydroxylated polychlorinated biphenyl (OH-PCB) bound to the catalytic estrogen binding site of human estrogen sulfotransferase. *Environ Health Perspect*, *111*, 884-888.

(158) Rehse, P. H., Zhou, M., and Lin, S. X. (2002) Crystal structure of human dehydroepiandrosterone sulphotransferase in complex with substrate. [erratum appears in Biochem J 2002 Jun 15;364(Pt 3):888.]. *Biochem J*, *364*, 165-171.

(159) Lee, K. A., Fuda, H., Lee, Y. C., Negishi, M., Strott, C. A., and Pedersen, L. C. (2003) Crystal structure of human cholesterol sulfotransferase (SULT2B1b) in the presence of pregnenolone and 3'-phosphoadenosine 5'-phosphate. Rationale for specificity differences between prototypical SULT2A1 and the SULT2BG1 isoforms. *J Biol Chem*, *278*, 44593-44599.

(160) Negishi, M., Pedersen, L. G., Petrotchenko, E., Shevtsov, S., Gorokhov, A., Kakuta, Y., and Pedersen, L. C. (2001) Structure and function of sulfotransferases. *Arch Biochem Biophys*, *390*, 149-157.

(161) Chapman, E., Best, M. D., Hanson, S. R., and Wong, C. H. (2004) Sulfotransferases: structure, mechanism, biological activity, inhibition, and synthetic utility. *Angew Chem Int Ed Engl*, *43*, 3526-3548.

(162) Otterness, D. M., Wieben, E. D., Wood, T. C., Watson, R. W. G., Madden, B. J., McCormick, D. J., and Weinshilboum, R. M. (1992) Human liver dehydroepiandrosterone sulfotransferase: molecular cloning and expression of cDNA. *Mol Pharmacol*, *41*, 865-872.

(163) Falany, C. N., Vazquez, M. E., and Kalb, J. M. (1989) Purification and characterization of human liver dehydroepiandrosterone sulphotransferase. *Biochem J*, *260*, 641-646.

(164) Thomae, B. A., Eckloff, B. W., Freimuth, R. R., Wieben, E. D., and Weinshilboum, R. M. (2002) Human sulfotransferase SULT2A1 pharmacogenetics: genotype-to-phenotype studies. *Pharmacogenomics J*, *2*, 48-56.

(165) Javitt, N. B., Lee, Y. C., Shimizu, C., Fuda, H., and Strott, C. A. (2001) Cholesterol and hydroxycholesterol sulfotransferases: identification, distinction from dehydroepiandrosterone sulfotransferase, and differential tissue expression. *Endocrinology*, *142*, 2978-2984.

(166) Barker, E. V., Hume, R., Hallas, A., and Coughtrie, W. H. (1994) Dehydroepiandrosterone sulfotransferase in the developing human fetus: quantitative biochemical and immunological characterization of the hepatic, renal, and adrenal enzymes. *Endocrinology*, *134*, 982-989.

(167) Falany, C. N., Comer, K. A., Dooley, T. P., and Glatt, H. (1995) Human dehydroepiandrosterone sulfotransferase. Purification, molecular cloning, and characterization. *Ann N Y Acad Sci*, *774*, 59-72.

(168) Falany, C. N., He, D., Dumas, N., Frost, A. R., and Falany, J. L. (2006) Human cytosolic sulfotransferase 2B1: isoform expression, tissue specificity and subcellular localization. *J Steroid Biochem Mol Biol*, *102*, 214-221.

(169) Elekima, O. T., Mills, C. O., Ahmad, A., Skinner, G. R., Ramsden, D. B., Bown, J., Young, T. W., and Elias, E. (2000) Reduced hepatic content of dehydroepiandrosterone sulphotransferase in chronic liver diseases. *Liver*, *20*, 45-50.

(170) Kitada, H., Miyata, M., Nakamura, T., Tozawa, A., Honma, W., Shimada, M., Nagata, K., Sinal, C. J., Guo, G. L., Gonzalez, F. J., and Yamazoe, Y. (2003) Protective role of hydroxysteroid sulfotransferase in lithocholic acid-induced liver toxicity. *J Biol Chem*, *278*, 17838-17844.

(171) Meloche, C. A., Sharma, V., Swedmark, S., Andersson, P., and Falany, C. N. (2002) Sulfation of budesonide by human cytosolic sulfotransferase, dehydroepiandrosterone-sulfotransferase (DHEA-ST). *Drug Metab Dispos*, *30*, 582-585.

(172) Falany, J. L., Macrina, N., and Falany, C. N. (2004) Sulfation of tibolone and tibolone metabolites by expressed human cytosolic sulfotransferases. *J Steroid Biochem Mol Biol*, *88*, 383-391.

(173) Gulcan, H. O., Liu, Y., and Duffel, M. W. (2008) Pentachlorophenol and other chlorinated phenols are substrates for human hydroxysteroid sulfotransferase hSULT2A1. *Chem Res Toxicol*, *21*, 1503-1508.

(174) Pasqualini, J. R. (2005) Enzymes involved in the formation and transformation of steroid hormones in the fetal and placental compartments. *J Steroid Biochem Mol Biol*, *97*, 401-415.

(175) Sasaki, K., Nakano, R., Kadoya, Y., Iwao, M., Shima, K., and Sowa, M. (1982) Cervical ripening with dehydroepiandrosterone sulphate. *Br J Obstet Gynaecol*, *89*, 195-198.

(176) Svec, F., and Porter, J. R. (1998) The actions of exogenous dehydroepiandrosterone in experimental animals and humans. *Proc Soc Exp Biol and Med*, *218*, 174-191.

(177) Gordon, G. B., Bush, D. E., and Weisman, H. F. (1988) Reduction of atherosclerosis by administration of dehydroepiandrosterone. A study in the hypercholesterolemic New Zealand white rabbit with aortic intimal injury. *The Journal of clinical investigation*, *82*, 712-720.

(178) Mohan, P. F. (1989) Dehydroepiandrosterone and Alzheimer's disease. *Lancet*, *2*, 1048-1049.

(179) Schwartz, A. G., and Perantoni, A. (1975) Protective effect of dehydroepiandrosterone against aflatoxin B1-and 7,12-dimethylbenz(a)anthracene-induced cytotoxicity and transformation in cultured cells. *Cancer Res*, *35*, 2482-2487.

(180) Barrett-Connor, E., and Goodman-Gruen, D. (1995) The epidemiology of DHEAS and cardiovascular disease. *Ann N Y Acad Sci*, *774*, 259-270.

(181) Khaw, K. T. (1996) Dehydroepiandrosterone, dehydroepiandrosterone sulphate and cardiovascular disease. *The Journal of endocrinology*, *150 Suppl*, S149-153.

(182) Kim, S.-B., Hill, M., Kwak, Y.-T., Hampl, R., Jo, D.-H., and Morfin, R. (2003) Neurosteroids: cerebrospinal fluid levels for Alzheimer's disease and vascular dementia diagnosis. *Journal of Clinical Endocrinology & Metabolism*, *88*, 5199-5206.

(183) Tagawa, N., Tamanaka, J., Fujinami, A., Kobayashi, Y., Takano, T., Fukata, S., Kuma, K., Tada, H., and Amino, N. (2000) Serum dehydroepiandrosterone, dehydroepiandrosterone sulfate, and pregnenolone sulfate concentrations in patients with hyperthyroidism and hypothyroidism. *Clin Chem*, *46*, 523-528.

(184) Pacifici, G. M., Ferroni, M. A., Temellini, A., Gucci, A., Morelli, M. C., and Giuliani, L. (1994) Human liver budesonide sulphotransferase is inhibited by testosterone and correlates with by testosterone sulphotransferase. *Eur J Clin Pharmacol*, *46*, 49-54.

(185) Mesia-Vela, S., and Kauffman, F. C. (2003) Inhibition of rat liver sulfotransferases SULT1A1 and SULT2A1 and glucuronosyltransferase by dietary flavonoids. *Xenobiotica*, *33*, 1211-1220.

(186) Mesia-Vela, S., Sanchez, R. I., Estrada-Muniz, E., Alavez-Solano, D., Torres-Sosa, C., Jimenez, M., Estrada, Reyes-Chilpa, R., and Kauffman, F. C. (2001) Natural products isolated from Mexican medicinal plants: novel inhibitors of sulfotransferases, SULT1A1 and SULT2A1. *Phytomedicine*, *8*, 481-488.

(187) Blat, Y. (2010) Non-competitive inhibition by active site binders. *Chem Biol Drug Des*, *75*, 535-540.

(188) Rebholz, K. L., and Northrop, D. B. (1994) Kinetics of enzymes with iso-mechanisms: dead-end inhibition of fumarase and carbonic anhydrase II. *Arch Biochem Biophys*, *312*, 227-233.

(189) Sahni-Arya, B., Flynn, M. J., Bergeron, L., Salyan, M. E., Pedicord, D. L., Golla, R., Ma, Z., Wang, H., Seethala, R., Wu, S. C., Li, J. J., Nayeem, A., Gates, C., Hamann, L. G., Gordon, D. A., and Blat, Y. (2007) Cofactor-specific modulation of 11beta-hydroxysteroid dehydrogenase 1 inhibitor potency. *Biochim Biophys Acta*, *1774*, 1184-1191.

(190) Wilson, D. K., Tarle, I., Petrash, J. M., and Quiocho, F. A. (1993) Refined 1.8 A structure of human aldose reductase complexed with the potent inhibitor zopolrestat. *Proc Natl Acad Sci U S A*, *90*, 9847-9851.

(191) Gulcan, H. O., and Duffel, M. W. (2011) Substrate Inhibition in human hydroxysteroid sulfotransferase SULT2A1: Studies on the formation of catalytically non-productive enzyme complexes. *Arch Biochem Biophys*.

(192) Marshall, A. D., McPhie, P., and Jakoby, W. B. (2000) Redox control of aryl sulfotransferase specificity. *Arch. Biochem. Biophys.*, *382*, 95-104.

(193) Blomquist, C. H., Kotts, C. E., and Hakanson, E. Y. (1978) A simple method for detecting steroid aggregation and estimating solubility in aqueous solutions. *Anal. Biochem.*, *87*, 631-635.

(194) Akaike, H. (1974) A new look at the statistical model identification. *IEEE. Trans Aut Control*, *19*, 716-723.

(195) Kullbuck, S., and Leibler, R. A. (1951) On information and sufficiency. *Ann Math Stat*, *22*, 79-86.

(196) Hurvick, C. M., and Tsai, C.-L. (1989) Regression and time series model selection in small samples. *Biometrika*, *76*, 297-307.

(197) Posada, D., and Buckley, T. R. (2004) Model selection and model averaging in phylogenetics: advantages of akaike information criterion and bayesian approaches over likelihood ratio tests. *Syst Biol*, *53*, 793-808.

(198) Copeland, R. A. (2005) Evaluation of enzyme inhibitors in drug discovery. A guide for medicinal chemists and pharmacologists. *Methods Biochem Anal*, *46*, 1-265.

(199) Copeland, R. A. (2000) *Enzymes, a Practical Introduction to Structure, Mechanism and Data Analysis*. 2nd ed., John Wiley and sons Inc. New York, NY. USA.

(200) Wang, L. Q., Falany, C. N., and James, M. O. (2004) Triclosan as a substrate and inhibitor of 3'-phosphoadenosine 5'-phosphosulfate-sulfotransferase and UDP-glucuronosyl transferase in human liver fractions. *Drug Metab Dispos*, *32*, 1162-1169.

(201) Wang, L. Q., Lehmler, H. J., Robertson, L. W., Falany, C. N., and James, M. O. (2005) In vitro inhibition of human hepatic and cDNA-expressed sulfotransferase activity with 3-hydroxybenzo[a]pyrene by polychlorobiphenylols. *Environ Health Perspect*, *113*, 680-687.

(202) Matsui, M., Takahashi, M., and Homma, H. (1993) Inhibition of Rat Liver Hydroxysteroid Sulfotransferase Activity by Alkylamines. *Biochem Pharmacol*, *46*, 465-470.

(203) Walle, T., Eaton, E. A., and Walle, U. K. (1995) Quercetin, a potent and specific inhibitor of the human P-form phenolsulfotransferase. *Biochem Pharmacol*, *50*, 731-734.

(204) Eaton, E. A., Walle, U. K., Lewis, A. J., Hudson, T., Wilson, A. A., and Walle, T. (1996) Flavonoids, potent inhibitors of the human P-form phenolsulfotransferase. Potential role in drug metabolism and chemoprevention. *Drug Metab Dispos*, *24*, 232-237.

(205) Barnett, A. C., Tsvetanov, S., Gamage, N., Martin, J. L., Duggleby, R. G., and McManus, M. E. (2004) Active site mutations and substrate inhibition in human sulfotransferase 1A1 and 1A3. *J Biol Chem*, *279*, 18799-18805.

(206) Cook, I. T., Leyh, T. S., Kadlubar, S. A., and Falany, C. N. (2009) Structural rearrangement of SULT2A1: effects on dehydroepiandrosterone and raloxifene sulfation. *Hormone Molecular Biology and Clinical Investigation*, *1*, 81-87.

(207) Whiteley, C. G. (1997) Enzyme Kinetics Partial and Complete Competitive Inhibition. *Biochemical Education*, *25*, 144-146.

(208) Vanderkooi, J., and Martonosi, A. (1969) Sarcoplasmic reticulum. 8. Use of 8-anilino-1-naphthalene sulfonate as conformational probe on biological membranes. *Arch Biochem Biophys*, *133*, 153-163.

(209) Doddgh, and Radda, G. K. (1969) 1-Anilinonaphthalene-8-sulphonate, a fluorescent conformational probe for glutamate dehydrogenase. *Biochem J*, *114*, 407-417.

(210) Rickenbacher, U., McKinney, J. D., Oatley, S. J., and Blake, C. C. (1986) Structurally specific binding of halogenated biphenyls to thyroxine transport protein. *J Med Chem*, *29*, 641-648.

(211) Niwa, T., Nomura, T., Sugiyama, S., Miyazaki, T., Tsukushi, S., and Tsutsui, S. (1997) The protein metabolite hypothesis, a model for the progression of renal failure: an oral adsorbent lowers indoxyl sulfate levels in undialyzed uremic patients. *Kidney Int Suppl*, *62*, S23-28.

(212) Niwa, T., Aoyama, I., Takayama, F., Tsukushi, S., Miyazaki, T., Owada, A., and Shiigai, T. (1999) Urinary indoxyl sulfate is a clinical factor that affects the progression of renal failure. *Miner Electrolyte Metab*, *25*, 118-122.

(213) Shibutani, S., Dasaradhi, L., Terashima, I., Banoglu, E., and Duffel, M. W. (1998) Alpha-hydroxytamoxifen is a substrate of hydroxysteroid (alcohol) sulfotransferase, resulting in tamoxifen DNA adducts. *Cancer Res*, *58*, 647-653.

(214) Liu, Y., Smart, J. T., Song, Y., Lehmler, H. J., Robertson, L. W., and Duffel, M. W. (2009) Structure-activity relationships for hydroxylated polychlorinated biphenyls as substrates and inhibitors of rat sulfotransferases and modification of these relationships by changes in thiol status. *Drug Metab Dispos*, *37*, 1065-1072.

(215) Lehmler, H. J., and Robertson, L. W. (2001) Synthesis of hydroxylated PCB metabolites with the Suzuki coupling. *Chemosphere*, *45*, 1119-1127.

(216) Sekura, R. D. (1981) Adenosine 3'-phosphate 5'-phosphosulfate. *Methods Enzymol*, *77*, 413-415.

(217) Sheng, J. J., and Duffel, M. W. (2003) Enantioselectivity of human hydroxysteroid sulfotransferase ST2A3 with naphthyl-1-ethanols. *Drug Metab Dispos*, *31*, 697-700.

(218) Bensadoun, A., and Weinstein, D. (1976) Assay of proteins in the presence of interfering materials. *Anal Biochem*, *70*, 241-250.

(219) Sheng, J., Sharma, V., and Duffel, M. W. (2001) Measurement of aryl and alcohol sulfotransferase activity. *Current Protocols in Toxicology*, pp. 4.5.1 - 4.5.9., John Wiley & Sons, Inc., New York.

(220) Sekura, R. D., and Jakoby, W. B. (1979) Phenol Sulfotransferases. *J Biol Chem*, *254*, 5658-5663.

(221) Duffel, M. W., Binder, T. P., and Rao, S. I. (1989) Assay of purified aryl sulfotransferase suitable for reactions yielding unstable sulfuric acid esters. *Anal Biochem*, *183*, 320-324.

(222) Jain, A. N. (1996) Scoring noncovalent protein-ligand interactions: a continuous differentiable function tuned to compute binding affinities. *J Comput Aided Mol Des*, *10*, 427-440.

(223) Jain, A. N. (2003) Surflex: fully automatic flexible molecular docking using a molecular similarity-based search engine. *J Med Chem*, *46*, 499-511.

(224) Ruppert, J., Welch, W., and Jain, A. N. (1997) Automatic identification and representation of protein binding sites for molecular docking. *Protein Sci*, *6*, 524-533.

(225) Katiyar, A., Lenka, S. K., Lakshmi, K., Chinnusamy, V., and Bansal, K. C. (2009) In silico characterization and homology modeling of thylakoid-bound ascorbate peroxidase from a drought tolerant wheat cultivar. *Genomics Proteomics Bioinformatics*, *7*, 185-193.

(226) Cramer III, R. D., Patterson, D. E., and Bunce, J. D. (1988) Comparative molecular field analysis (CoMFA). 1. Effect of shape on binding of steroids to carrier proteins. *J Am Chem Soc*, *110*, 5959-5967.